Relationship between flotation operational factors and froth behaviour

Tanaka Casandra Shumba

BSc (Eng) Chemical Engineering (University of Cape Town)

A thesis submitted to the University of Cape Town in fulfilment of the requirements for the degree of Master of Science in Engineering (Chemical Engineering)

May 2014

DECLARATION

I hereby certify that this thesis is the result of my own work and has not been submitted prior to this for any higher degree to any other university or institution. I know the meaning of plagiarism and declare that all the work in the document, save for that properly acknowledged, is my own.

Tanaka Casandra Shumba

q

ACKNOWLEDGEMENTS

I would like to thank my supervisors, Mrs Jenny Wiese and Dr Belinda McFadzean for their invaluable guidance and encouragement throughout this MSc study.

I would also like to acknowledge the following people and institutions:

- Amira P9P project for their financial support
- Professor Cyril O'Connor and Mr Martin Harris, for their insight in this study.
- The staff at the Centre for Minerals Research, especially Shireen Govender for all her assistance; Kenneth Maseko and Moegsien Southgate for their technical input in setting up and modifying the experimental apparatus used in this study.
- Santosh Pani, Tafadzwa Marozva, Jemitias Chivava, Mehdi Safari and Innocent Achaye for assisting me at the various stages of this study.
- Motena Takalimane, Tonderai Mupandi, Runyararo Dikinya, Theodore Subramoney, Tanita Gandidze, Wadzanai Kajawo, Margreth Tadie, Thandazile Moyo, Pharoah Muzanenhamo and Constance Nyambayo for their support and encouragement
- Most of all a big thank you to my parents, "Vabereki" and my siblings Marilyn and Chiko Shumba for all their love and reassurance, and for believing in me when I doubted myself.

SYNOPSIS

This study utilised laboratory-scale column flotation experiments to investigate froth stability, with respect to, water recovery and top-of-froth bubble burst rate. Tests were conducted at different froth heights, superficial air rates and depressant dosages in a 2 m high Plexiglass column, using a PGM bearing UG2 ore from the Bushveld Igneous Complex. Four concentrate and tailings samples were simultaneously collected and solids and water recoveries were determined. Assays of the concentrates were conducted to establish the amount of platinum, palladium and chromite that was recovered under each operating condition. Video footage of the top of the froth was recorded and was used to measure the top-of-froth bubble burst rate. The stability of the froth was analysed qualitatively by comparing the relationship between water recovery and the bubble burst rate at the different operating conditions.

A key finding from this study was that the concentration of particles had a large effect on the stability of the froth. The maximum concentration of particles was obtained when the tests were conducted in the absence of depressant. Under these conditions it was established that the froth produced was so stable that increasing the air rate only showed minor changes in the stability of the froth phase. This stability has been attributed to the presence of hydrophobic gangue, which stabilised the froth phase by embedding between adjacent bubbles and preventing bubble coalescence. Conversely, when a high depressant dosage was used the froth became unstable such that no trends could be established when either air rate or froth height were altered. The instability of the froth has been attributed to the depression of the majority of the froth stabilising gangue, which resulted in increased bubble coalescence.

When a depressant dosage of 100 g/t was used, the froth formed was moderately stable which resulted in more pronounced froth stability trends being observed as the air rate was increased. When evaluating the effect of changing superficial air rate, a peak in the stability of the froth was observed at the intermediate air rate (1.60 cm/s). The initial increase in froth stability was due to the shorter froth residence time which reduced the time over which bubble coalescence could occur thus making the froth more stable. The increase in air rate also resulted in more solids entering the froth which led to reduced bubble coalescence. Further increases in air rate, however, increased the amount of turbulence in the system which destabilised the froth phase.

A decrease in the stability of the froth was observed when the froth height was increased at depressant dosages of 0 and 100 g/t, and this has been attributed to an increase in the drainage of water and particles from the froth back into the pulp phase. This drainage decreased the liquid layer between adjacent bubbles which promoted bubble coalescence and decreased the stability of the froth.

In this study the concentration of particles was altered by varying the depressant dosage; increasing the depressant dosage decreased the concentration of particles which affected the stability of the froth. When the tests were conducted at constant superficial air rates of 1.35 and 1.85 cm/s, there was a decrease in the stability of the froth phase as the depressant dosage was increased. This decrease was due to the depression of the naturally floatable gangue. However, when the tests were conducted at an air rate of 1.60 cm/s there were no changes in the stability of the froth. It was found that when tests were conducted at the different superficial gas rates, maximum froth stability was attained when an air rate of

1.60 cm/s was used. As a result the effect of changing depressant dosage was overshadowed by the air rate used.

An anomaly was noted when evaluating the effect of changing depressant dosage. When increasing the depressant dosage it was expected that the amount of solids and ultimately water recovered would begin to decrease due to the depression of gangue. However, it was noted that with increasing depressant dosage the recoveries first increased and then decreased. This has been attributed to high bubble loading which occurred when no depressant was used in the system. This resulted in the slower transportation of froth and solids from the column into the launder. As the depressant dosage was increased the bubble loading decreased and as a result the solids recovery increased. A further increase in depressant dosage resulted in the expected lowering of solids and water recoveries due to the depression of most of the naturally floatable gangue.

This study has qualitatively demonstrated the different trends observed when changes in froth height, superficial air rate and depressant dosage are made in a flotation system.

TABLE OF CONTENTS

LIST OF TABLES

LIST OF FIGURES AND PICTURES

ABBREVIATIONS AND NOMENCLATURE

cm/s	Centimetres per second
CMR	Centre for Minerals Research
C1	First concentrate
C2	Second concentrate
C3	Third concentrate
C4	Fourth concentrate
FH	Froth height
g/min	Grams per minute
g/t	Grams per tonne
Jg	Superficial gas rate
PAR	Peak Air Recovery
PGE	Platinum group elements
PGM	Platinum group mineral
PSD	Particle Size Distribution
SIBX	Sodium Isobutyl Xanthate
T1	First tails
T2	Second tails
T3	Third tails
T4	Fourth tails
UG2	Upper Group 2
UCT	University of Cape Town
µm	Microns

CHAPTER ONE : INTRODUCTION

1.1. Background

Froth flotation is widely used in the mineral processing industry to aid the recovery of valuable minerals from the bulk ore. Flotation operates on the differences in the physico-chemical properties of particles, which include particle size and particle hydrophobicity. Efficient flotation depends on the characteristics of both the pulp and froth phases. The performance of the froth depends on its stability and mobility. The mobility of the froth can be described as the froth's ability to move from the flotation cell into the launder, whilst stability of the froth phase is the time of the froth's persistence or the froth's ability to resist bubble rupture and coalescence (Subrahmanyam and Forssberg, 1988; Farrokhpay, 2011).

Froth stability is important as it affects both the grade and recovery of the concentrate collected, with changes in stability having opposite effects on the grade and the recovery. If the froth phase is very stable then recovery will be good but the selectivity of the froth will decrease due to the recovery of unwanted gangue material, which decreases the grade of the concentrate. Conversely, if the froth is unstable this reduces the overall concentrate recoveries, but may enhance the grade. Acquiring the correct stability of the froth is therefore of paramount importance.

Air bubbles and conditioned slurry are combined within the pulp phase in a flotation cell. Hydrophobic particles then attach onto the bubble surface forming a bubble-particle aggregate. Along with other bubbles, these bubble-particle aggregates rise to the top of the flotation cell forming a froth layer. The bubbles have a liquid film surrounding them and when three bubbles are adjacent to each other they form a Plateau boarder which usually contains liquid in it (Farrokhpay, 2011). If the liquid between adjacent bubbles drains back into the pulp phase the bubbles coalesce forming larger less stable bubbles that are prone to rupturing which can be seen by an increase in top of froth burst rate (Hunter et al.,2008). The drainage of water back into the pulp ultimately results in a decrease in the amount of water that is collected in the concentrate.

The number of bursting events and amount of drainage that can occur also depends on the rate at which the concentrate is transported to the launder. Froths that are transported slowly to the launder have a longer residence time in the flotation cell which results in increased coalescence and drainage and ultimately less water is recovered in the final concentrate and more bubbles burst at the top of the froth. From the above description it is evident that there is a strong relationship between bubble coalescence within the froth phase, top of froth bubble burst rate and the amount of water recovered in the concentrate. The stability of the froth has thus been defined as the froth's ability to resist coalescence and bursting (Farrokhpay, 2011).

Previous research has been conducted to gain a better understanding of the behaviour of the froth phase with different operational conditions in an attempt to quantify the stability of the froth (Bikerman, 1973; Ventura-Medina & Cilliers, 2002; Barbian et al, 2003; Hadler and Cilliers, 2009; Morar et al., 2012). Until recently, most test work had been conducted in two phase or in discontinuous, non-overflowing systems (Dippenaar, 1982a; Barbian et al., 2003; Aktas et al., 2008). Using this information, researchers have settled on different factors such as water recovery and changes in froth appearance as measures of froth stability. However,

at present there is no universal method that can be used to quantify the stability of the froth phase. A more robust method which takes into account the relationship between the different measured factors is required to quantify froth stability.

This projects aims to investigate the effect of various operating conditions on the stability of the froth phase, using an in-line aerated column. The conditions that will be varied are depressant dosage, froth height and superficial air rate, and the stability of the froth phase will be determined by investigating the changes in water recovery, top of froth bubble burst rate and rate of bubble coalescence within the froth phase. The top of froth bubble burst rate and rate of coalescence will be measured by analysing video footage of the froth phase captured during each test. Assays of the concentrates will be conducted to determine their mineralogical composition.

1.2. Research Objectives

The aim of this project is to study the effect of changing flotation operational factors on the stability of the froth phase. This will be achieved by completing the following objectives:

1. Investigate froth stability using a real ore (UG2 ore) by changing the following operating conditions; froth height, superficial air rate and pulp chemistry (depressant dosage) in a laboratory scale column cell.
2. Develop an experimental procedure that can be used to capture and analyse the burst rate and coalescence rate of bubbles within the froth phase.
3. Establish a procedure that combines water recovery, top of froth bubble burst rate and coalescence rate to study the stability of the froth phase.

1.3. Key Questions

The key questions that will be answered through this study are:

1. What is the effect of altering froth height on stability of the froth in a flotation column?
2. What is the effect of increasing aeration rate on the stability of froth in a flotation column?
3. What is the effect of altering depressant dosage on the stability of the froth in a flotation column?
4. How do changes in froth stability affect the recovery of valuable minerals?

1.4. Thesis Scope

There are many different factors that affect the efficiency of the flotation system as summarised in Figure 1.1, this project will focus on the factors that affect the stability of the froth phase.

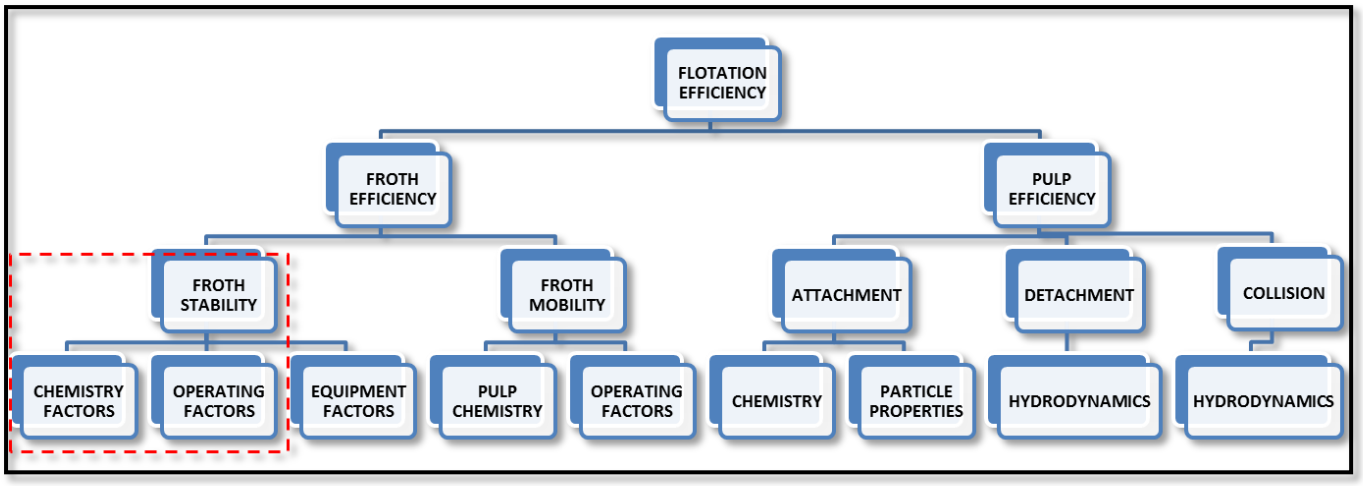

Figure 1. 1: Schematic representation of factors affecting flotation efficiency, the highlighted area lies within scope of the thesis

The factors that will be varied are classified as chemistry and operational factors. In this study the operational factors that will be altered are the froth height within the flotation column and the superficial air rate. The chemistry factor that will be changed is the depressant dosage which would change the concentration of naturally floatable gangue in the pulp.

Changes in frother dosage and particles properties are known to influence the stability of the froth, these effects are, however, not part of the scope of this project. The frother will be used at a concentration above its critical coalescence concentration (CCC) to reduce coalescence within the pulp phase. And particle properties such as size and hydrophobicity will be kept constant throughout the tests.

This project will focus on the development of a procedure that can be used to determine the stability of the froth. This will include determining a relationship between coalescence, bubble burst rate and water recovery. Whilst the measurement of water recovery is a simple sampling procedure, a method will have to be established to determine burst rate and rate of bubble coalescence. This method will incorporate the use of video footage and still images of the froth phase for the burst rate and coalescence rate respectively.

1.5. Structure of the Thesis

The progression of the thesis is shown in Figure 1.2 followed by a brief description of the contents of each chapter.

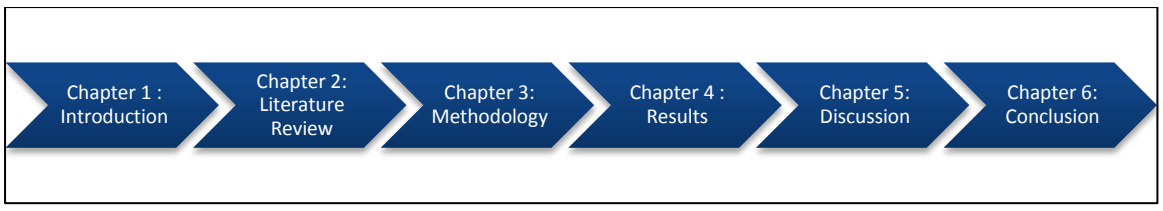

Figure 1. 2: Structure of the thesis

Chapter One: Chapter one provides some background to the study as well as its relevance to the mineral processing industry. The chapter also

highlights the scope of the study and the key questions and objectives which will be addressed.

Chapter Two: The second chapter is a review of the literature that is pertinent to this study. This includes a description of the froth structure and the causes of froth instability. The chapter also contains the various factors that affect the stability of the froth, and the different measures that have been used in an attempt to quantify froth stability.

Chapter Three: The third chapter describes the experimental methods that were used in conducting the study. It includes descriptions of the equipment, materials and reagents that were used in the study as well as the methods that were used to analyse the stability of the froth. The chapter also contains an analysis of the reproducibility of the tests and the initial experiments that were conducted during the commissioning phase.

Chapter Four: The fourth chapter is an analysis of the data obtained from changing froth height, air rate and depressant dosage. This includes water and solids recoveries, bubble burst rates and mineral recoveries. It also shows an analysis of the relationship between water recovery and top of froth bubble burst rate.

Chapter Five: The fifth chapter is a discussion of the results shown in chapter four. It incorporates the findings from the different tests conducted in an attempt to answer the key questions posed.

Chapter Six: Chapter six concludes the work discussed in this thesis and revisits the key questions and objectives mentioned in chapter one to assess if all the goals were achieved. The key findings from the study are highlighted and recommendations for further work are stated

CHAPTER TWO : LITERATURE REVIEW

2.1. Introduction

In mineral processing, flotation is widely used in the beneficiation of valuable minerals from gangue. The regions within the flotation cell can be divided into the pulp phase and the froth phase. In the pulp phase, hydrophobic particles in the ore attach onto air bubble surfaces creating a bubble-particle aggregate which rises to the top of the flotation cell forming a froth phase. Regulating the stability of the froth phase is imperative as high froth stabilities compromise the grade of the concentrate, whilst low froth stabilities reduce the recovery. Different researchers have investigated the properties of the froth phase and how stability affects flotation performance. However, at present there is no set method that has been used to quantify froth stability.

This chapter outlines the current knowledge on froth stability, including the structure of the froth and the different methods that have been employed in quantifying froth stability on laboratory and plant scale.

2.2. Background

Flotation is widely used in the mineral processing industry to separate valuable minerals from the non-valuable gangue .This process is driven by the differences in the physico-chemical surface properties of the solid particles in the feed pulp, such as hydrophobicity, which causes selective adsorption of the valuable solid particles onto air bubbles (Wills & Napier-Munn, 2006). Figure 2.1 shows a cross sectional view of a flotation cell highlighting the attachment of hydrophobic particles onto the bubble surface.

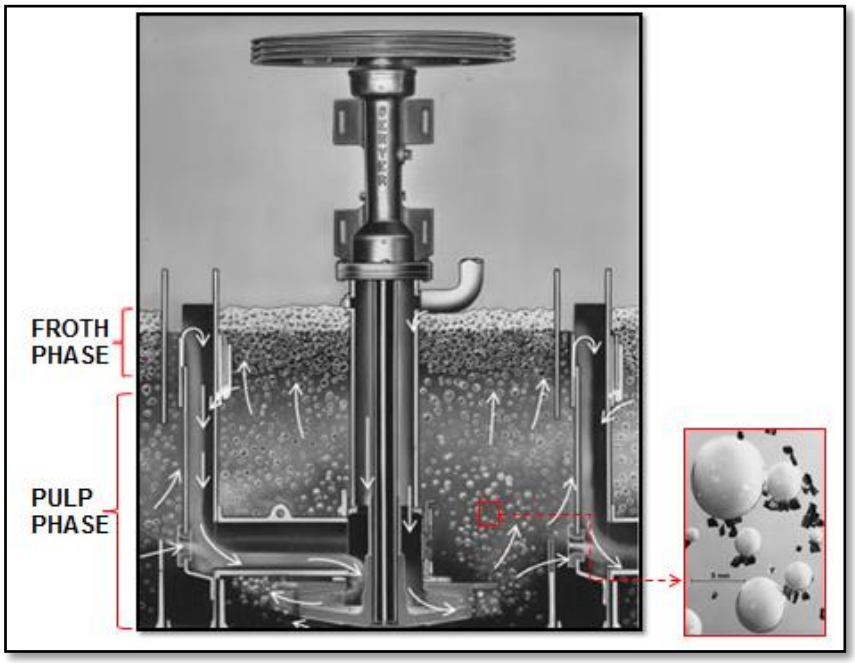

Figure 2. 1: Flotation cell showing pulp phase and froth phase and attachment of particles on to bubble surface [Adapted from (Ciros Mining Equipment, 2012)

The bubble-particle aggregates formed, ascend through the pulp phase into the froth phase until they are eventually collected in the launder, where after subsequent processing the valuable mineral can be further concentrated. Conversely hydrophilic particles do not attach onto the bubble surface and usually remain suspended within the pulp phase where they are subsequently collected in the tailings stream (Whelan and Brown, 1956). However, hydrophilic particles can be recovered in the concentrate through entrapment and entrainment which are non-selective processes that occur when particles are trapped between bubbles and when they are carried up into the froth phase by the water in the slurry.

In order to efficiently support the attached solid particles the froth phase must be sufficiently stable. Unstable froth results in the bursting of the bubble particle aggregates which causes the release of the hydrophobic particles back into the pulp phase. Conversely if the froth is too stable the amount of hydrophilic particles that can be recovered through entrainment and entrapment increases, which ultimately reduces the grade of the concentrate. Froths with small, closely-knit bubbles are favourable for increasing recoveries, whilst loosely knit froth with large bubbles improves grades (Subrahmanyam and Forssberg, 1988).

The presence of particles in the froth improves its stability, which affects the maximum achievable froth height, drainage capacity and improves the froth's ability to support other solid particles (Johansson and Pugh, 1992). Stable froths also enable the addition of wash water in a flotation column, which can be used to reduce the amount of entrained particles.

2.3. Fundamentals of froth stability

The words "foam" and "froth" are readily interchanged to mean the same thing. However, in this thesis they will have distinctly different meanings. Foam is a two phase system composed of air and liquid, which typically consists of polyhedral gas bubbles with liquid film in between them. When three bubbles are clustered together they form a plateau border which contains liquid as show in Figure 2.2. (Farrokhpay, 2011).

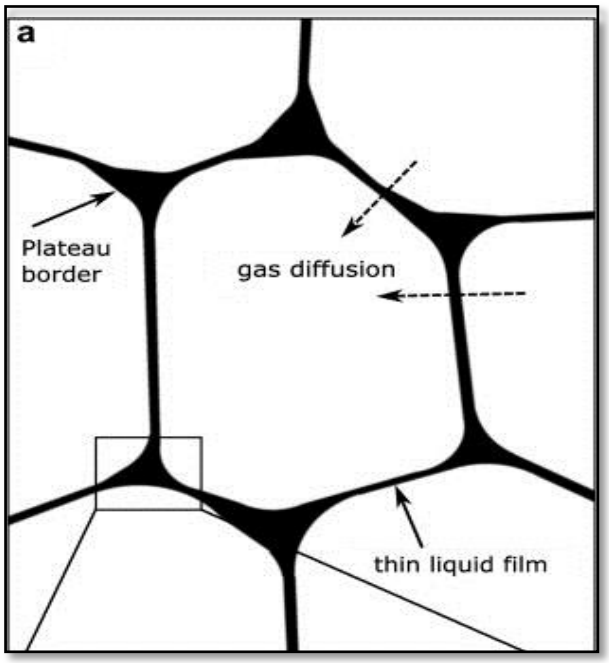

Figure 2. 2: Structure of froth phase (Baete et al., 2008)

Froth on the other hand, is a three phase structure which consists of air bubbles, solids and water. It can be characterised as either bulk froth or surface froth. Froth surface stability has been related to the bursting of bubbles at the surface and the subsequent loss of air into the atmosphere, whilst the bulk froth stability is related to bubble size on the froth surface and coalescence rates within the froth bed (Morar et al., 2006).

Froth stability can thus be defined as the froth's ability to resist coalescence and bubble bursting (Farrokhpay, 2011) or a measure of the lifetime of the froth (Subrahmanyam and Forssberg, 1988). Froths can be either metastable or unstable; metastable froths are more persistent and have a longer life time, whilst unstable froths constantly breakdown due to liquid drainage from between the bubbles and back into the pulp phase (Harris, 1982). This results in the merging of the two bubbles and the formation of one larger less stable bubble (Hunter et al., 2008).

2.4. Factors affecting froth stability

The stability of froth is influenced by the presence of particles and to a lesser extent by the presence of surface active agents and operating conditions (Hunter et al., 2008). The properties of particles that affect stability are the size, shape and the hydrophobicity of suspended particles. The main surface active agents that affect the stability of the froth are frothers which adsorb at the gas liquid interface and change the interfacial properties. Changes in frother type and concentration modify the stability of the froth (Harvey et al., 2005). Operating factors such as process water and gas dispersion also affects the stability of the froth (Farrokhpay, 2011).

2.4.1. Particle properties

The presence of solid particles within a flotation cell affects the stability of the froth phase through the interaction of the bubble surface and the particle during true flotation or entrainment. During true flotation the attachment of particles on to the bubble is dependent

on the hydrophobicity and size of the particles, and this affects the type of particles that report to the froth phase. However, these particle characteristics also have a large effect on the stability of the froth phase which may override the effects in the pulp phase (Johansson and Pugh, 1992; Aktas et al., 2008).

In 1982 Dippenaar established that a stable film was formed when a particle bridged both bubble surfaces (Johansson and Pugh, 1992). Dippenaar also concluded that froth stability could be reduced by the presence of a small number of hydrophobic particles. However a large number of particles could form a mono-layer (stearic barrier) which could prevent interfaces from touching and in so doing prevent coalescence (Johansson and Pugh, 1992). The bridging of the particles between the bubbles reduced the contact area in the foam and thus allowed for better drainage and dryer froth as shown in Figure 2.3 (Hunter et al., 2008).

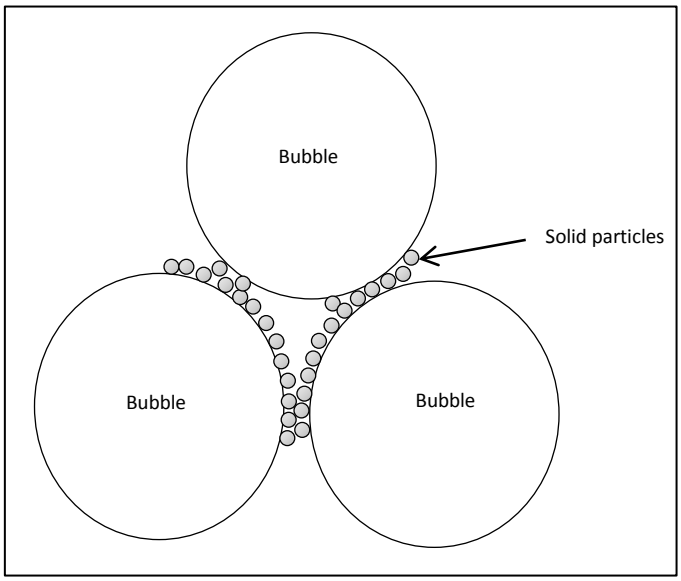

Figure 2. 3: Effect of particles on bubble interface [Adapted from (Hunter et al., 2008)]

Hydrophobicity

The ability of particles to attach onto bubbles during flotation is determined by the hydrophobic (water repelling) nature of the solid particles. This interaction is determined by the interfacial energies between the solid particles, liquid and gas bubbles, which can be determined by the Young/ Dupre Equation show by equation 2.1 (Fuerstenau and Han, 2003).

$$\gamma_{lv} cos\theta = \gamma_{sv} - \gamma_{sl} \qquad 2.1$$

Where γ_{lv} is the surface energy of the liquid/ vapour interface, γ_{sv} is the surface energy of the solid/vapour interface and γ_{sl} is the surface energy of the solid/liquid interface and Ɵ is the contact angle as shown in Figure 2.4. This interfacial energy can also be used to determine how particles of different contact angles can stabilise froth (Hunter et al., 2008).

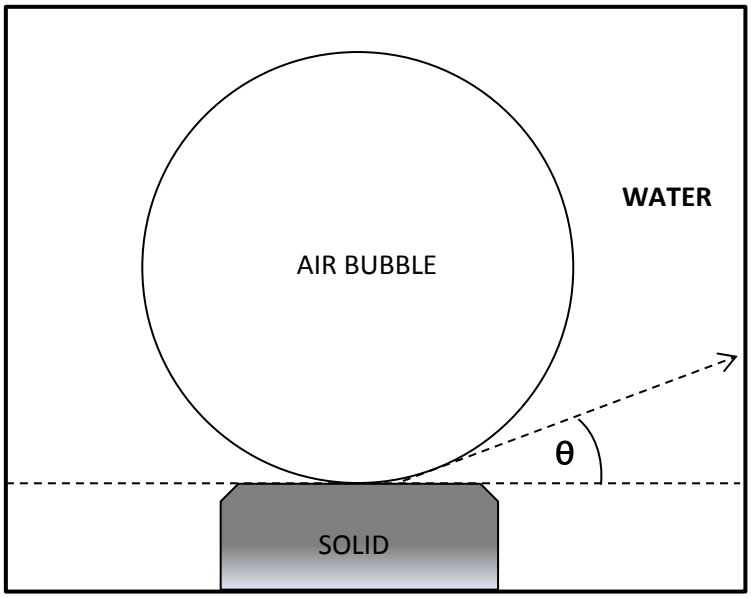

Figure 2. 4: Attachment of solid particle onto bubble, highlighting the contact angle

Initially it was hypothesized that the larger the contact angle the greater the work of adhesion between particle and bubbles and more resilient to external forces (Wills & Napier-Munn, 2006) which was assumed to result in the formation of more stable foam. Robinson (1960) deduced that there was a critical degree of hydrophobicity at which maximum floatability could be achieved, this maximum or threshold level increased with increasing particle size as depicted by Figure 2.5.

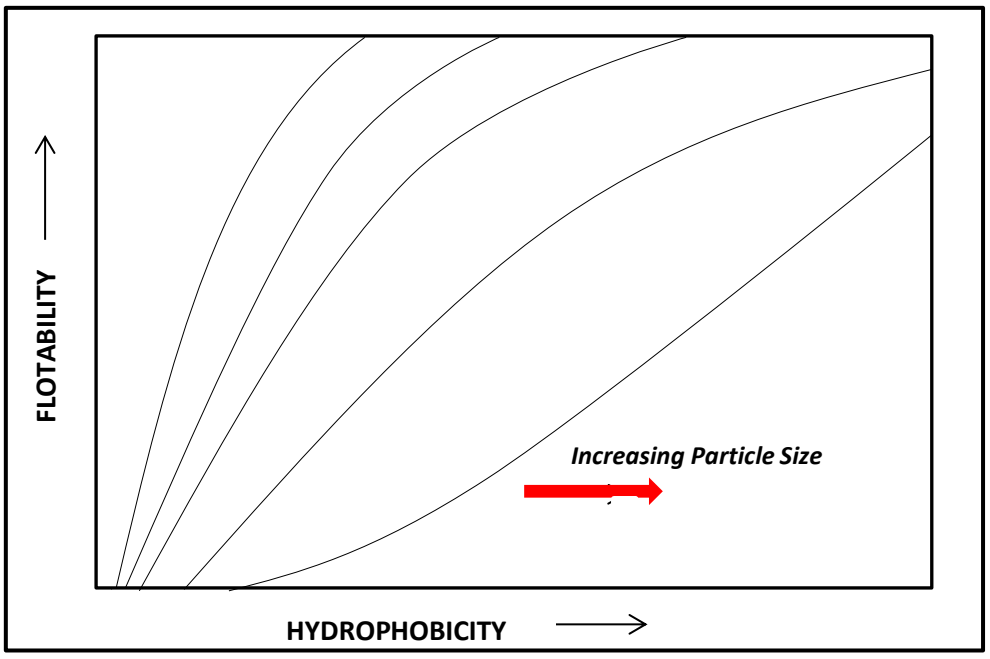

Figure 2. 5: Qualitative representation of influence of particle size on the relationship between floatability and hydrophobicity [Adapted from (Trahar, 1980)]

The floatability of the particles was linked to the stability of the froth which is a key factor in optimising flotation. Dippenaar (1982a) found that hydrophobic spherical particles with contact angles greater than 90 degrees destabilized the froth (Johansson and Pugh, 1992).

Johansson and Pugh (1992) also found that hydrophobic particles between 26 and 44 microns with contact angles larger than 80 degrees reduced the froth stability whilst those with intermediate hydrophobicity (65 degrees) increased it; which showed that there was some optimum contact angle or hydrophobicity which could stabilise the froth. Highly hydrophobic particles (with contact angles larger than 82 degrees) penetrated the interface to such an extent that the film ruptured, whilst particles with low hydrophobicity (less than 40 degrees) streamlined in the lamellae around the bubble not contributing to the froth film stability (Ata et al., 2003). Aveyard et al. (1994) found that maximum stability was attained at contact angles between 80 and 95 degrees.

Dippenaar (1982a) also suggested that increasing the particle hydrophobicity would increase the bubble rupture which was also reported by Livshits and Dudenkov (1965). This was contrary to the reports of Klassen and Mokrousovk (1963) who suggested the stronger the hydrophobicity the greater the froth stability. Ata et al. (2003) deduced that moderately hydrophobic particles produced the greatest stability. They also suggested that hydrophilic particles aided the stabilization of the froth, through increasing the bulk viscosity or by blocking the liquid flow in the froth (mechanical blocking). This was because particles with high hydrophobicity penetrated the interface to a large extent consequently rupturing the film, and particles with low hydrophobicity streamlined into the lamellae and did not contribute to the stability of the froth.

Particle size

The size of particles plays an important role in promoting stabilisation of the froth phase and it has been established that hydrophobic particles can stabilise or destabilise the froth depending on particle size and concentration (Aktas et al., 2008). This was also noted by Tang et al. (1989) who found that the stability of foam was directly proportional to the particle concentration and inversely proportional to the particle size.

Fine Particles

During flotation it has been observed that the rate of fines recovery was relatively low, and this has been attributed to the low probability of collision between particles and air bubbles (Trahar and Warren, 1976). As a result fine particles are streamlined in the water surrounding the bubbles and are recovered through entrainment as shown in Figure 2.6.

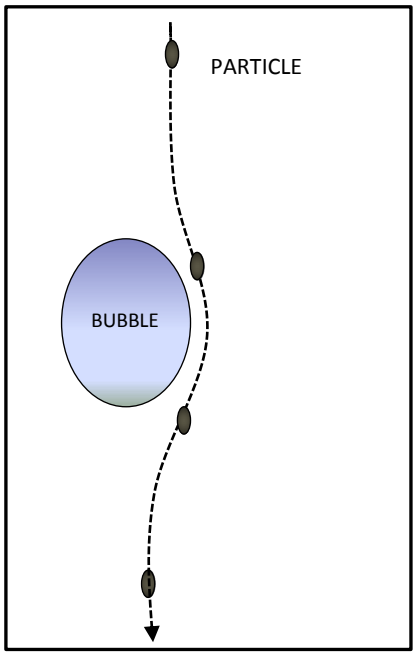

Figure 2. 6: Flotation of fine particles around air bubbles

In 1913 Hoffman hypothesized that the presence of fine particles affected the stability of the froth (Hunter et al., 2008). This was further explained by Szatkowski and Freyburger in 1985 who found that fine quartz particles made bubbles more resistant to coalescence and thus increased froth stability (Rahman et al., 2012). Using the dynamic froth stability factor as a measure of froths stability, Aktas et al. (2008) also found that using feed with finer particles increased the dynamic froth stability factor.

Rahman et al. (2012) reported that the presence of fines improved the stability of the froth by decreasing the bubble size and that this increase in stability increased the recovery of coarse and medium particles in both the collection and froth zones. This was also observed by Lange et al. (1997) and Viera and Peres (2007).

Intermediate Sized Particles

Generally fine particles and coarse particles are difficult to float whilst the flotation of intermediate particles yields larger recoveries (Trahar, 1980).Intermediate sized particles are mainly recovered through true flotation, whilst a small proportion at the end of the boundary region is recovered through entrainment (Trahar, 1980). The intermediate size range is dependent on the mineral being floated and types of collector added to aid flotation.

Experiments by Livshits and Dudenkov (1965) showed that coarse and fine particles did not destroy the froth as coarse particles would act as a buffer between two bubbles thus preventing coalescence, and slowing down the drainage of the liquid film between bubbles; fine particles would drain back with the liquid to the pulp phase. They proposed that there was an optimum size at which coalescence would occur. This however is contrary to later studies which showed that coarse particles destabilised the froth (Rahman et al, 2012).

Coarse Particles

The majority of coarse particles are recovered through true flotation and a negligible amount through entrainment (Trahar, 1980).Coarse particles easily collide with bubbles, however

due to their substantial weight they are easily detached from the bubble surface as shown in Figure 2.7.

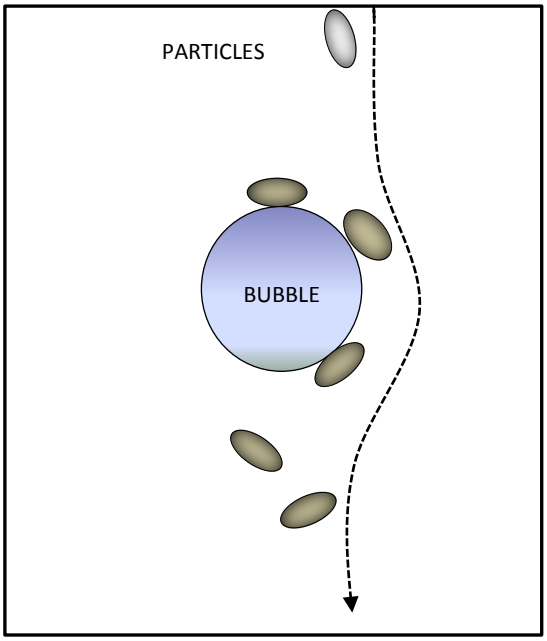

Figure 2. 7: Flotation of coarse particles around air bubbles

As a result large amounts of collectors or collectors with longer hydrocarbon chains are required to increase the hydrophobicity of the coarse particles (Kakovsky et al., 1961). Due to their size, particles larger than 50 microns are seldom recovered by entrainment; so hydrophilic coarse particles are largely transported via entrapment or other mechanisms (Ekmekci et al., 2003; Zheng et al., 2006).

A study conducted by Moudgil (1992) showed that coarse particles are likely to destabilise the froth phase and this was most likely due to the weight of the particles which resulted in the bursting of bubbles because of their weight.

Particle concentration

The concentration of particles within the feed has an effect on froth stability and ultimately flotation performance. Increasing the concentration of particles in the pulp increases bubble loading which reduces the mobility of the froth phase. This consequently increases the froth residence time (time over which coalescence can occur) and the froth becomes less stable with increasing time. Conversely increasing bubble loading also increases the coating of bubbles by particles, which could potentially reduce coalescence effects and increase stability (Perez-Garibay et al., 2002). The increased bubble coating would also increase the amount of solids recovered in the concentrate.

The effect of solids concentration is also intertwined with that of particle size. Tao et al. (2000) found that particles less than 100 microns destabilized the froth at lower concentrations and stabilised it at higher concentrations. Aktas et al. (2008) found that froth stabilisation at high concentrations was due to an increase in particle size agglomeration; and the destabilisation at lower solid concentration could be attributed to hydrophobicity.

2.4.2. Chemistry factors

In order to intensify the characteristics that promote efficient flotation, the feed pulp is conditioned using various chemical reagents. Some chemicals are added to alter the mineral surfaces so that there is selective adherence of the valuable mineral on to bubble surfaces; whilst other chemicals are used to regulate conditions within the pulp phase and air bubble properties.

The reagents that were used in this study were collectors, frothers and depressants.

Frothers

Frothers are hetero-polar surface active organic reagents which according to the Leja-Schulman penetration theory, accumulate preferentially on the water gas interface (Laskowski, 2004) as shown in Figure 2.8. The addition of frother helps to reduce the surface tension of the air-liquid interface which enhances the stability of the froth phase (Subrahmanyam and Forssberg, 1988). The polar section of the frother reacts with water, whilst the non-polar hydrocarbon tails are non-reactive and are subsequently thrust into the air phase as shown in (Wills & Napier-Munn, 2006).

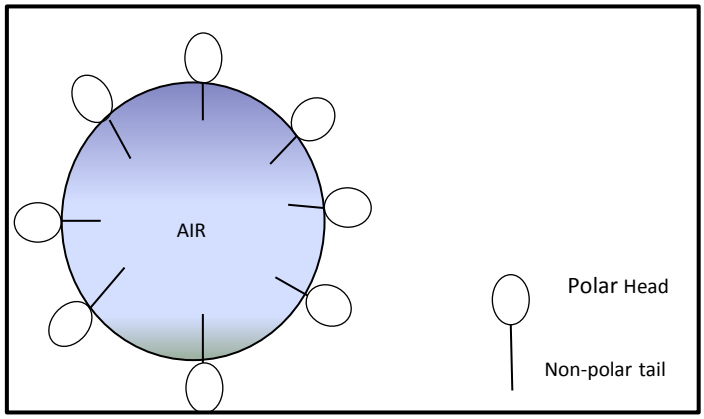

Figure 2. 8: Effect of frothers on air bubbles

This results in a reduction in surface tension which in turn stabilizes the bubbles allowing them to be recovered in the launder without bursting (Wills & Napier-Munn, 2006). Cho and Laskowski (2002) deduced that frothers also control the stability of the bubbles in the pulp phase by decreasing the rate at which they coalesce. This results in a lower bubble burst rate and more water recovered in the concentrate. A study conducted by (Tang et al., 2010) showed that there was an increase in the stability of the froth phase as the frother concentration was increased. This was depicted in the increase in water recovery and maximum froth height as shown as shown in Figure 2.9.

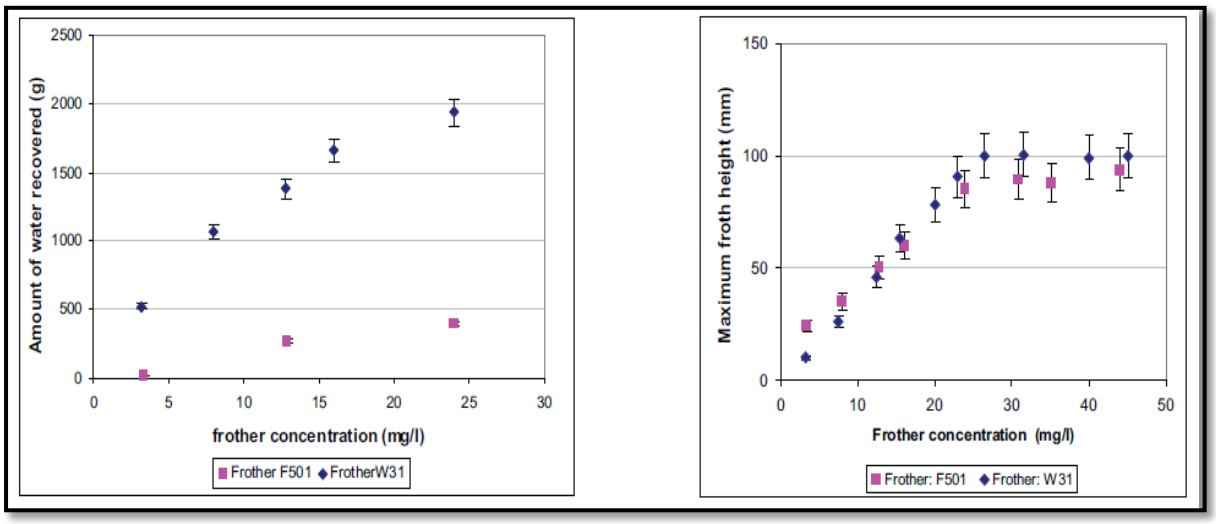

Figure 2. 9: Amount of water recovered and maximum froth height as a function of frother type and concentration in two phase system (Tang et al., 2010)

Increasing the frother dosage has been found to increase the recovery of solids. This however also decreases the selectivity of the froth phase which reduces the grade of the concentrate (Klimpel, 1995). The frother dosage was maintained constant during the experiments and therefore frother was not expected to affect the froth stability.

Collectors

Collectors are added to the pulp to increase the hydrophobicity of the valuable minerals. These molecules consist of a polar hydrophobic tail and a non-polar hydrophilic head. Due to the physical, chemical and electrical attraction between the polar head and the mineral surface; collectors adsorb onto the solid particles through their hydrophilic heads thus suspending their non-polar hydrophobic tails in the bulk solution (Wills & Napier-Munn, 2006). The physical and chemical attraction can be described as physisorption and chemisorption respectively. The addition of a collector results in the formation of a mono-layer of non-polar hydrophobic hydrocarbons around the solid particles as shown in Figure 2.10.

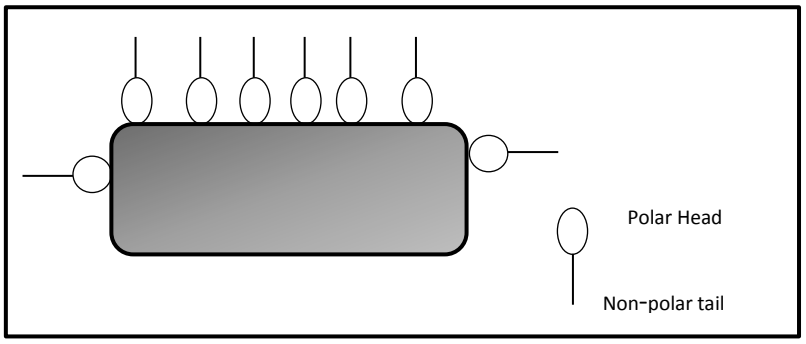

Figure 2. 10: Effect of collectors on solid particles

The formation of the mono-layer around the solid reduces the stability of the hydrated layer that separates the mineral surface from the air bubble which allows the attachment of the particle to the bubble to occur on contact (Wills & Napier-Munn, 2006).

Collectors alter the stability of the froth by altering the hydrophobicity of the particles; so whilst addition of collector might help improve the barrier between particles which prevents coalescence, too much collector could potentially destabilise the froth.

The most commonly used collectors for sulphide minerals are sulfhydryl collectors such as Xanthates and Dithiophosphates which are highly selective and do not have an affinity for non-sulphide gangue minerals (Corin and Harris, 2010).

Synergistic interactions between collectors and frothers

Whilst frothers and collectors individually influence the stability of the froth phase, the interaction between the two molecules also impacts the froth. At the mineral water interface, the frother and collector alkyl chains are united by van der waal's forces; a hydrogen bond is formed between the frother and the oxygen atom in the collector which results in the formation of a stable three phase froth (Bradshaw et al, 1998).

Depressants

Depressants are added to the pulp phase to aide flotation selectivity by making gangue minerals hydrophilic which subsequently hinders their flotation and recovery (Wills & Napier-Munn, 2006).

Modified guar gum and carboxymethyl cellulose (CMC) are generally used for the flotation of sulphide minerals (Corin and Harris, 2010). Whilst they are interchangeable in use, their basic structure and effects on froth stability are markedly different (Harris, 1982).Typical guar gums are uncharged or have very low charge and have been found to be stronger depressants of naturally floating gangue than CMC at low dosages (Wiese, 2009). CMC's are strongly negatively charged which induces the surfaces of the gangue minerals to become negatively charged and results in dispersed pulps and destabilised froths. For this reason a guar gum has been chosen as the depressant for this study

Previous research has shown that the addition of depressants especially at high concentrations affects the stability of the froth phase (Bradshaw et al., 2005). This was attributed to the removal of froth stabilising gangue such as talc (which is naturally floatable), and also due to the nature of the depressant polymer molecule (Bradshaw et al., 2005).

2.4.3. Operating factors

Effect of air rate on froth stability

The froth phase largely consists of a collection of bubble particle aggregates, with small bubbles forming more stable froth than larger bubbles. These bubbles are formed when air is fed into the collection zone of the flotation cell; the bubbles formed then rise through the pulp phase attracting and appending to hydrophobic particles which are eventually recovered in the launder. The parameters that influence the dispersion of gas in flotation systems are the superficial gas velocity (J_g), gas hold up (ε_g), bubble size (D_b) and the bubble surface area flux (S_b) (Finch et al., 2007). The relationship between the gas hold up and gas rate is used as a basis for hydrodynamic characterization and is shown in Figure 2.11.

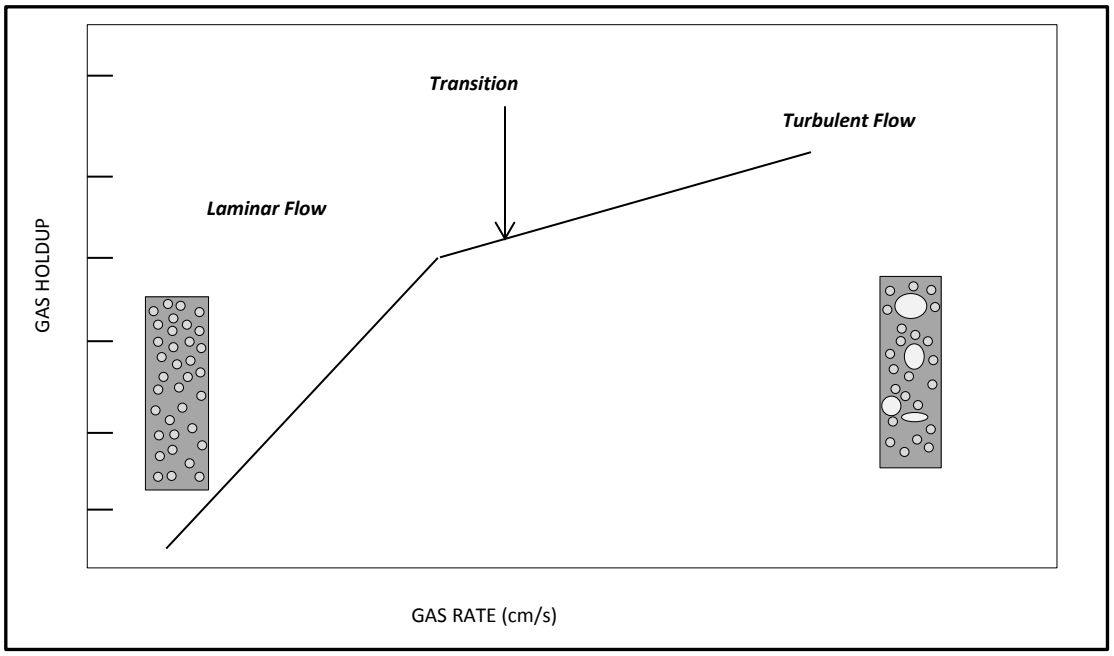

Figure 2. 11: Relationship between gas hold up and gas rate showing the two principle flow regions [Adapted from (Finch et al., 2007)]

As can be seen from the figure, at lower gas hold up the relationship between the gas rate and gas holdup is essentially linear forming laminar flow. At higher gas hold up the flow becomes chaotic and turbulent. The transition between linear and chaotic flow usually occurs between 15 and 20% gas hold up in flotation systems (Finch et al., 2007). In laminar flow the bubbles produced are of a uniform size and they rise through the pulp at uniform velocity. In comparison turbulent flow produces larger bubbles which rapidly ascend through the collection zone displacing slurry and fine bubbles downwards (Finch et al., 2007).

At high shear and turbulence rates fine particles can easily collide with the bubbles produced, however for coarse particles there is a higher probability of detachment of particles from the bubble surface (Schulze, 1984). A large amount of gas also causes a reduction in the grade and recovery of the concentrate. As a result laminar flow is much more ideal for optimum flotation in columns (Finch and Dobby, 1990).

Changes in air also alter the froth structure and retention time of water and entrained particles in the froth which affects drainage (Zheng et al., 2006). Initially there were two contrasting opinions on the influence of air rate on the stability of the froth phase. The first school of thought was that increasing the gas rate resulted in the formation of more stable froth and a subsequent increase in water recovery (Klassen and Mokrousov, 1963; Tao et al., 2000). Increasing air rate increased water recovery because more bubbles were generated at higher air rates and, assuming constant bubble size and thickness of liquid film, more water would be recovered in the launder (Engelbrecht and Woodburn, 1975). It was observed that increasing the air rate decreased the bubble residence time in the froth, which decreased the time over which coalescence could occur. An improvement in froth recovery with increasing Jg was also noted which could be attributed to the reduction in the residence time of particles in the froth phase, which reduced the probability of particle detachment from the bubbles (Rahman et al., 2012).

The second school of thought was that increasing air rate destabilised the froth phase. A study conducted by Barbian et al. (2003) showed that high froth stability conditions occurred at lower air flowrates as shown in Figure 2.12, where the dynamic stability factor (∑) was used as a measure of froth stability.

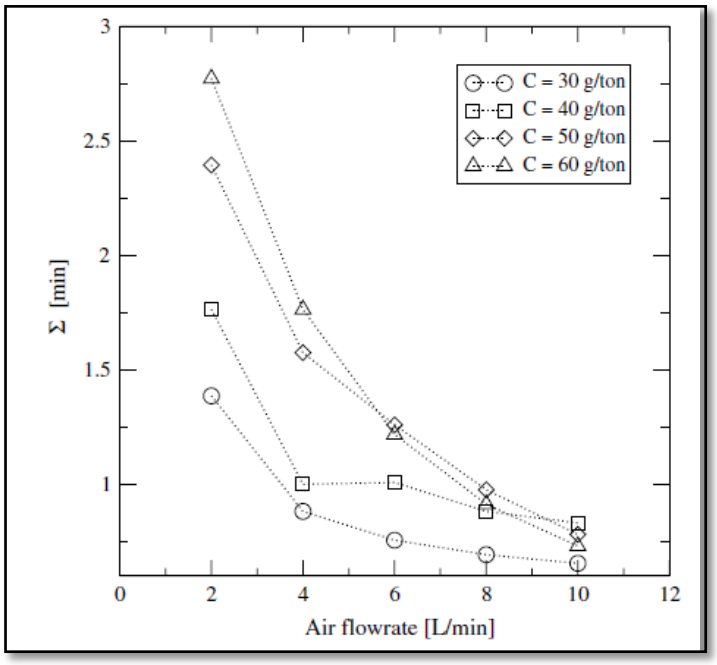

Figure 2. 12: Dynamic stability factor as a function of air flowrate for different frother concentrations (Barbian et al., 2003)

A similar conclusion was drawn by Ventura-Medina et al. (2003) from image analysis of the froth surface. In this study froth stability was estimated as the faction of bubbles bursting on the surface of froth and solids loading on the bubbles at the top of the surface. And they found that high air flowrates resulted in a decrease in froth stability which was noted by a decrease in the fraction of air overflowing and a decrease in the solids loading. Low air rates were therefore preferential as they promoted high particle bubble loading which promoted high bubble stabilisation and low gangue entrainment which improved flotation performance (Ventura-Medina et al., 2003).

The two schools of thought were later combined by Hadler and Cilliers (2009) who found that as the superficial air rate was increased, the stability of the froth went through a maximum or peak which corresponded to a peak in air recovery (PAR). They found that when the air rate was less than PAR the froth produced was highly laden and formed bubbles with low mobility that were prone to collapsing before overflowing the cell lip. These froths had low air and mineral recoveries but high concentrate grades. At air rates above PAR the froths were free flowing but produced bubbles with low particle loading which also resulted in bubbles bursting before overflowing. These froths produced moderate mineral recoveries but low concentrate grades. At intermediate air rates there was equilibrium between bubble loading and froth mobility, which resulted in the formation of a stable froth. As a result there was a peak in air recovery and a high mineral recovery and an acceptable concentrate grade as shown in Figure 2.13 (Hadler and Cilliers, 2009).

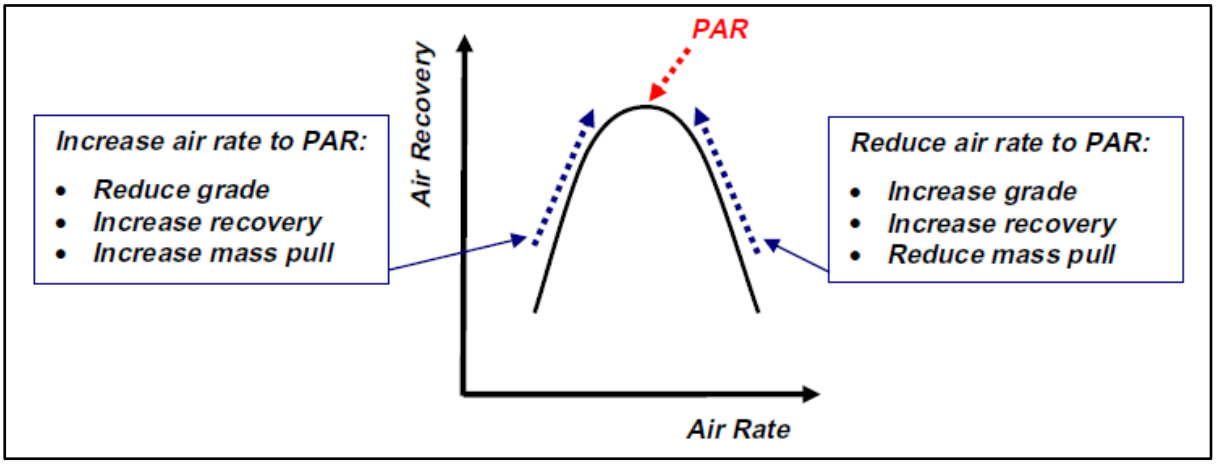

Figure 2. 13: Schematic showing general effect of air recovery optimisation on flotation performance (Hadler et al., 2010)

Effect of froth height on froth stability

Changing froth depth can be used as a means of altering the recoveries and grade of the final concentrate; these changes also have an effect on the stability of the froth phase. It has been observed that increasing froth height decreases the amount of water that is recovered in the concentrate (Bisshop and White, 1976). Previous researchers have also noted that there is a linear negative relation between these two factors (Englebrecht and Woodburn, 1975; Laplante et al., 1983b; Feteris et al., 1987; Tao et al., 2000). Increasing froth height increases the froth retention time, which allows for more drainage of liquid film from the froth back into the pulp phase. The lamellae and plateau boarders become thinner, causing more bubble coalescence and bursting events which are indicative of a less stable froth. As a result the froth becomes less stable as the froth height increases, resulting in its eventual collapse (Englebrecht and Woodburn, 1975; Feteris et al., 1987; Tao et al., 2000).

These observations were also made in a study by Ventura Medina et al. (2003) who found that increasing froth height decreased air recovery (a measure of froth stability). However an industrial campaign conducted by Hadler et al. (2012) at a South African platinum concentrator showed that when increasing froth height, the air recovery passed through a peak, at a constant air rate. The froth depth at which the PAR was observed was dependent on the air rate, with low air rates resulting in shallower froth depth than higher air rates as illustrated by Figure 2.14.

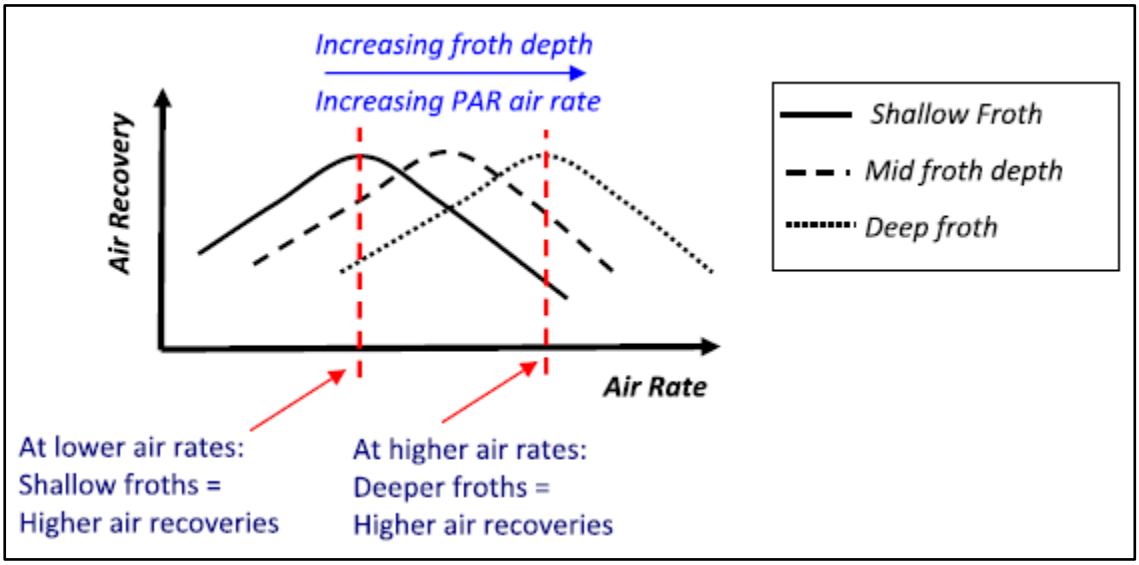

Figure 2. 14: Schematic showing relationship between froth depth, air rate and air recovery (Hadler et al., 2012)

The entrainment of hydrophilic gangue was found to be closely related to the amount of water recovered (Engelbrecht and Woodburn, 1975). This was also observed in a study by Alavarez-Silva et al. (2012) which showed that there was a decrease in both water and chromite (hydrophilic gangue in UG2 ore) as the froth height was increased. This decrease was attributed to an increase in the drop back of particles due to the increased froth depth. The presence of entrained solids in the froth phase usually stabilises the froth by providing a barrier between adjacent bubbles thus preventing coalescence from occurring. The drainage of these solids back into the pulp phase therefore results in a reduction in the stability of the froth phase.

The froth depth can also be used to regulate the grades and the recoveries of the final concentrates. Increasing froth depth increases concentrate grade but decreases mass rate (Ata et al., 2002; Farrokhpay, 2011). Deep froth reduces recovery by reducing the residence time in the pulp phase whereas shallow froth reduces grade by reducing residence time in the froth phase, which decreases selectivity (Tao, et al., 2000). The study by Alavarez- Silva et al. (2012) showed that at a constant superficial gas velocity chromite recovery could be reduced by increasing froth height; however there was little effect on the chromite grade. However above a certain maximum froth height, the amount of gangue recovered would become constant (Moys, 1978; Subrahmanyam and Forssberg, 1988).

Effect of pulp rheology on froth stability

Rheology is the study of the deformation and flow behaviour of fluid under stress and whilst the majority of this study in mineral processing has been focused on comminution process, it is also known to have an impact on flotation (Farrokhpay, 2012). The rheology of the pulp phase affects both the stability and mobility of the froth. A study conducted by Farrokhpay and Zanin (2011) showed that at lower pH values higher froth stabilities were attained which was attributed to an increase in slurry viscosity and particle aggregation. Similarly Xu et al (2011) found that the stability of bubble particle aggregates was higher when the viscosity of the suspending medium was high.

2.5. Froth stability measurements

At present there is no agreed upon method that is used to quantify froth stability during flotation operation. However, based on the knowledge of froth and foam stability various methods have been proposed. The majority of the research that has been conducted has been carried out on non-overflowing systems.

2.5.1. Non-overflowing systems

Bikerman Test

Bikerman (1973) quantified foam stability by defining a dynamic foam stability factor (∑) based on the ratio of the foam volume (V_f) to gas flow rate (Q).

$$\sum = \frac{V_f}{Q} = \frac{H_{max} \times A}{Q} \qquad 2.2$$

This factor was obtained by observing the rate at which foam grows to an equilibrium height (H_{max}) in a sparged foam column with cross- sectional area, A, and it has been implemented by many researchers in both two-phase and three phase systems (Dippenaar,1982a; Barbian et al.,2003; Aktas et al.,2008).

2.5.2. Overflowing Systems

Methods such as the Bikerman test are most applicable in non-continuous systems such as non-overflowing columns. Industrial operations are however open, continuous systems and froth stability measures would have to be devised taking this into consideration. Most industrial flotation operations deduce froth stability by observing the surface of the froth and noting the froth colour, bubble size, surface bursting rate and froth velocity (Farrokhpay, 2011). A link is therefore required between froth stability measures used in the laboratory and those that can be used on an industrial scale.

Froth growth rate

This was attempted by Barbian et al. (2005) in which they adapted Bikerman's foam test, using a non-overflowing froth column inserted below the pulp-froth interface in a flotation cell. Using the pulp-froth interface as the reference, the height of froth within the column was noted as a function of time, H(t), and the equilibrium height was measured, (H_{max}).

These were then used to calculate the expected fraction of air overflowing the weir β(H) as shown in equation 3 which can then be used to calculate the froth stability factor (τ) which is a characteristic of the froth growth rate. Where Q is the air flowrate and A is the cross sectional area of the column used.

$$\beta(H) = \frac{(H_{max} - H(t)}{\tau} \frac{A}{Q} \qquad 2.3$$

The froth stability results obtained were found to be comparable to those obtained from image analysis which estimated bubble size distribution, average bubble size and froth velocity (Barbian et al., 2005).

This method is however difficult to use on continuous operation on a plant scale as columns are intrusive to the process and disrupt the flow of froth thus decreasing the flotation cell efficiency (Morar et al., 2012). They are also difficult to use in small flotation cells with moving parts.

Air recovery

Another method that has been used to measure froth stability is that of measuring the air recovery (α) which was first proposed by Moys (1984) and later modified by Woodburn et al. (1994). Air recovery is the fraction of air that overflows the flotation cell lip as unburst bubbles and can be calculated from equation 3 (Ventura-Medina and Cilliers, 2002; Hadler and Cilliers, 2009).

$$\alpha = \frac{V}{Q_a} = \frac{v_f \, h_{lip} \, w}{Q_a} \qquad 2.4$$

Where V is the volume of overflowing froth, Q_a is the air feed to the flotation cell, v_f is the velocity of the froth at the top surface, h_{lip} is the height of the froth overflowing at the weir, and w is the overflowing weir length.

Rate of bubble coalescence

Unstable froths are characterised by increased coalescence due to thinning of lamellae between bubbles. The rate at which bubbles coalesce as a function of distance from the pulp-froth interface can then be used as an indicator of froth stability. The average size of the bubbles at various froth heights is calculated using the Sauter mean diameter (d_{32}).

$$d_{32} = \frac{\sum n_i d_i^3}{\sum n_i d_i^2} \qquad 2.5$$

This method was utilised by Ata et al. (2003) who found that there was an increase in bubble size as the distance from the interphase increased as shown in Figure 2.15.

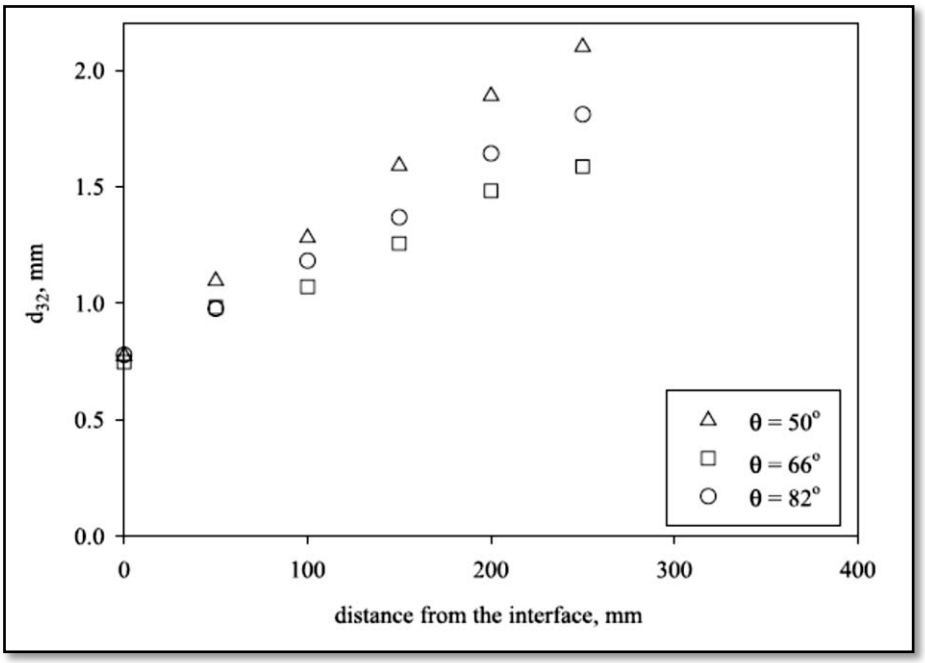

Figure 2. 15: Variation of the Sauter mean bubble diameter as a function of froth height for glass beads having various degrees of hydrophobicities (Ata et al., 2003)

From this study they also found that the presence of gangue decreased the coalescence rate which was attributed to an increase in the viscosity of the slurry between the bubbles which blocked channels between the lamellae and prevented drainage.

Bubble burst rate

The large bubbles formed from coalescence are generally much weaker and are prone to bursting. The rate at which these bubbles burst can be used as an indicator of the stability of the froth, with more bursting events indicating an unstable froth. Previous researchers have proposed the use of imaging software to measure the top of froth bubble burst rate (Moolman et al., 1995).

These machine vision measurements have been proposed based on the comparison of consecutive frames as shown in Figure 2.16, which shows the top of froth before and after a bursting event occurs.

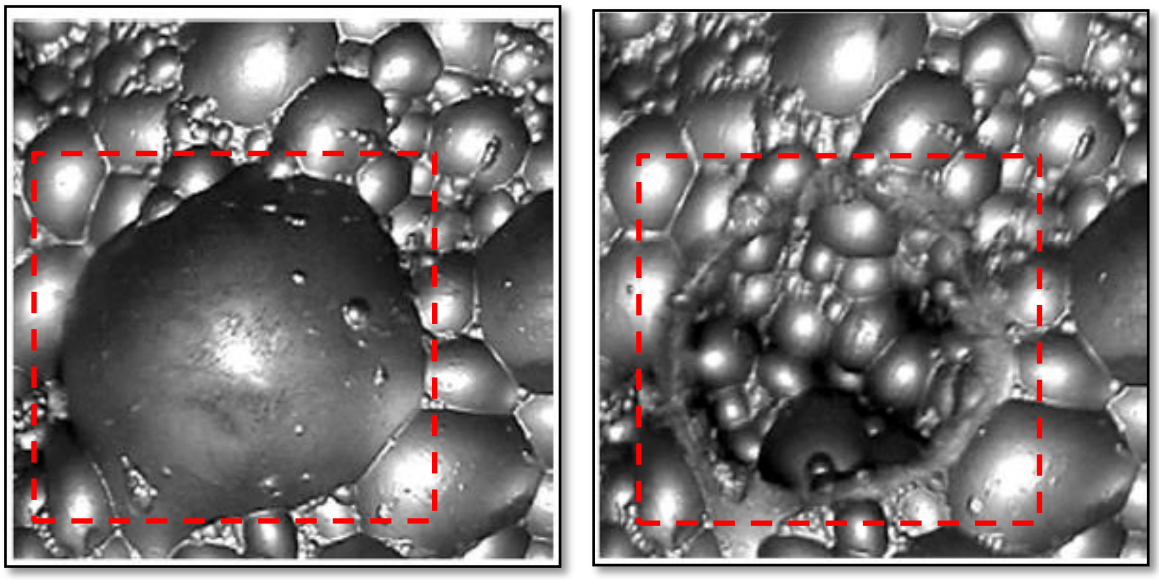

Figure 2. 16: Bubbles bursting in two consecutive frames where the highlighted area is the region where the burst bubble is located [Adapted from (Morar et al., 2012)]

These images were obtained by (Morar et al., 2012) who focused on the burst rate by detecting and counting the number of bubble bursting events. Image analysis has however been found to be slightly inefficient in prediction as different operating parameters can result in similar images (Moolman et al., 1995).

Water recoveries

Water recovery can be defined as the fraction of water in the feed that is recovered in the concentrate or as the flow rate of water in the concentrate. It is the most widely used indicator of froth stability in continuous systems (Tao et al., 2000; Wiese et al., 2011). When a froth is unstable the liquid in the froth phase drains back into the pulp phase, which leads to coalescence and bursting of bubbles. The bursting of these bubbles results in the release of the liquid film surrounding bubbles back into the pulp phases; ultimately reducing the amount of water that could have been collected in the concentrate.

The froth stability measures that were used for this study were the rate of coalescence, bubble burst rate and solid-water recoveries; these three measures are directly related and could therefore be used together to quantify froth stability.

2.6. Equipment used in the measurement of froth stability

The type of flotation cell as well as the configuration and dimensions of the chosen cell play a vital role in studying flotation performance. There are many different kinds of equipment that is used on laboratory or pilot scale which can be used to simulate plant operation in batch or continuous operation as a means of understanding the froth phase.

2.6.1. Froth Columns

Frothing columns are widely used in the implementation of discontinuous or non-overflowing test work, such as for the Bikerman test. They are usually transparent with a sintered bottom through which air is bubbled; an agitator can be added to prevent the settling of solids when

operating in three phase. Frothing columns are typically non-overflowing discontinuous systems. A typical example of a frothing column is shown in Figure 2.17.

Figure 2. 17: Frothing column used in Bikerman tests

A modification of the conventional frothing column was proposed by (Barbian et al., 2005) for use on industrial flotation cells. This was an attempt to adapt the frothing column to continuous test work.

2.6.2. Mechanical flotation cell

The most common flotation cell used in test work and on an industrial scale is the mechanical flotation cell shown in Figure 2.18.

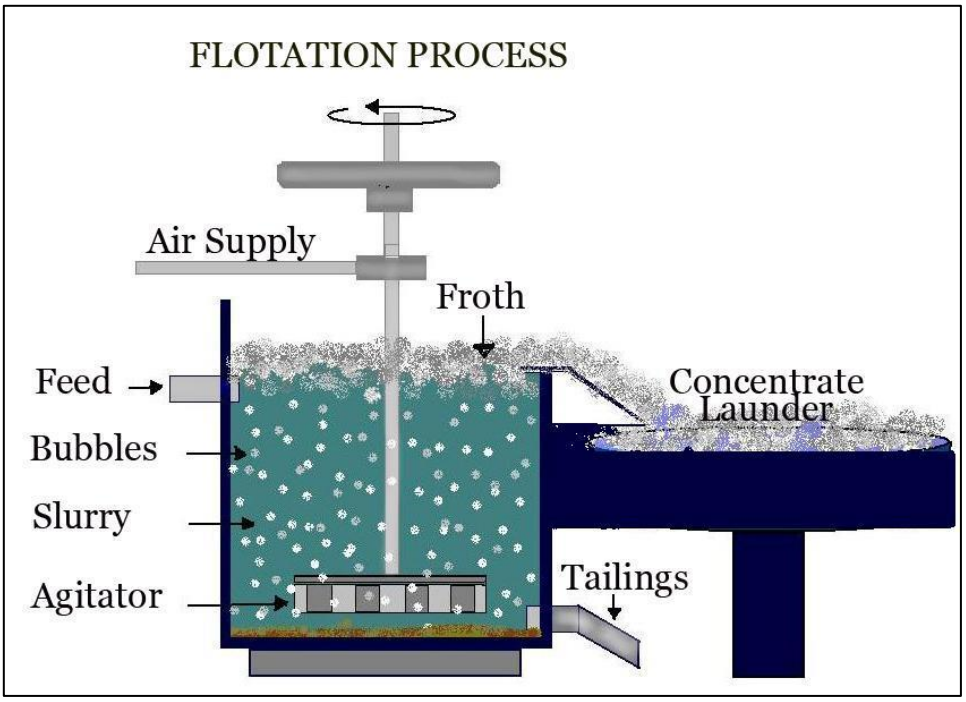

Figure 2. 18: Diagram illustrating the froth flotation process (Aldo Miners, 2012)

In this cell air is introduced through a hollow stand pipe around the agitator shaft; as the agitator rotates air is drawn from the stand pipe resulting in the formation of fine bubbles which rise through the pulp phase (Wills & Napier-Munn, 2006). The turbulence created by the agitator causes the collision of particles and bubbles, which results in the attachment of hydrophobic particles and the formation of a mineral froth at the top of the cell (Wills & Napier-Munn, 2006). Due to the fine size of the bubbles produced this flotation cell is most useful in the flotation of fine particles, as small bubbles tend to drop their load or burst if the particles weight is too large (Wills & Napier-Munn, 2006). When mechanical flotation cells are used on an industrial scale several stages in a flotation circuit are required to ensure that the final product is of an economically acceptable quality (Wills & Napier-Munn, 2006). Mechanical batch cells are not ideal for studying effects in the froth since the maximum achievable froth height is very small.

2.6.3. Column flotation cell

Flotation columns are widely used in the study of the flotation process and are gaining popularity on an industrial scale. The first industrially successful column was invented by Boutin and Tremblay in Canada during the 1960s, and these columns have been commonly implemented in industry since the 1980s (Yianatos, 1989).The flotation column can be divided into two sections; the collection zone, where solid particles come into contact with a rising bubble swarm produced by a sparger, and the froth phase, where the bubble-particle aggregates accumulate prior to being removed in the launder. In a column, air or a mixture of air and water are fed into the column through its base, and slurry through its mid points. This results in the sinking of ore particles and the rising of bubbles creating counter current action which can be enhanced by the addition of wash water from the top of the column as shown in Figure 2.19. One of the largest differences between a column and a mechanically agitated cell is that in the former the collection occurs in the majority of the cell volume,

whereas in the latter the collection zone is concentrated around the impeller. In addition, the energy imparted by a mechanically agitated cell is far greater than in a column cell.

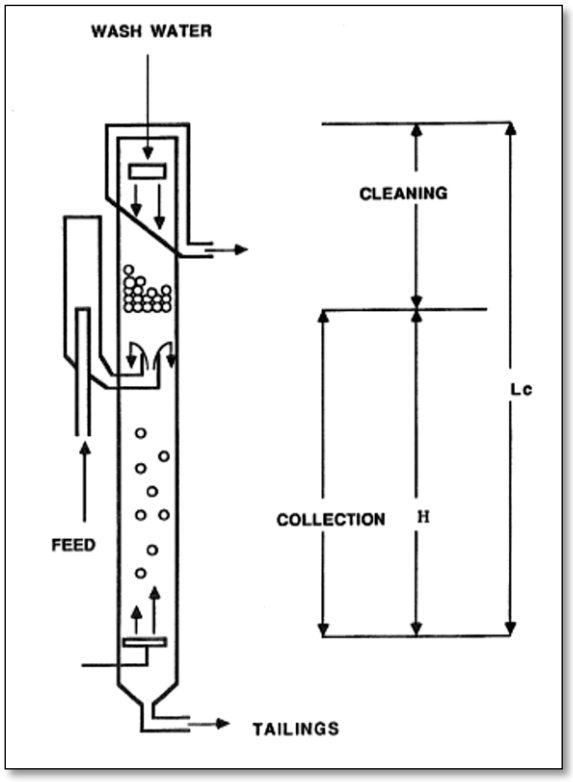

Figure 2. 19: Flotation column with collection zone (H) and height of column (Lc) (Yianatos, 1989)

Flotation columns are increasingly becoming popular industrially, especially in the flotation of coarse particles as the absence of an agitator in the system decreases the detachment of particles from bubbles (Kawatra and Eisele, 2001). Flotation columns also aide the flotation of fine particles as they produce small bubbles which have greater collision probabilities with the fine particles. Columns can be operated with deep froths which reduce the amount of entrained gangue thus improving the metallurgy of the floated minerals. .This can be further increased through the addition of wash water which reduces the amount of solids that are entrained. Flotation columns are also easier to control than batch cells and can be easily arranged in circuits that optimise productivity (Yianatos, 1989).

2.6.4. In-line aerated column

The column that will be used in the experiments is an in-line aerated column adapted from (Xu et al., 1996). The main difference between the conventional column and the in-line aerated column is that in the latter the feed and air are mixed together prior to being fed into the bottom of the column as shown in Figure 2.20.

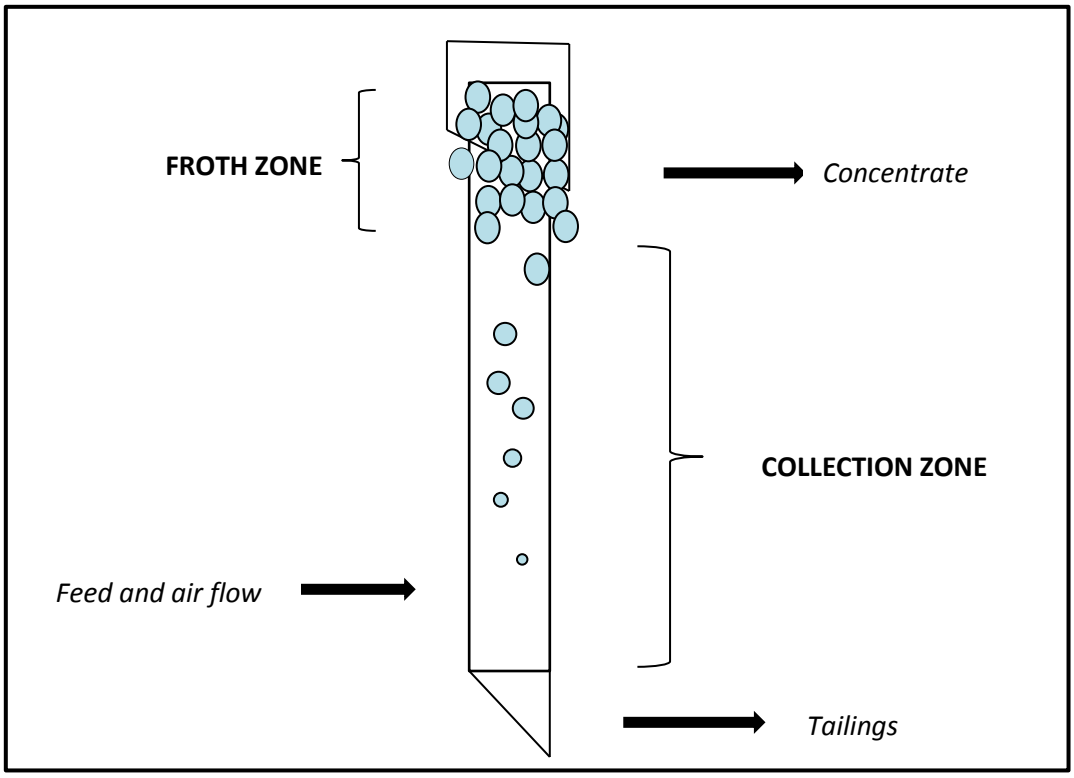

Figure 2. 20: Schematic of in-line aerated flotation column

2.8. Summary of Literature and Hypotheses

This chapter has reviewed the different literature pertaining to the concept of froth stability, beginning with the basic structure of froth and the processes that lead to the destabilisation of the froth phase. This includes how various factors such as particle properties, chemical reagents, and operational factors influence the stability of the froth. The chapter also covers the methods that have been used to measure the instability of the froth phase and the equipment that was used to conduct these tests.

From this literature review the following hypotheses were proposed to answer the key questions that were posed in Chapter One.

1. Increasing the height of the froth in a cell will decrease the stability of the froth due to an increase in the drainage of liquid and froth stabilising gangue from the froth into the pulp phase.
2. Increasing the air rate will increase the stability of the froth up to a peak air rate due to a decrease in the time available for bubble coalescence in the froth phase as well as an increase in froth stabilising gangue in the froth; after this peak air rate, the froth destabilises due to increased turbulence in the system
3. Increasing depressant dosage will decrease the stability of the froth by depressing froth stabilising gangue.

CHAPTER THREE : EXPERIMENTAL DETAILS

3.1. Introduction

As explained in the previous chapter, there are many different measures that have been used to quantify the stability of the froth phase for both overflowing and non-overflowing systems. This project aims to combine some of the methods that have been used in order to find a practical relationship that can be used to indicate the stability of the froth.

The chapter describes the experimental procedure that was used to investigate the stability of the froth phase, when subjected to variations in chemistry and operating factors. It begins with a brief description of the equipment that was used and how it was calibrated; and the chemical reagents that were used in conditioning the slurry.

This is followed by a summary of the project commissioning phase, including how the range of operating parameters was established and the method by which variability was determined. The process that was developed to conduct the experiments is then outlined; including the measurements that were taken and how the data obtained was analysed.

The chapter concludes with a description of the different methods proposed for analysing the stability of the froth and some of the preliminary results obtained.

3.2. Equipment and material

3.2.1. Milling equipment

The ore that was used in the experiment was delivered in 5 kg bags with particle size less than 3 mm. This had to be milled to reduce the size of the particles to 60% passing 75 μm. The mill that was used to achieve this was a 3 kg SALA stainless steel rod mill which is shown in Figure 3. 1.

The mill has an internal diameter and length of 30 cm and was operated with 22 stainless steel rods. Each rod was 25 mm in diameter and 28.5 cm in length. The mill was operated at a speed of 77.1 rpm

Figure 3. 1: 3kg rod mill used in ore preparation

Milling curve

A milling curve was developed to determine the amount of grinding time necessary to reduce the ore sample to a particle size distribution of 60% passing 75 µm. The curve was created by wet milling 2.5 kg of ore in the rod mill with 1.5L of water, for various times.

The milled slurry was then wet screened using a 75 µm sieve, and after filtering and drying Figure 3. 2 was plotted using the mass of solids found in the filtrate. A mass balance of the solids in the filtrate and solids left on the sieve was used as validation. From the milling curve it was determined that the time required to produce the required PSD i.e. 60% passing 75 µm was 21 minutes. This process was repeated and similar milling curve was obtained.

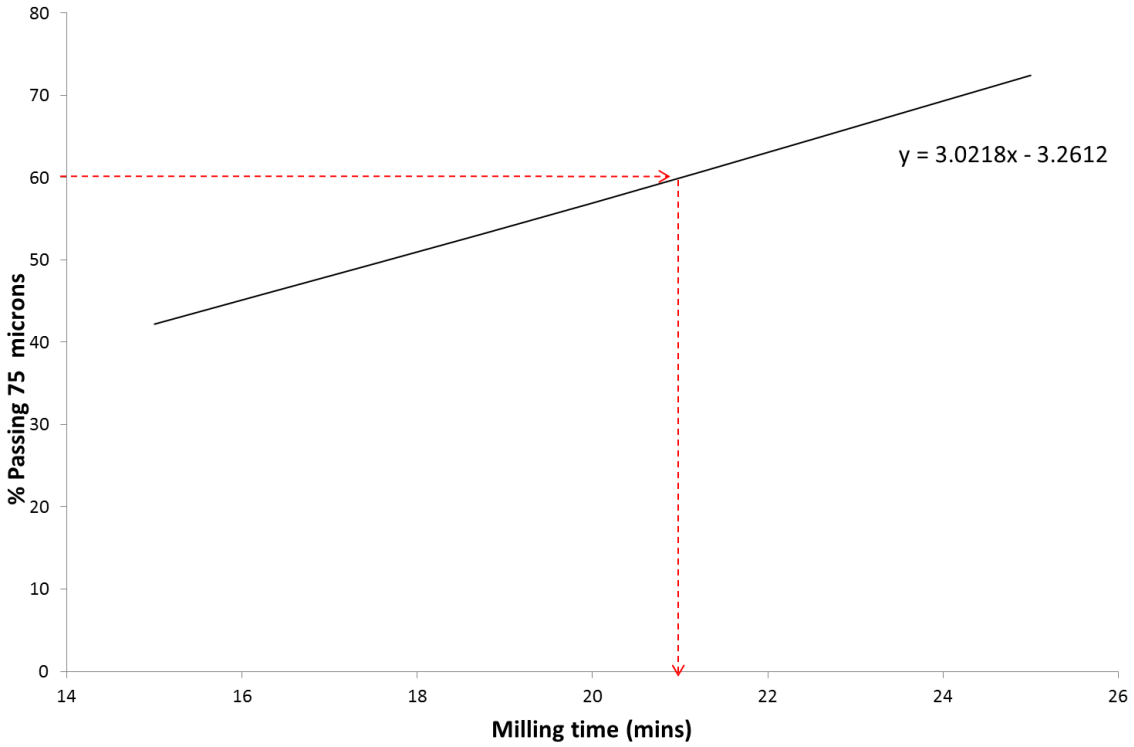

Figure 3. 2: Waterval ore milling curve using 3 kg rod mill

3.2.2. Flotation equipment

The flotation experiments conducted in this study were carried out in an in-line aerated column which is a modification of the conventional column. This column and the experimental set up used (shown in Figure 3. 3) were based on a design suggested by Xu et al. (1996).

The column was constructed from Plexiglass, and has an internal diameter of 4.6 cm and a cross sectional area of 16.62 cm^2. The column was initially 200 cm in length, but was later adjusted to a length of 196 cm to enable the determination of bubble coalescence when operating the column using shallow froths. The air and slurry feed point was situated about 30 cm from the bottom of the column and the recycle line was situated at the same level. The concentrates obtained were collected in the launder at the top of the column, and the tailings were pumped out through the bottom. Three peristaltic pumps were used to transport the feed, recycle and tails flows.

A pressure transducer located 80 cm from the bottom of the column was used to measure the pressure difference caused by the pulp level in the column. The pressure detected was then transmitted to a Proportional Integral Derivative controller (PID) that was used to control the level in the column by altering the speed of the variable speed pump that regulated the tailings flow.

.

Figure 3. 3: In-line aerated column used in experiments

The in-line aerated column differs from a conventional column in how the slurry and air are fed into the systems. In a conventional column the feed enters midway from the bottom of the column, whilst the air enters from the bottom creating counter-current flow patterns. In an in-line aerated column the feed and air are combined prior to being fed through a sparger located at the bottom of the column as shown Figure 3.4. A recycle stream also leaves the column below the feed inlet and combines with the feed and air prior to being fed back into the column. The tail stream then exits through the bottom of the column after which it can be collected.

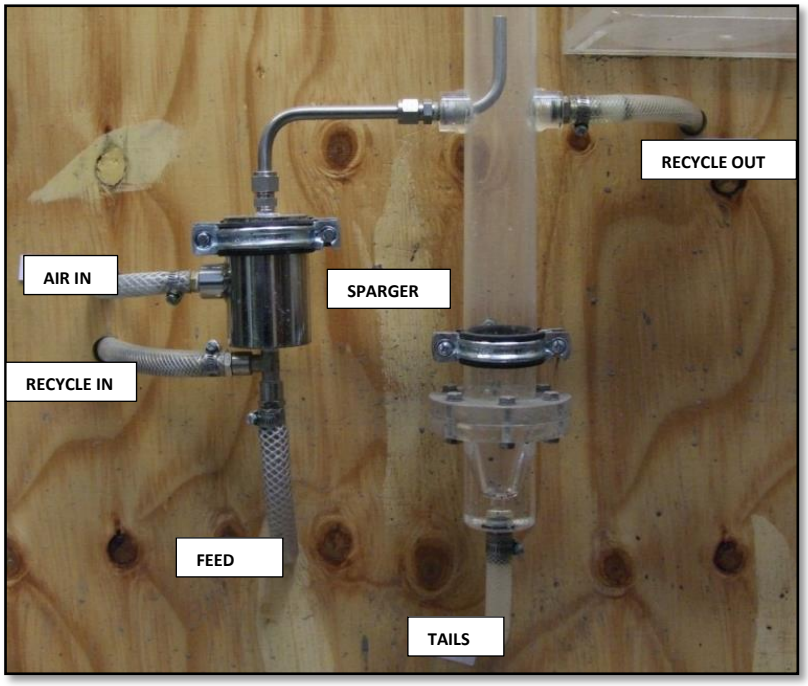

Figure 3. 4: Bottom part of column showing the sparger and inlet and outlet streams

Pump calibrations

The pumps used in this study were Watson Marlow peristaltic pumps and they were connected to the feed, tailings and recycle lines. The pumps were calibrated using water, by varying the pump frequency and noting the amount of water delivered. The resulting curves are shown in Figures 3.5 and 3.6.The feed and tailing pump that were used yielded the same pump calibration curves.

From these figures the frequency could then be adjusted so that the pumps would deliver the required flowrate.

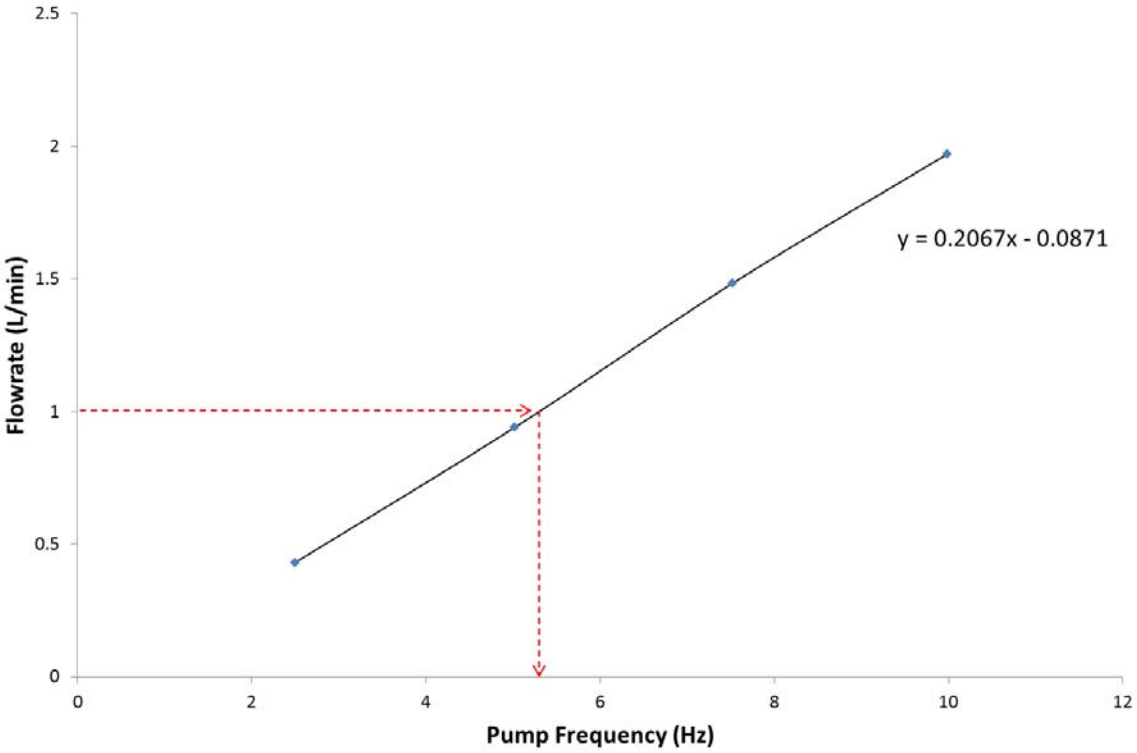

Figure 3. 5: Calibration of feed and tails pump

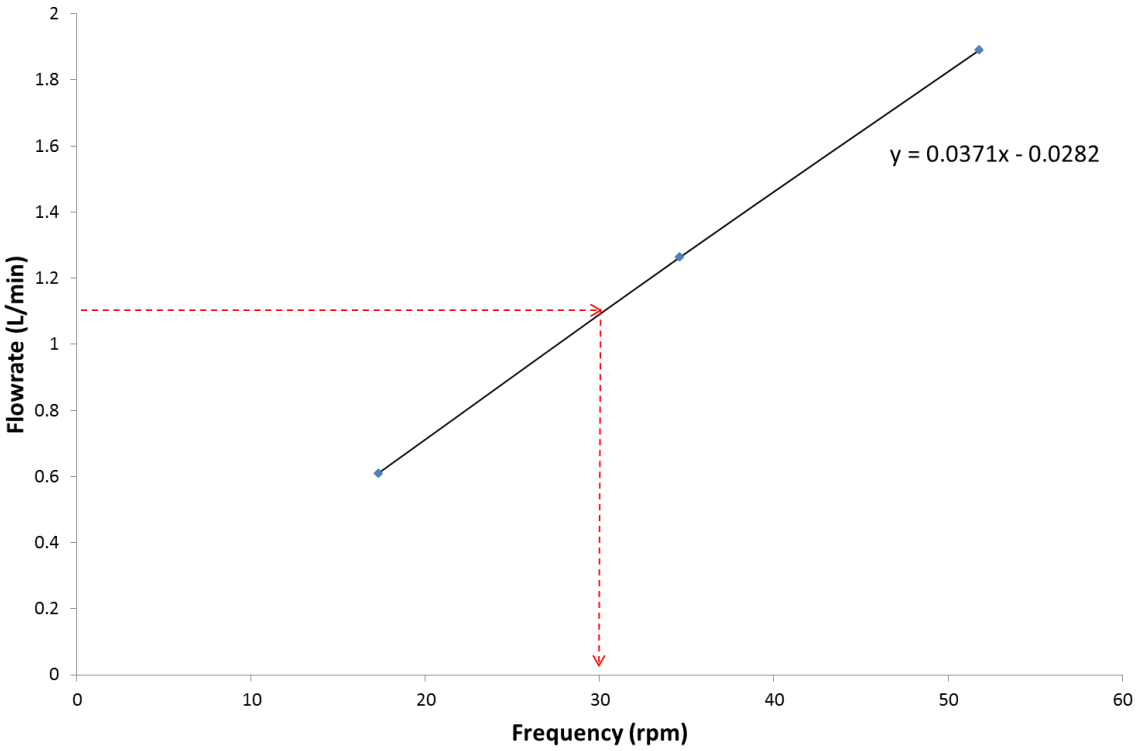

Figure 3. 6: Calibration of recycle pump

3.2.3. Image capturing equipment

Part of the experimental program included the measurement of bubble burst rate and rate of bubble coalescence in the froth. The top of froth bubble dynamic images were recorded using video footage from a Sony MiniDV digital Handycam. The rate of coalescence was measured from a bubble coalescence profile which was obtained from photographs take on a Fujifilm Finepix F60 FD camera with 12 megapixels adjusted to macro settings. Post-processing of these images is discussed in Section 3.3.4.

3.2.4. Chemical reagents

The three flotation reagents used in this study were collector, depressant and frother.

Collector

The collector used in all the column flotation experiments was sodium isobutyl xanthate (SIBX) which was maintained constant at 80 g/t during the experiments and therefore changes in hydrophobicity were not expected to affect the froth stability. The collector was supplied by Senmin in powdered form at a purity of close to 90%. Before use it was made up to achieve a 1% solution using synthetic plant water.

Depressant

Sendep 348, a modified guar gum supplied by Senmin in powdered form, was used as a gangue depressant in this test work. Average characteristics of Sendep 348 are shown in Table 3.1.

Table 3. 1: Characteristics of Sendep 348

	Molecular Mass (g/mol)	Purity (%)	Insolubles (%)
Sendep 348	239 000	92	7.02

The depressant was made up as a 1% solution by hydrating the powdered depressant in synthetic plant water for 2 hours using a magnetic stirrer.

Frother

The frother used in all the column flotation experiments was the polyglycol type frother, DOW 200. This was supplied by Betachem in liquid form at close to 100% purity and was dosed as is at 25.2 ppm, which is above the critical coalescence concentration of this frother (Grau et al., 2005).

3.2.5. Synthetic plant water used in test work

All column flotation experiments were conducted using synthetic plant water, which was prepared using a recipe based on the analysis of ions present in a Merensky concentrator located on the Western Limb. This recipe involves the modification of distilled water through the addition of various chemical salts to achieve specific total dissolved solids content (Wiese et al., 2005). The ionic concentration of the synthetic plant water is based on the typical values found on concentrators processing PGM bearing ores. The water was prepared in 40 L batches for use in the column flotation tests. The ionic concentrations of the synthetic plant water are shown in Table 3.2.

Table 3. 2: Ions present in synthetic plant water [Adapted from (Wiese et al., 2005)]

Ion	Concentration (ppm)
Ca^{2+}	80
Mg^{2+}	70
Na^{+}	153
Cl^{-}	287
SO_4^{2-}	240
NO_3^{-}	176
NO_2^{-}	-
CO_3^{2-}	17

3.2.6 Ore Mineralogy

The ore used in this study was UG2 ore from Waterval mine in the Bushveld complex of South Africa .The UG2 chromitite ore body contains one of the largest known reserves of Platinum Group Elements (PGE) in the world (Cawthorn, 1999). However the concentration of PGE's in the body is low, 4-7 g/tonne, and consists of 60-90% chromite by volume (Schouwstra and Kinloch, 2000). There are six platinum group metals, platinum, palladium, rhodium, ruthenium, iridium and osmium and the main gangue minerals are pyroxene (15-20%), feldspar (3-5%) and talc (1-3%) (Hay and Roy, 2010).

Depending on the type and degree of the post magnetic charge of the ore, platinum group assemblages could be predominantly sulphide minerals, with some non-sulphide minerals, the most common PGE sulphides being laurite, cooperite, malarite, braggite and vystokite (Penberthy et al., 2000). The presence of platinum group minerals can be associated with the presence of base metal sulphide minerals or gangue minerals like chromite and silicate as shown in Figure 2.21 (Penberthy et al., 2000).

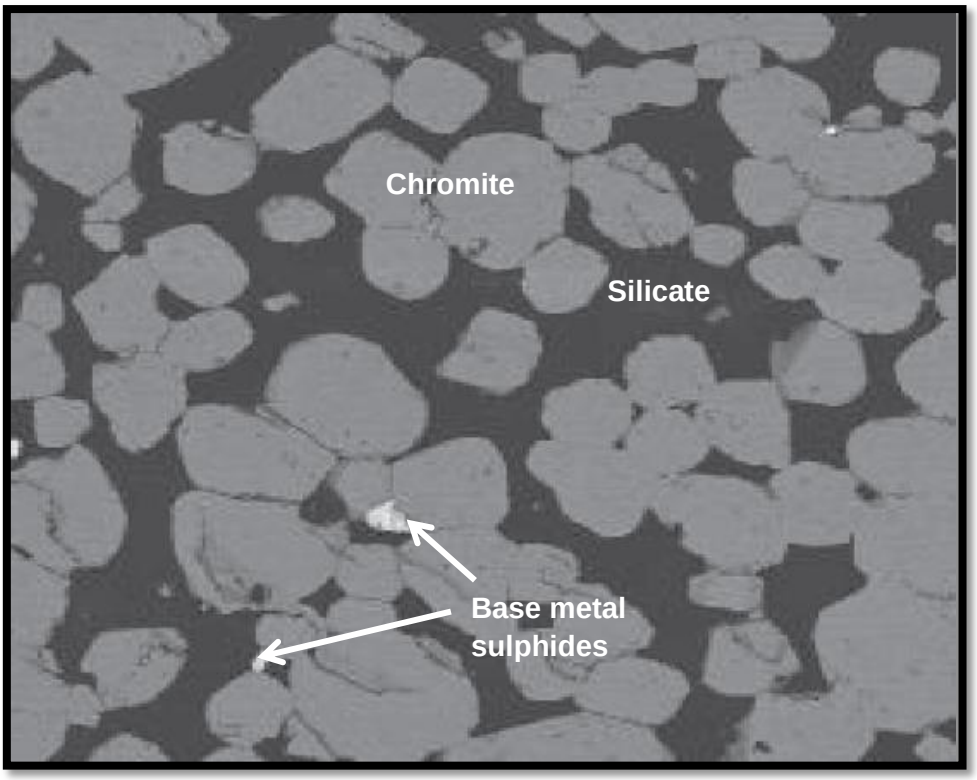

Figure 2. 21: General view of UG2 ore [Adapted from (Hay and Roy, 2010)]

Talc is a naturally hydrophobic gangue, so during flotation it can attach on to bubble surfaces and be recovered in the concentrate. The presence of talc in the concentrate reduces the PGM grades and has detrimental effects on the functioning of the smelters due to the resulting high magnesium oxide content (Pugh, 1988a). Talc also changes the stability of the froth. A large amount of talc results in the formation of more rigid froth which takes time to disintegrate. It is therefore essential to depress talc along with other silicate gangue minerals to improve flotation efficiency (Nashwa, 2007).

Chromite, a rock containing $FeO.Cr_2O_3$ as its major constituent, is the largest gangue mineral constituent in UG2 ore and, if it is not efficiently removed during flotation, it has detrimental effects on the efficiency of the furnace (Hay and Roy, 2010). As a naturally hydrophilic oxide mineral, chromite has a low floatability and mainly passes into the concentrate through entrainment in the water that is carried from the pulp into the froth (Hay and Roy, 2010). In some cases talc rimming of the chromite grains occurs which renders the chromite minerals more floatable than usual. In this case, the chromite could be prevented from floating by adding a suitable depressant, without affecting PGM recovery (Hay and Roy, 2010). Ekmekci et al. (2001) found that changes in depressant dosage from 0-100g/t and frother from 15-40g/t changed the recovery and grade of chromite in the concentrate. This was also observed by Valenta (2007) who noted that increasing both depressant and frother dosage increased the grade of chromite due to a reduction of silicate mass. A study conducted by Ekmekci et al. (2003) showed that the chromite grade could be decreased by increasing the froth height which increased drainage of entrained gangue particles and coarse particles with low hydrophobicity (Hay and Roy, 2010).

3.3. Operating procedure

3.3.1. Scoping experiments

In order to establish the operating range for the experimental conditions varied in the study, scoping tests were performed. The tests determined the maximum froth height and minimum air rate at which the column could be operated such that froth could be recovered. Scoping tests also included the maximum solids concentration that could be used in the column.

The results of the scoping tests showed that the highest air flow rate at which the column could operate efficiently was 1.85 cm/s. At flow rates higher than 1.85 cm/s the pulp froth interface was not visible due to equal gas hold up in both the pulp and froth phases. At higher gas rates more bubbles are generated in the pulp phase and these subsequently carry more water into the froth resulting in a decrease in gas hold up in the froth and a subsequent increase in the collection zone (Tao et al., 2000). The minimum flow rate was determined as the lowest flow rate that could be used to obtain solids and water recoveries when operating at the maximum froth height. This was an air flow rate of 1.35 cm/s at a froth height of 20 cm.

Initially the experiments were conducted using slurry of 11% solids concentration, which is significantly lower than the 30% solids concentration which is the minimum threshold that is used in industry (Yianatos, 1989). The solids concentration was then increased to give a better depiction of reality. At solids concentrations higher than 30%, the pulp froth interface was difficult to distinguish due to the large amount of solids in the froth zone. Since the high air rates also had an effect on the visibility of the pulp froth interface, the density tests were conducted at 1.85 cm/s. At this air rate the solids concentration was gradually decreased until a pulp froth interface could be identified. This was obtained at solid concentration of 29.5 % which is close to the minimum industrial concentration.

3.3.2. Flotation and sample collection

Prior to flotation the ore was ground in the rod mill in 2.5 kg batches to make up 12.5 kg of ore. The ore was wet milled with 1.5 L of synthetic plant water to achieve a grind of 60 % passing 75 µm. After grinding, all 12.5 kg of ore was combined with synthetic plant water to produce slurry that was 30% solids by mass. This was agitated in a feed tank for 15 minutes to ensure complete particle suspension after which it was conditioned with collector, depressant and frother sequentially at 1 minute intervals according to the dosages shown in Table 3.3.

Table 3. 3: Reagent dosages

Reagent	Dosage
Frother (ppm)	25.2
Depressant (g/t)	0,100,300
Collector (g/t)	80

The slurry was then agitated for a further 30 minutes before being co-fed with air into the column at a feed rate of 1 L/min which resulted in a column residence time of 3.25 minutes. The different air flow rates investigated are shown in Table 3.4. The recycle rate was set at 1.1 L/min to aide bubble generation which resulted in increased mixing.

Table 3. 4: Experimental conditions

Conditions	
Air flow rate (cm/s)	1.35 , 1.60, 1.85
Depressant dosage (g/t)	0, 100, 300
Froth height (cm)	10, 15, 20

A schematic of the experimental procedure followed is shown in Figure 3. 7.

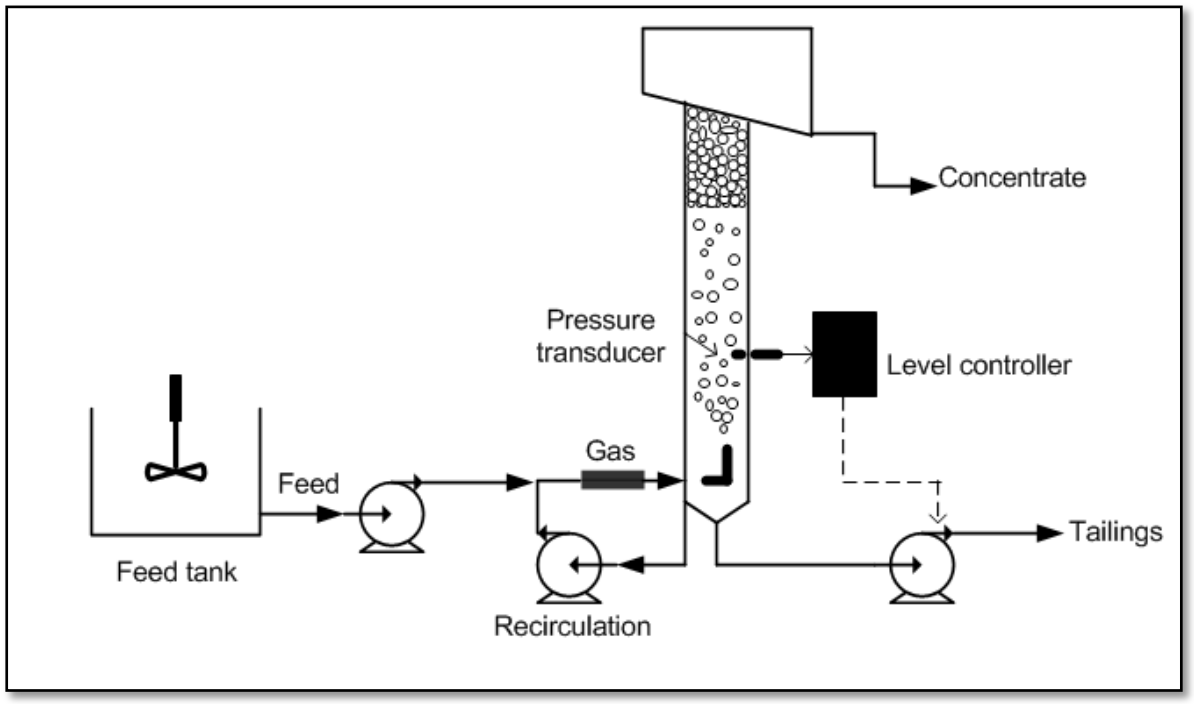

Figure 3. 7: Schematic of the experimental procedure (Alvarez-Silva et al., 2012)

A PID controller was used to maintain the pulp froth interface at different levels (froth heights) as shown in Figure 3.7.

To ensure that the system was operating at steady state, the pulp froth interface was maintained at the set level for a period of 2.5 residence times prior to sample collection. After establishing steady state, photographs of bubbles in the froth zone were taken from the side of the column, concentrate and tailings samples were then collected simultaneously for 1 minute at 30 second intervals, whilst concurrently capturing video footage of the bubble burst rate from the top of the column. After collection the gas hold up in the column was measured by switching off the air supply and measuring the change in pulp-froth interface level.

The samples collected were weighed before and after drying to determine water and solids recovery. The dried feed, concentrate and tailings samples were sent to an independent laboratory for PGM and chromite assays. Platinum and palladium assays were conducted by performing a fire assay followed by dissolution of the silver prill and analysis for the desired elements using ICP-OES. The chromite content was determined using ICP-OES after fusion of the ore sample and dissolution in hydrochloric acid or nitric acid. Particle size analysis of all samples was also conducted using a Malvern Mastersizer.

3.3.3. Reproducibility analysis

Due to the large amount of ore required for each experiment, it was not feasible to conduct the experiments in duplicate. It was therefore essential to establish the repeatability of experiments carried out under the same conditions, based on the solids and water recoveries.

This was accomplished by selecting a set of conditions and conducting the experiments in triplicate. The conditions that were chosen were a froth height of 15 cm, an air flowrate of 1.5 cm/s and a depressant dosage of 100 g/t. The solids and water recoveries obtained from these tests are shown in Figure 3. 8 and the corresponding error analysis is shown in Table 3.5.

Each repeat consists of the masses of dry solids and water of the concentrates that were collected during each experiment. For each repeat, the average solids and water recovered was calculated, and these averages were then analysed to determine the repeatability of the experiments.

From the three repeats, it was determined that there is 2.5 % error for solids recoveries between experiments, and 6.4 % error for the water recovery. Due to the small margins or differences the experiments were deemed to be reproducible.

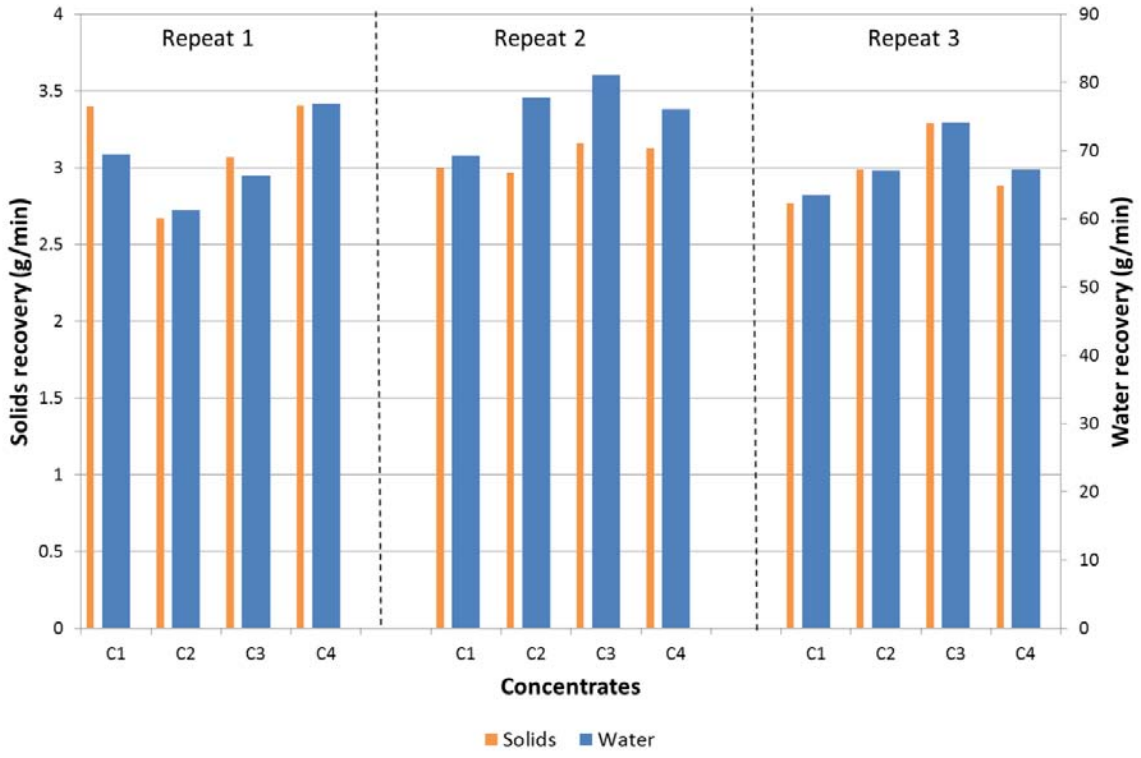

Figure 3. 8: Solids and water recoveries from tests conducted to determine experimental reproducibility

Table 3. 5: Error analysis for tests conducted to determine experimental reproducibility

	Solids	Water
Average (g/min)	3.06	70.8
Absolute Error(g/min)	0.08	4.52
Relative error (%)	2.53	6.38

3.3.4. Measurement of burst rate and coalescence profile

The top of froth bubble burst rate and side of froth coalescence rate was measured using video analysis software called Tracker.

Burst rate

For the top of the froth measurements, 100 frames were selected from the beginning of the video footage, the frame rate was then slowed down to 0.5 frames/s. At this reduced speed, the number of bubbles that burst over the entire period could be counted and the bubble burst rate was calculated using equation 3.1.

$$Burst\ rate = bubbles\ bursting\ in\ 100\ frames \times video\ speed \qquad 3.1$$

This was repeated using 100 frames from the middle and end of the video footage. An average burst rate for the video was then calculated using the three burst rates.

A still image of the top of the froth is shown in Figure 3. 9.

Figure 3. 9: Still image of top of froth during flotation test

Coalescence

The bubble coalescence profile was obtained by zooming into different regions of the froth through the side of the column as shown in Figure 3. 10. The size of the bubbles in different regions of froth was then measured using Tracker's built-in tools.

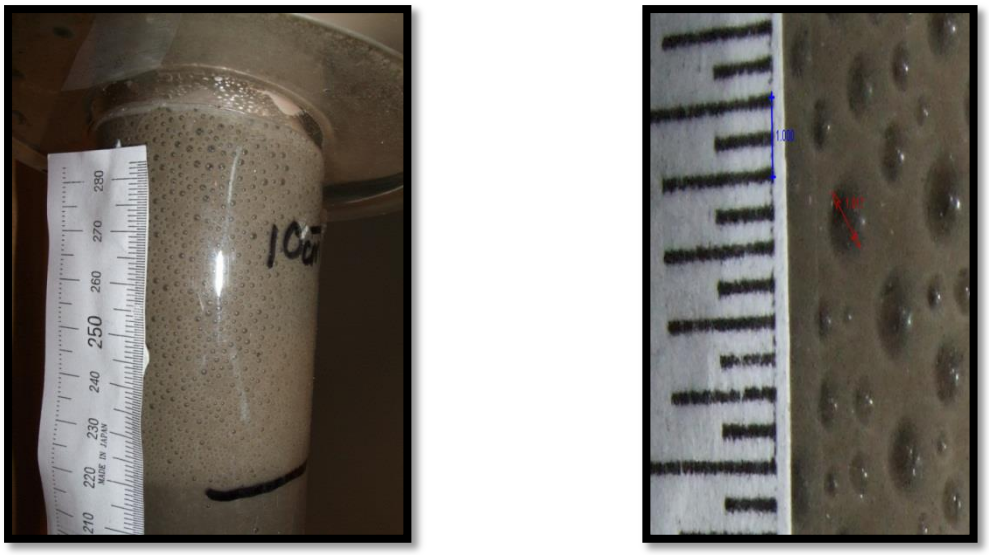

Figure 3. 10: Side of froth before and after zooming in

In order to get an accurate measurement of the size of bubbles in the froth, Tracker's measuring tools were calibrated using a ruler mounted on the side of the column. The size of bubbles was then measured starting from the pulp froth interface and continuing upwards at 1 cm intervals. Bubbles were only measured from the mounted ruler to the middle of the column in attempt to reduce convex/wall effects. At each level the average bubble size was determined using the Sauter mean diameter given by equation 3.2.

$$Sauter\ mean\ diameter = \frac{\sum d_i^3}{\sum d_i^2} \qquad 3.2$$

The bubble size within the pulp phase was also incorporated in the coalescence profile and this was calculated using a method proposed by Zhou et al. (1993), where the bubble radius (R_v) can be calculated using equation 3.3.

$$R_v = \frac{B_c^{0.5}}{0.84 - C_c B_c} \qquad 3.3$$

C_c is the contamination factor and B_c is a coefficient given by equation 3.4.

$$B_c = \frac{\frac{J_g(1-\varepsilon_g)}{\varepsilon_g + J_l}}{A(1-1.06\varepsilon_g)} \qquad 3.4$$

Where ε_g is the gas hold up; J_g and J_l are superficial gas and liquid velocities respectively and A is a constant given by equation 3.5.

$$A = \frac{g(\rho_L - \rho_G)}{9\mu} \qquad 3.5$$

Where g is the gravitational acceleration, μ is the bulk liquid viscosity and ρ_L and ρ_G are the liquid and gas densities.

The coalescence profile was obtained by plotting the size of the bubbles against the height in the froth from the bottom of the column as shown in Figure 3. 11.

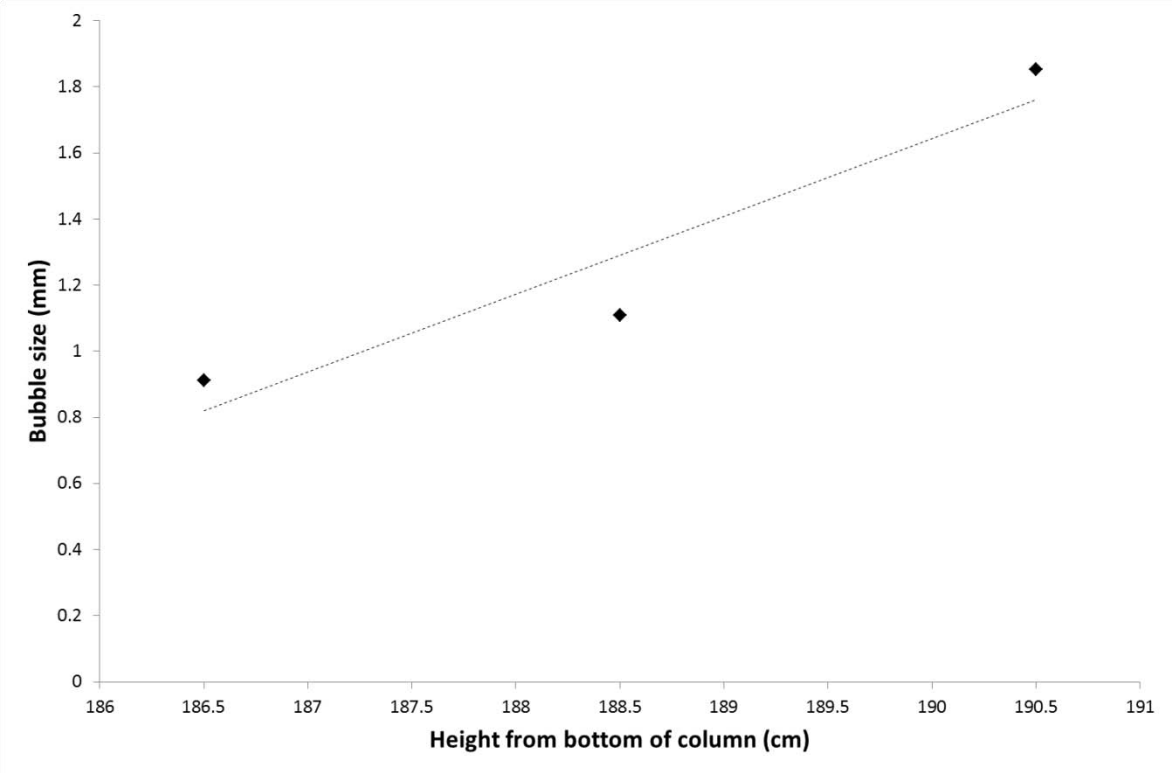

Figure 3. 11: Rate of bubble coalescence in the froth phase

The gradient of the curve could then be used to indicate froth stability which is given by equation 3.6.

$$Rate\ of\ coalescence = \frac{Change\ in\ bubble\ size}{Change\ in\ height} \qquad 3.6$$

The first investigation was conducted at froth heights of 10, 15 and 20 cm, using a superficial air rate of 1.35 cm/s in the absence of depressant. The coalescence profiles obtained are shown in Figure 3.12, and these include the pulp bubble size which was calculated 150 cm from the bottom of the column. The linear trend lines did not fit the data very well, which is shown by each trend line's relatively low R^2 value. As a result there was little confidence that the gradients of the trend lines could be used to represent the coalescence rate. The low accuracy of fit was thought to be due the pulp bubble size which had been calculated using an indirect method which had been proposed in a two phase system. It was considered that the method was giving poor results for a three-phase system. The data set was then plotted again without the pulp bubble size as shown in Figure 3. 13.

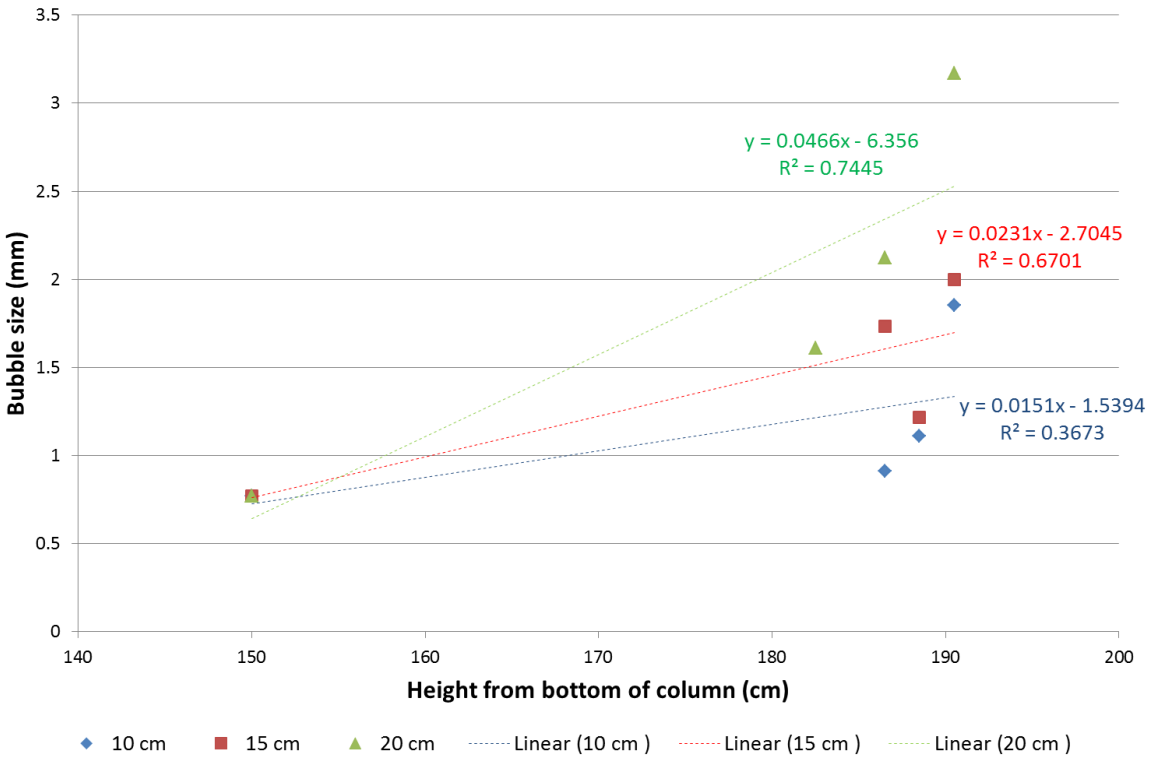

Figure 3. 12: Bubble size in different regions of the froth phase including pulp bubble size

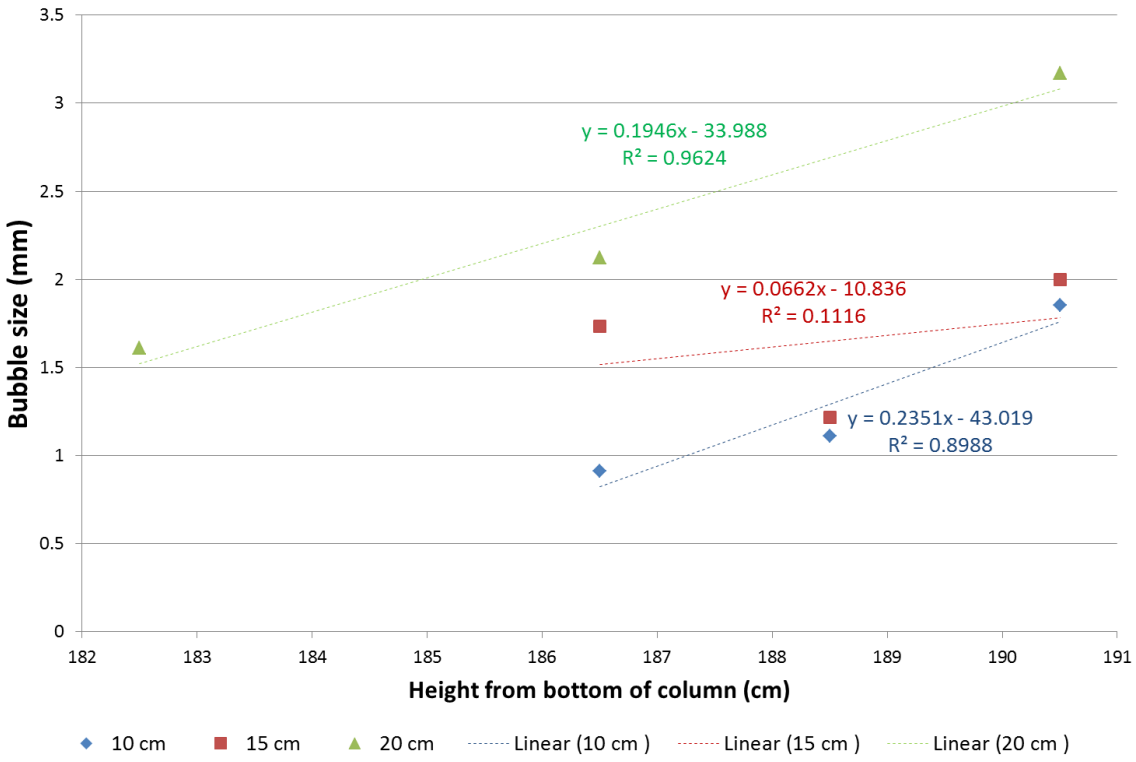

Figure 3. 13: Bubble size in different regions of the different froth phase

The trend lines drawn at froth heights of 10 and 20 cm resulted in a better fit without the pulp bubble size, whilst the trend line at 15 cm resulted in a much lower R^2 value.

Coalescence profile data is presented in the following sections of this chapter. The data is confined to the Experimental chapter since it was ultimately disregarded in the analysis of the results. However, for the sake of completeness and to assist in future work in this area, a discussion of this data is included.

3.4 Froth stability analysis

Bubble burst rate, rate of coalescence and water recoveries as measures of froth stability are discussed in the following section. Several of the methods were subsequently discarded in an analysis of the results and this section provides the motivation for which froth stability analysis tools proved to be fit for purpose.

Method 1: Using rate of coalescence as a measure of froth stability

One of the factors proposed as an indicator of froth stability was the rate of bubble coalescence within the froth. The procedure that was followed in determining this rate has been described in section 3.3.4.

This method was applied at all the experimental conditions that were investigated, and the following is an analysis of whether this method can be applied in this system.

Preliminary results

The first investigation tested the effect of changing air rate and froth height on rate of coalescence when no depressant was used, shown in Figure 3. 14. It was expected that as the froth height was increased the froth would become less stable thus increasing the coalescence rates. As air rate was increased the coalescence rate would decrease due to the shorter froth residence time.

At the three air rates investigated there was a decrease in coalescence rate between 10 and15 cm followed by a subsequent increase between 15 and 20 cm. This trend was most pronounced at a Jg of 1.85 cm/s where there was no change in coalescence at a froth height of 15 cm. The results obtained when increasing air rate seemed to have a bit more scatter in them. At a froth height of 10 cm the coalescence rate was constant between 1.35 and 1.60 cm/s, after which there was a decrease. A 15 cm froth height showed a decrease in coalescence rate as air rate increase. At 20 cm there was a decrease in coalescence rate between 1.35 and 1.60 cm/s followed by an increase thereafter.

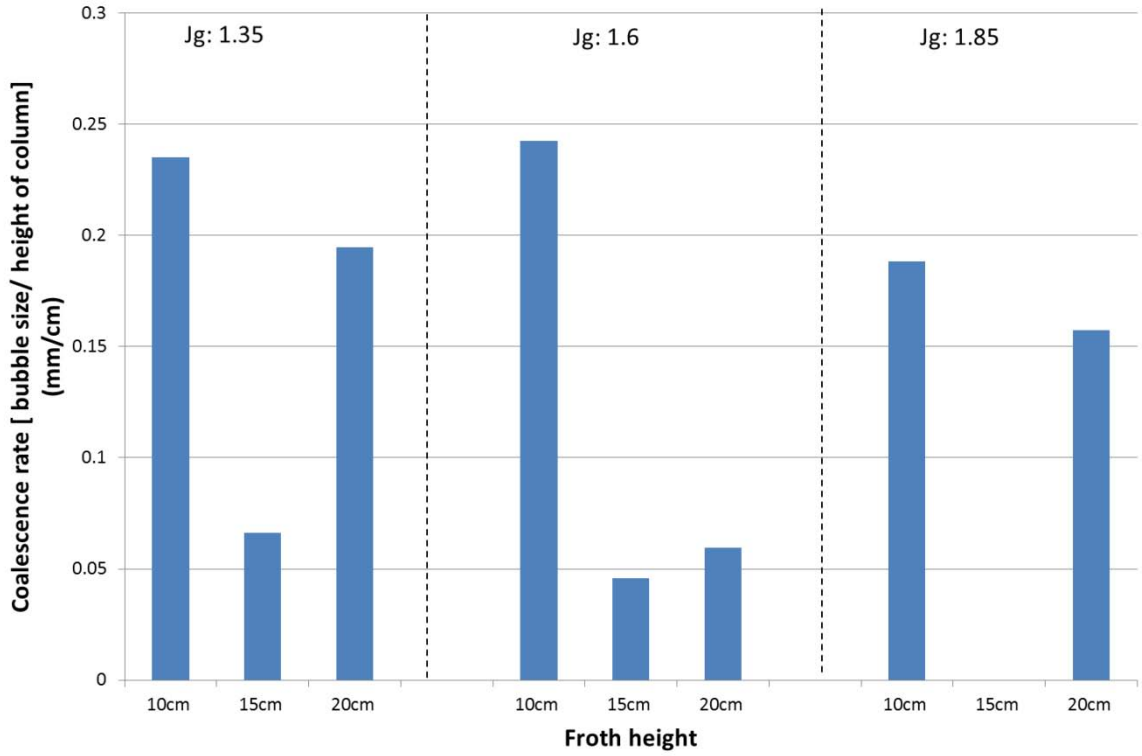

Figure 3. 14: Bubble coalescence rate for tests conducted at froth heights of 10, 15 and 20 cm and Jg of 1.35, 1.60 and 1.85 in the absence of depressant.

The experiments were repeated using a depressant dosage of 100 g/t and the results obtained are shown in Figure 3. 15. At a constant air rate of 1.35 and 1.60 cm/s there was a decrease in coalescence rate between 10 and 15 cm followed by an increase. However at an air rate of 1.85 cm/s there was a decrease in coalescence as the froth height was increased. When testing the effect of increasing air rate, different trends were observed for the different froth heights. At a froth height of 10 cm, there was an increase in coalescence rate between 1.35 and 1.60 cm/s followed by a subsequent decrease. At 15 cm there was an increase in coalescence rate as the air rate was increased; and at 20 cm froth height the rate was constant between 1.35 and 1.60 cm/s followed by a decrease thereafter.

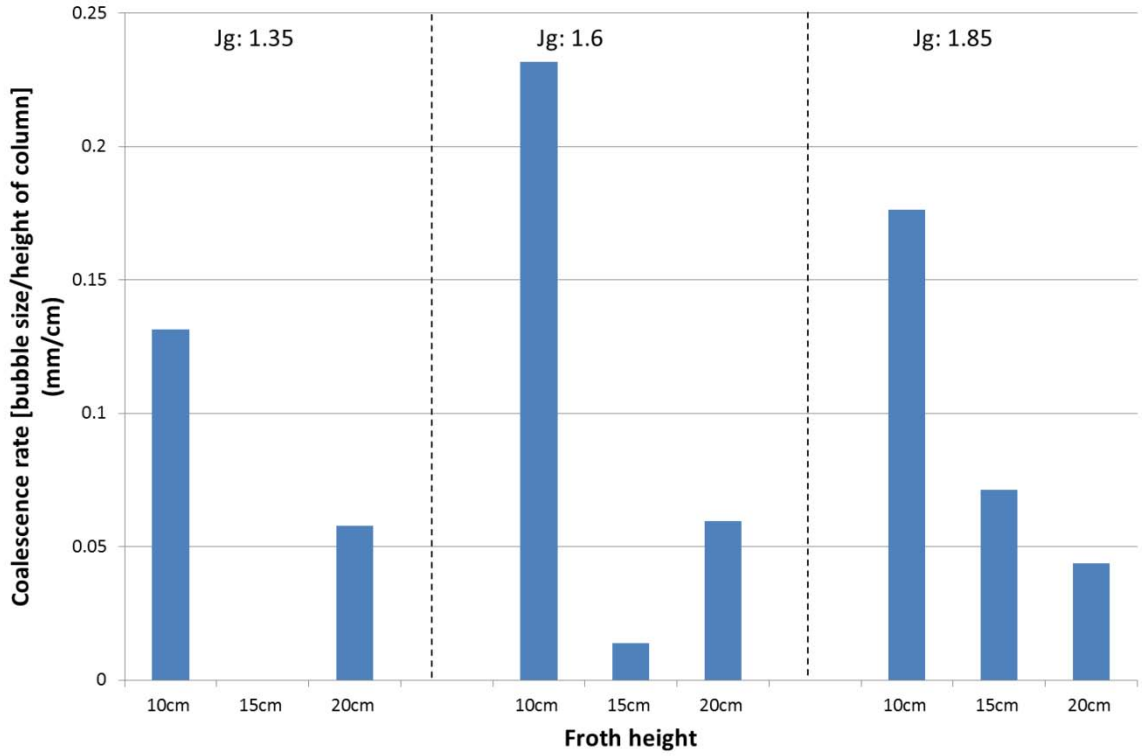

Figure 3. 15: Bubble coalescence rate for tests conducted at froth heights of 10, 15 and 20 cm and Jg of 1.35, 1.60 and 1.85 with 100 g/t depressant.

The last set of experiments was conducted at a depressant dosage of 300 g/t and the results are shown in Figure 3. 16. At this depressant dosage there was more variation in the trends when testing the effect of changing froth height. At a constant air rate of 1.35 cm/s there was a decrease in air rate between 10 and 15 cm, after which the coalescence rate increased. At 1.60 cm/s there was an increase in rates between 10 and 15 cm followed by a subsequent decrease. Whilst at 1.85 cm/s there was a decrease in coalescence as the froth height was increased. When testing the effect of changing air rate, it was observed that at 10 cm froth height the coalescence rate decreased between 1.35 and 1.60 cm/s after which it increased. At 15 cm the rate increased between 1.35 and 1.60 cm/s after which it decreased. And at 20 cm the coalescence rate decreased continuously.

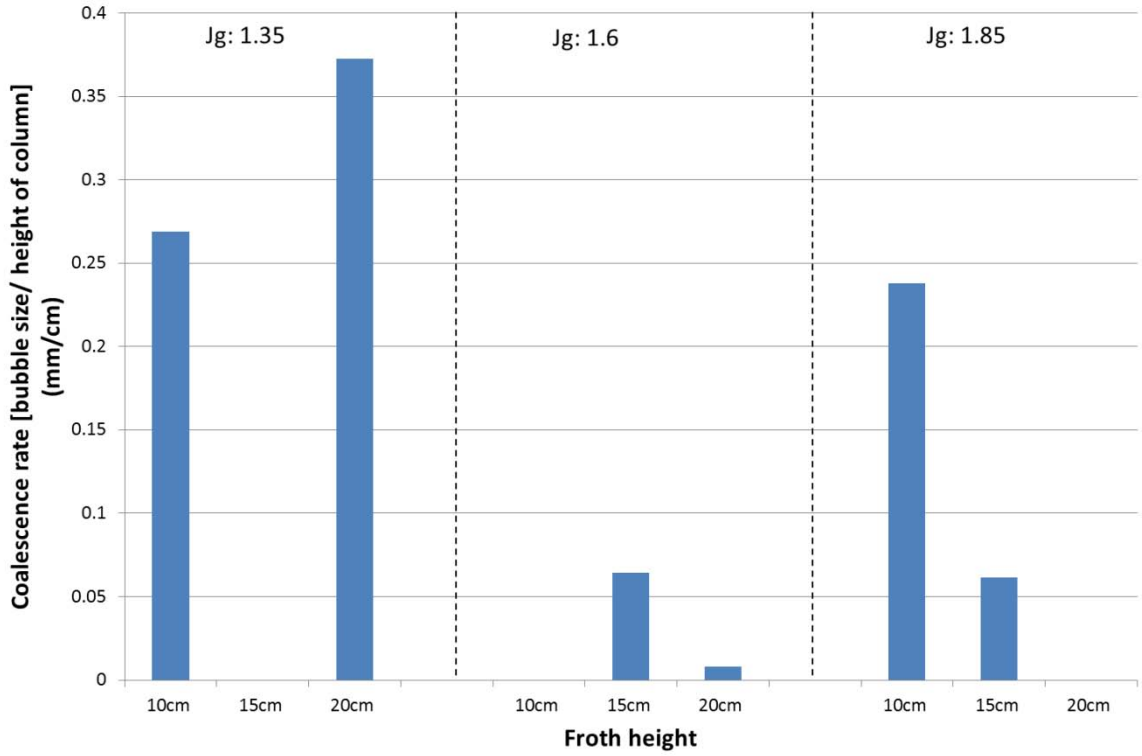

Figure 3. 16: Bubble coalescence rate for tests conducted at froth heights of 10, 15 and 20 cm and Jg of 1.35, 1.60 and 1.85 with 300 g/t depressant.

Due to the lack of consistency in trends observed between changing air rates and changing froth heights, and for the reasons discussed earlier in this chapter, the coalescence data could not be used accurately in this system to indicate froth stability. In addition, there was a lack of consistency with regard to coalescence rates compared to the other froth stability measures of bubble burst rate and water recovery.

The inconsistency in trends could be attributed to the poor fit that was obtained when linear trend lines were applied on the bubble size data .The inconsistency might also be due to distortions in measurement caused by the convex nature of the column. Also the size of bubbles near to the column wall might be different to those at the centre of the column, so the bubbles measured would give a poor indication of the coalescence rate.

As a result of this analysis, coalescence could not be used as an indicator of froth stability, and bubble burst rate and water recovery were the only indicators used.

Method 2: Using the stability factor

The second method that was proposed to quantify froth stability was to calculate a stability factor from the burst rate and froth height. This method was applied in a study conducted by Harris and McFadzean (2013)[1] at a platinum concentrator in South Africa.

The stability of the froth was calculated using an adaptation of the stability factor defined by Bikerman (1973) shown in equation 3.7.

[1] McFadzean,B J.& Harris,M.C., 2013, Froth stability measurements on a platinum concentrator rougher bank (Personal Communication), Cape Town: Unpublished Research Report

$$\alpha = \frac{H}{J_L} \qquad 3.7$$

Where α is the froth stability in seconds, H is the froth height i.e. the distance from the interface to the froth surface (m) and J_L is the superficial gas rate of air leaving the surface (m/s)

J_L could be calculated from the bubble burst rate obtained from equation 3.8.

$$J_L = \frac{Burst\ rate\ \times Volume\ of\ 1\ bubble}{Cross\ sectional\ area\ of\ column} \qquad 3.8$$

The volume of a bubble was obtained by extrapolating the coalescence profiles to the surface of the froth.

Preliminary results

This method was first applied when the effects of changing froth height and air rate were investigated with no depressant in the system as shown in Figure 3. 17. The first observation made from this analysis was the magnitude of the stability numbers. The numbers calculated were larger than expected ranging from 2000 to 25000 seconds, which implies that the froth was stable for at least 30 minutes before breaking down. This was contrary to the observations that were made whilst conducting the experiments which showed that the froth barely lasted a minute before deteriorating.

When the effect of changing froth height was tested, similar trends were noted at superficial air rates of 1.35 and 1.60 cm/s; a decrease in stability number between 10 and 15 cm, followed by an increase thereafter. At a superficial air rate of 1.85 cm/s, the opposite effect was noted i.e. the stability number increased between 10 and 15 cm, and decreased thereafter.

Changes in air rate also yielded a lot of variation in froth stability. At 10 cm froth height the stability number decreased with increasing air rate, and at 15 cm the stability was initially constant between 1.35 and 1.60 cm/s and increased thereafter. When a 20 cm froth height was used, the stability number increased between1.35 and 1.60 cm/s and decreased between 1.60 and 1.85 cm/s.

The tests were repeated using a depressant dosage of 100 g/t, and just as observed when no depressant was used, the stability number was larger than expected as shown in Figure 3.18. When the effect of froth height was investigated the stability number increased between 10 and 15 cm, and subsequently decreased which was noted at the three air rates. The data obtained when changing air rate was also more consistent, as the air rate was increased the stability number also decreased.

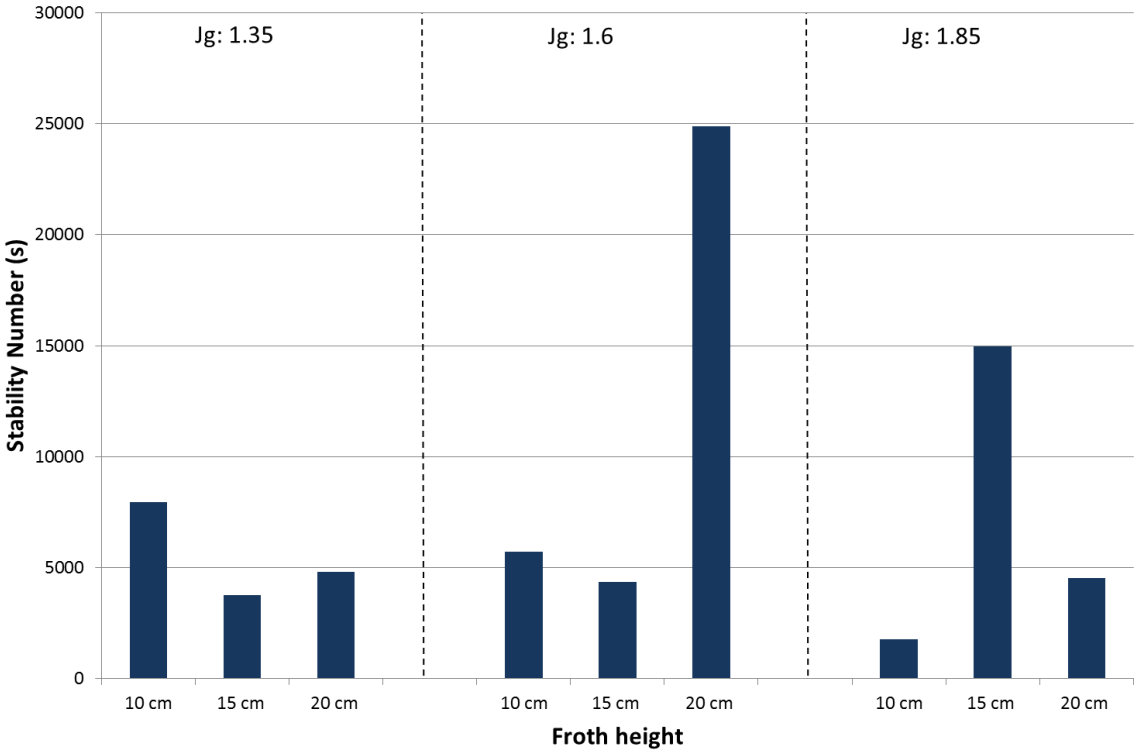

Figure 3. 17: Stability numbers for tests conducted at froth heights of 10, 15 and 20 cm and Jg of 1.35, 1.60 and 1.85 in the absence of depressant.

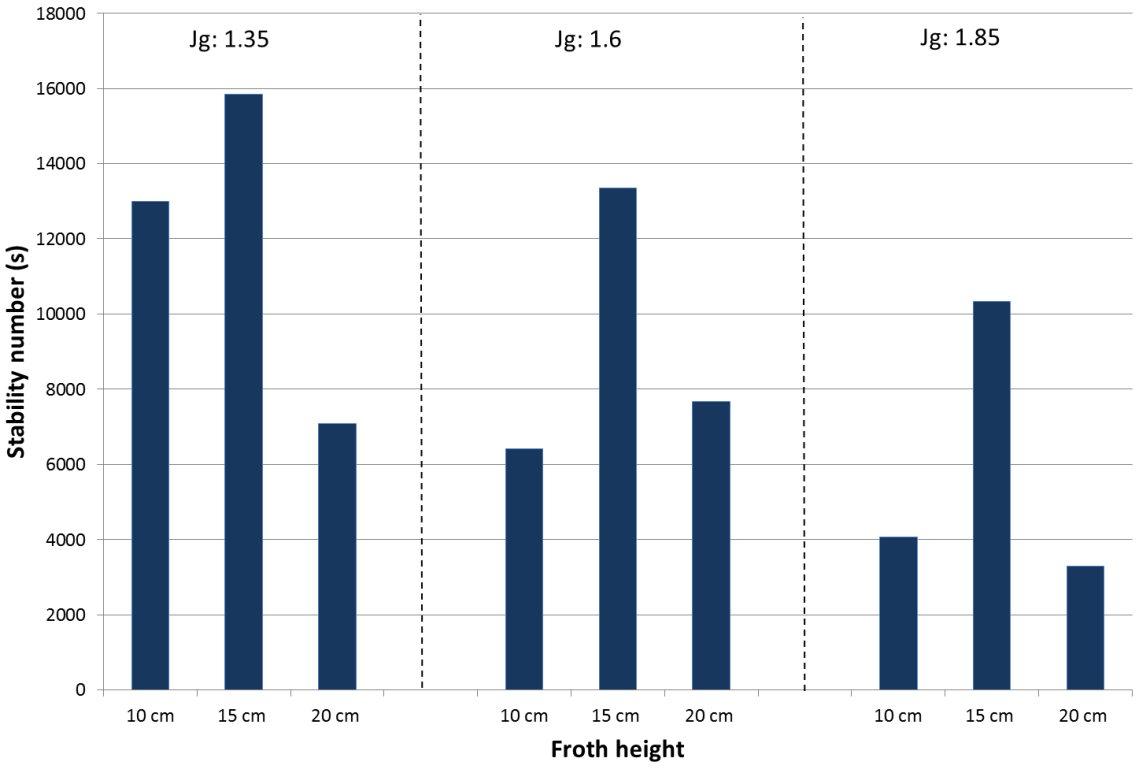

Figure 3. 18: Stability numbers for tests conducted at froth heights of 10, 15 and 20 cm and Jg of 1.35, 1.60 and 1.85 with 100 g/t depressant.

The last investigation was conducted using a depressant dosage of 300 g/t and the results are show in Figure 3.19. Similar to the results obtained at 0 and 100 g/t, the stability numbers were larger than expected. When the effect of changing froth height was investigated three distinct trends were noted. At a superficial air rate of 1.35 cm/s the stability number decreased then increased thereafter; at 1.60 cm/s the number increased then decreased, and at 1.85 cm/s the stability number continuously increased with increasing froth height.

When the air rate was increased a continuous decrease in stability number was noted when a 10 cm froth height was used. Froth heights of 15 and 20 cm showed an increase between 1.35 and 1.60 cm/s, followed by a decrease thereafter.

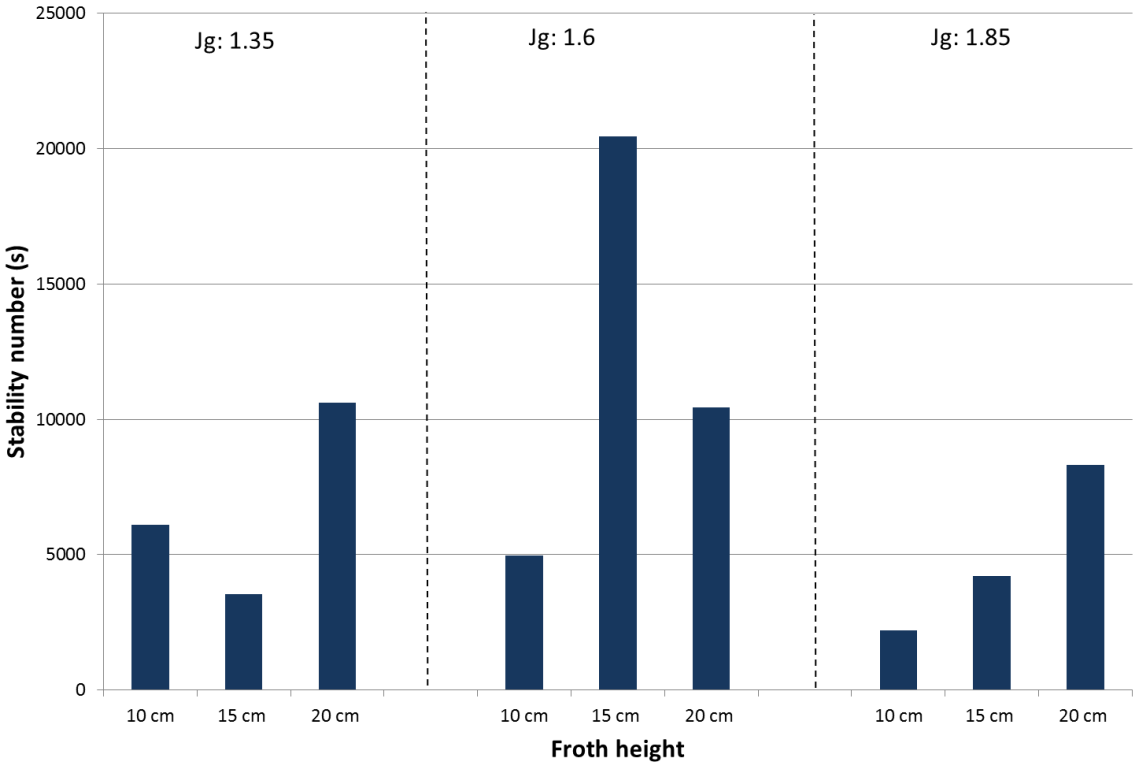

Figure 3. 19: Stability numbers for tests conducted at froth heights of 10, 15 and 20 cm and Jg of 1.35, 1.60 and 1.85 with 300 g/t depressant.

For all the tests that were conducted the stability numbers that were calculated were larger than feasible. This could be because the top of froth bubble size was extrapolated from the bubbles in the froth phase which might have yielded smaller bubble sizes than those observed in reality; direct measurement of these bubbles might give more realistic numbers. Due to these discrepancies this method could not be applied in this system to predict or analyse the stability of the froth.

Method 3: Relationship between water recovery and burst rate

The bursting of bubbles in the froth phase results in the release of water from the froth back into the pulp, which ultimately reduces the amount of water recovered in the concentrate. There is an inverse relationship between the top of froth burst rate and the water recovered, which can be further substantiated by the relationship between water recovery and air recovery in equation 3.9 (Cilliers, 2007).

$$Water\ recovered = kA_{column}\frac{J_g^2}{d_{bubble}^2}(1-\propto) \propto \qquad 3.9$$

Where A_{column} is the cross sectional area of the column, k is a constant, J_g is the superficial air rate, d_{bubble} is the sauter mean diameter of bubbles flowing over the weir and α is the air recovery. Air recovery has been defined as the fraction of air entering the pulp that exits the cell by overflowing the weir. Thus 1-α represents the fraction of air that leaves the flotation cell when the bubbles burst. The relationship between water recovery and air recovery is non-linear; however it does increase monotonically (Cilliers, 2007). Therefore, water recovery should monotonically decrease as the top of froth bubble burst rate increases.

The relationship between water recovery and top of froth bubble burst rate could then be used to highlight changes in the stability of the froth with changing operational factors. Along each trend line the stability of the froth decreases with increasing bubble burst rate as shown by direction 1 in Figure 3.20.

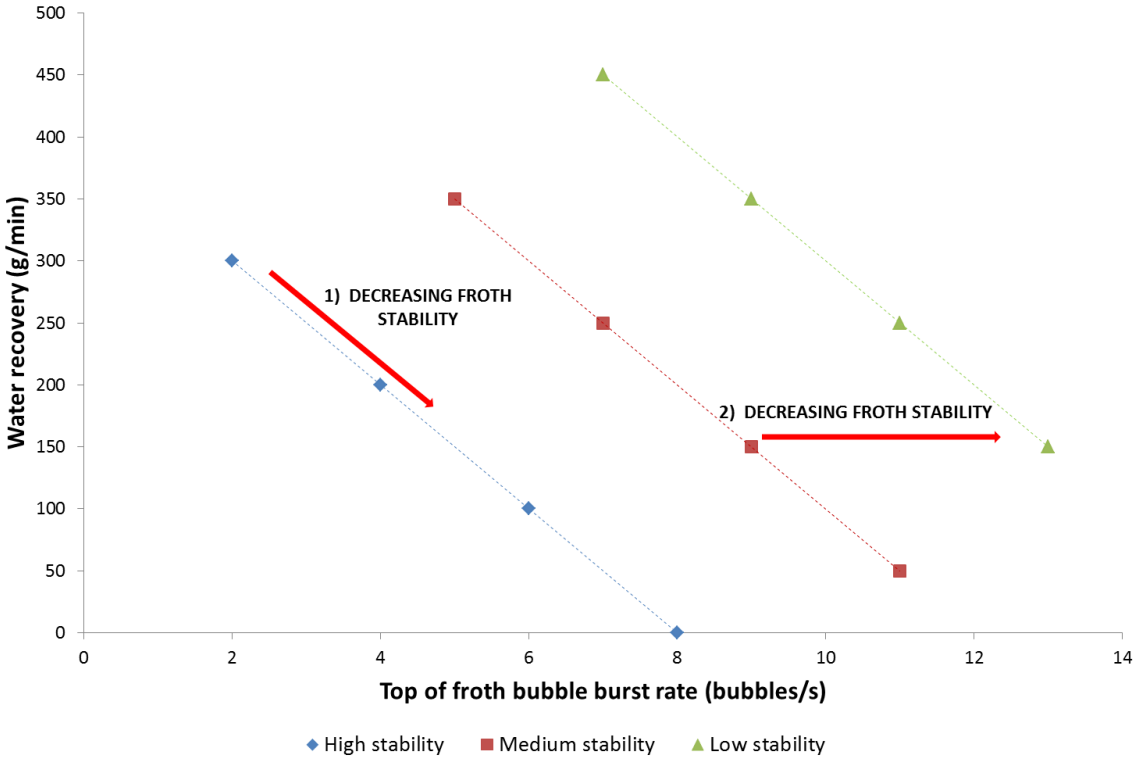

Figure 3. 20: Water recovery as a function of top of froth bubble burst rate showing the different levels of froth stability

A comparison of the different trend lines could also be used determine which conditions the highest stability is attained as shown by direction 2. As illustrated by the figure, an increase in the burst rate will correspond to a decrease in the stability of the froth

This method produced results that were more consistent than the previous two methods and was thus selected for use in this study; the results obtained are presented in Chapter Four.

CHAPTER FOUR : RESULTS

4.1: Introduction

The aim of this study was to investigate the effect of froth height, superficial air rate and depressant dosage on the stability of the froth phase.

In order to achieve this, the burst rate and solids and water recoveries were measured; the burst rate shown for each test is an average from three rates measured and the solids and water recoveries are an average of four samples collected during each test, the complete data set is shown in the appendix. The water recovery was used in conjunction with the top of froth bubble burst rate to analyse the stability of the froth phase. The chapter also includes average particle sizes for the solids collected during the flotation tests and their corresponding mineral assays, showing the amount of chromite, palladium and platinum recovered in the concentrate. The details of the procedure that were used in conducting this investigation are described in Chapter Three.

The chapter is divided into two sections, the first section focuses on the effect of froth height and air rate on the stability of the froth, whilst the second section focuses on the effect of depressant dosage.

4.2. The effect of froth height and air rate on froth stability at a constant depressant dosage

This first section is divided into three sub-sections each focusing on changes in the stability of the froth phase when varying froth height and superficial air rate at different depressant dosages viz. 0 g/t, 100 g/t and 300 g/t.

Test conditions

The first set of flotation tests was conducted in the absence of depressant with other flotation reagents added as follows: collector, SIBX at a dosage of 80 g/t and frother, Dow 200 at a dosage of 25.2 ppm.

The conditioned pulp was combined with air prior to being fed into the column, at superficial air rates of 1.35, 1.60 and 1.85 cm/s for the different tests. The height of froth in the column was maintained at 10, 15 and 20 cm, depending on the flotation test being conducted.

The tests were then repeated using depressant dosages of 100 and 300 g/t.

4.2.1 Effect of froth height and air rate on froth stability in the absence of depressant

The solids and water recoveries obtained when using these conditions are shown in Figure 4.1. The solids and water recovery trends were similar when the air rates and froth heights were varied. The figure also shows that when changing froth height similar trends were observed at superficial air rates of 1.60 and 1.85 cm/s whilst that at 1.35 cm/s showed a different trend.

When tests were conducted using a superficial air rate of 1.35 cm/s there was a decrease in solids and water recoveries as the froth height was increased, this trend was most pronounced between 10 cm and 15 cm, after which the recoveries plateaued off between 15

and 20 cm. At a superficial air rate of 1.60 cm/s the solids and water recoveries remained relatively constant as the froth height was increased; the differences between the maximum and minimum values for the solids and water recoveries were 2.50 g/min and 31.2 g/min respectively, which are relatively small in comparison to the 9.49 g/min and 123 g/min solids and water ranges observed at a superficial air rate of 1.35 cm/s. Similarly, the solids and water recoveries at a superficial air rate of 1.85 cm/s can also be deemed as constant with recoveries with ranges of 2.33 g/min and 22.8 g/min for the solids and water respectively.

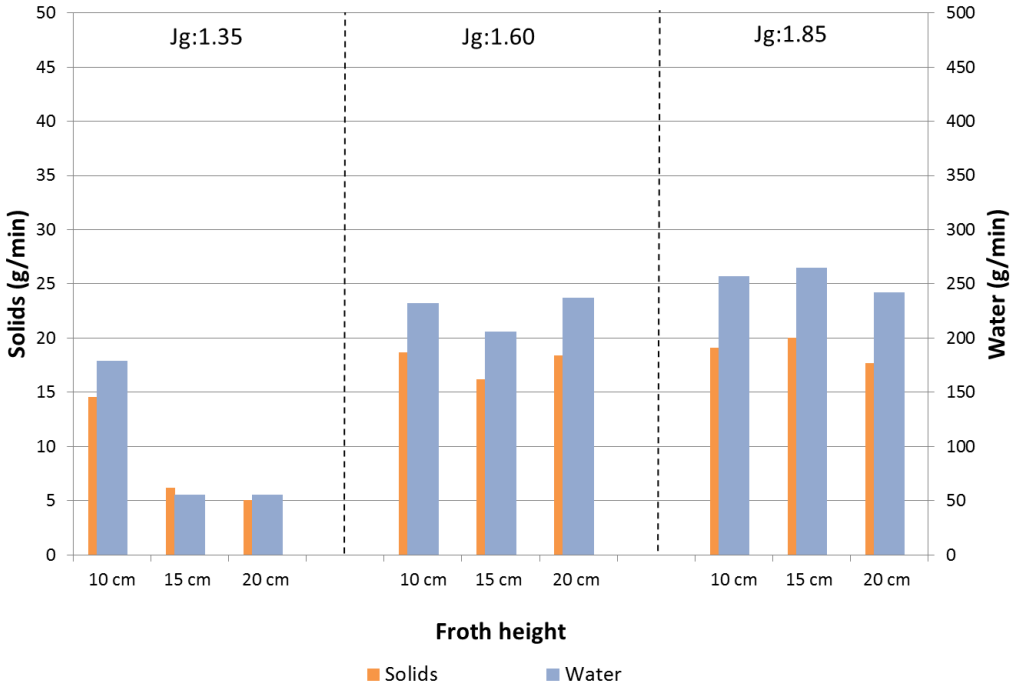

Figure 4.1: Solids and water recovered from tests conducted at froth heights of 10, 15 and 20 cm and Jg of 1.35, 1.60 and 1.85 in the absence of depressant.

To investigate the effect of increasing superficial air rate on the recovery of solids and water, the tests were conducted at a constant froth height whilst changing the air rate. Figure 4.1 illustrates that there was an increase in solids and water recoveries as the air rate was increased. This trend was observed for all three froth heights evaluated.

The top of froth bubble burst rate was measured for these tests and the results are shown in Figure 4.2. When the tests were conducted at an air rate of 1.35 cm/s an increase in the bubble burst was observed as the froth height was increased, the increase was most pronounced between the froth heights of 10 and 15 cm. Tests conducted at superficial air rates of 1.60 and 1.85 cm/s showed more subtle changes in bubble burst rate as the froth height was increased, with ranges of 0.03 and 0.04 bubbles/s for the 1.60 and 1.85 cm/s superficial air rates respectively. These ranges are very small in comparison to the 0.17 bubbles/s observed at a superficial air rate of 1.35 cm/s, and thus the trends observed at 1.60 and 1.85 cm/s can be regarded as constant.

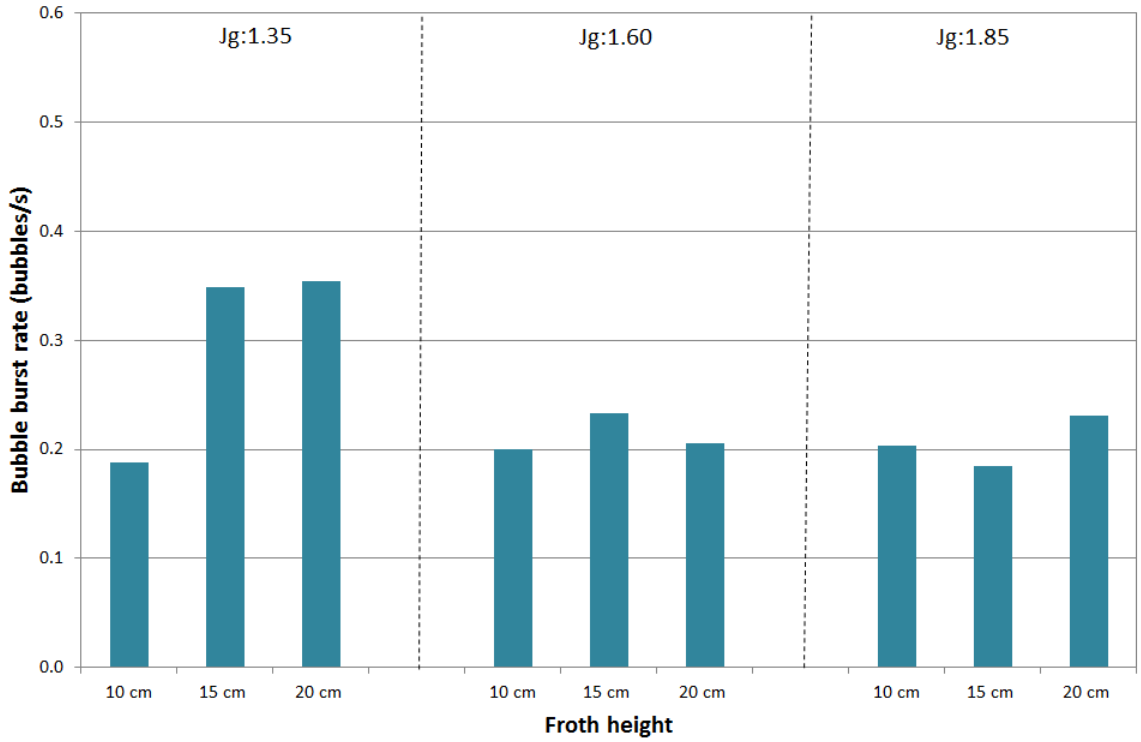

Figure 4.2: Top-of-froth bubble burst rate for tests conducted at froth heights of 10, 15 and 20 cm and Jg of 1.35, 1.60 and 1.85 in the absence of depressant.

The bubble burst rate trends that were observed when increasing the superficial air rate at a constant froth height, are different for the three froth heights investigated. At a froth height of 10 cm the bubble burst rate remained relatively constant at a rate of 0.2 bubbles/s. Tests conducted at a 15 cm froth height showed a decrease in bubble burst rate as the air rate was increased whilst a 20 cm froth height showed a decrease between superficial air rates of 1.35 and 1.60 cm/s, followed by a slight increase between superficial air rates of 1.60 and 1.85 cm/s.

The relationship between the bubble burst rate and water recovery when changing froth height and air rate are shown in Figure 4.3.The figure shows that there is an inverse relationship between water recovery and top of froth bubble burst rate with increasing froth height. As the froth height was increased there was a corresponding increase in the burst rate which suggests that the froth formed was less stable. This trend was noted at all three air rates investigated. As the air rate was increased the water recovery and burst rate relationship were shifted to the right (increased bubble burst rate) which suggest that the froth became less stable with increasing air rate. The difference between the trends formed at superficial air rate of 1.60 and 1.85 cm/s is small, showing that there was little change in the stability of the froth.

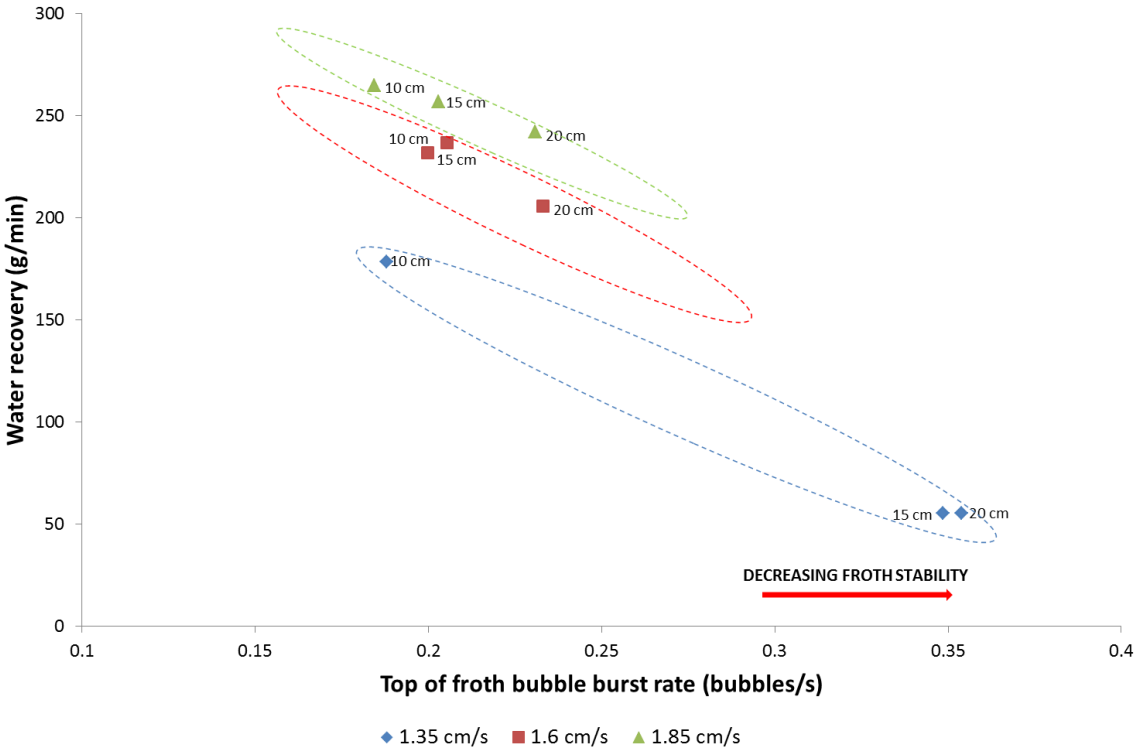

Figure 4. 3: Water recovery as a function of top of froth bubble burst rate for tests investigating the effect of changing froth height and air rate on froth stability at 10, 15 and 20 cm at Jg's of 1.35, 1.60 and 1.85 in the absence of depressant.

The concentrates collected were assayed to determine the amounts of PGM that were recovered under these conditions. Figure 4.4 shows the percentages of palladium and platinum in the feed that were recovered in the concentrates.

At an air rate of 1.35 cm/s there was a decrease in the recoveries of both platinum and palladium from about 65% to about 55% as the froth height was increased from 10 to both 15 cm and 20 cm. This may be as a result of the increased occurrence of bubbles bursting under these conditions as shown in Figure 4.2 and the subsequent loss of attached PGM. For air rates of 1.60 and 1.85 cm/s the PGM recoveries remained relatively constant as the froth height was increased; the difference between maximum and minimum values was less than 5% for both platinum and palladium when using a superficial air rate of 1.60 cm/s, and less than 2% for a superficial air rate of 1.85 cm/s.

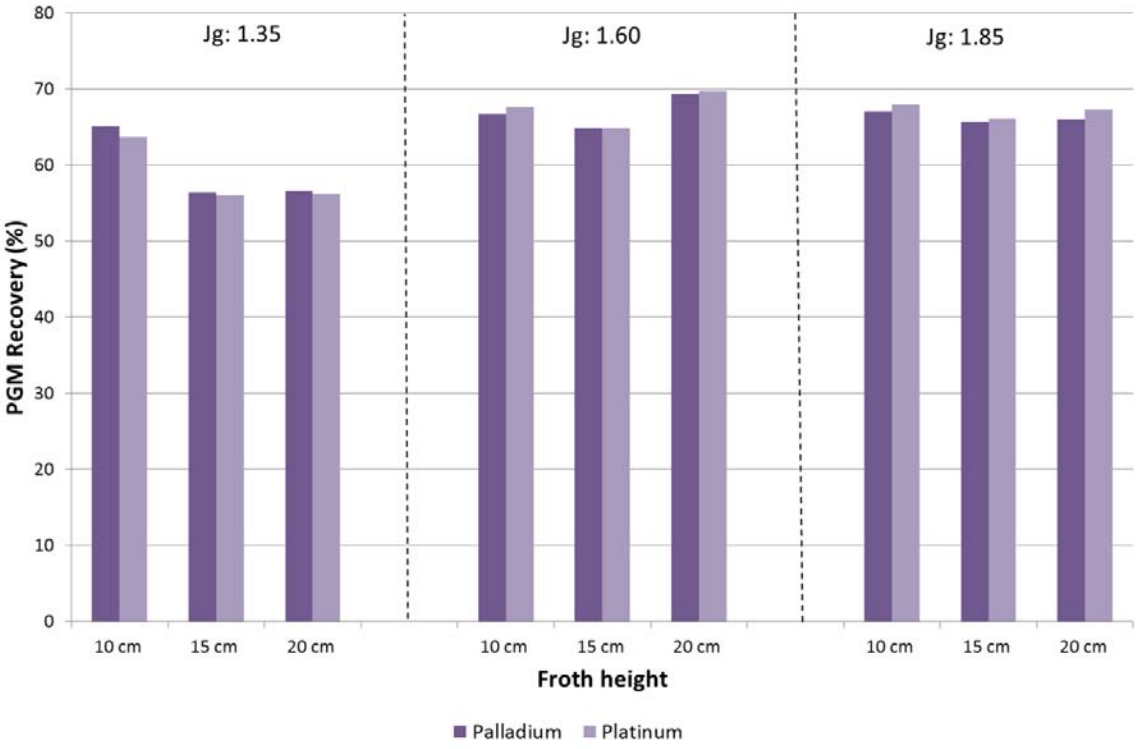

Figure 4. 4: Platinum and palladium recoveries for tests conducted at froth heights of 10, 15 and 20 cm and Jg of 1.35, 1.60 and 1.85 in the absence of depressant.

At a constant froth height of 10 cm, there was very little change in platinum and palladium recoveries as the superficial air rate was increased. For tests conducted at 15 cm froth height there was an increase in PGM recovery when the superficial air rate was increased. And at 20 cm there was an increase in PGM recovery when the superficial gas rate was increased from 1.35 to 1.65 cm/s followed by a slight decrease when it was increased from 1.6 to 1.85 cm/s.

The amount of chromite present in the feed that was recovered to the concentrates was calculated from the assays, and the results obtained are presented in Figure 4.5.
At a superficial air rate of 1.35 cm/s there was a decrease in chromite recovery as the froth height was increased. This was most pronounced when the superficial air rate was increased from 1.35 and 1.60 cm/s, after which the recovery increased only slightly when the superficial air rate was increased from 1.60 to 1.85 cm/s, this increase is less than 0.1% and can therefore be deemed constant. This trend is very similar to the water recovery trend shown in Figure 4.1. The trend for chromite recovery at a superficial air rate of 1.85 cm/s is comparable to that observed at a superficial air rate of 1.35 cm/s, showing a decrease in recoveries when froth height was increased from 10 to 15 cm and reaching a plateau thereafter. At a superficial air rate of 1.60 cm/s there was a decrease in chromite recovery when froth height was increased from 10 and 15 cm, followed by an increase when the froth height was increased from 15 and 20 cm.

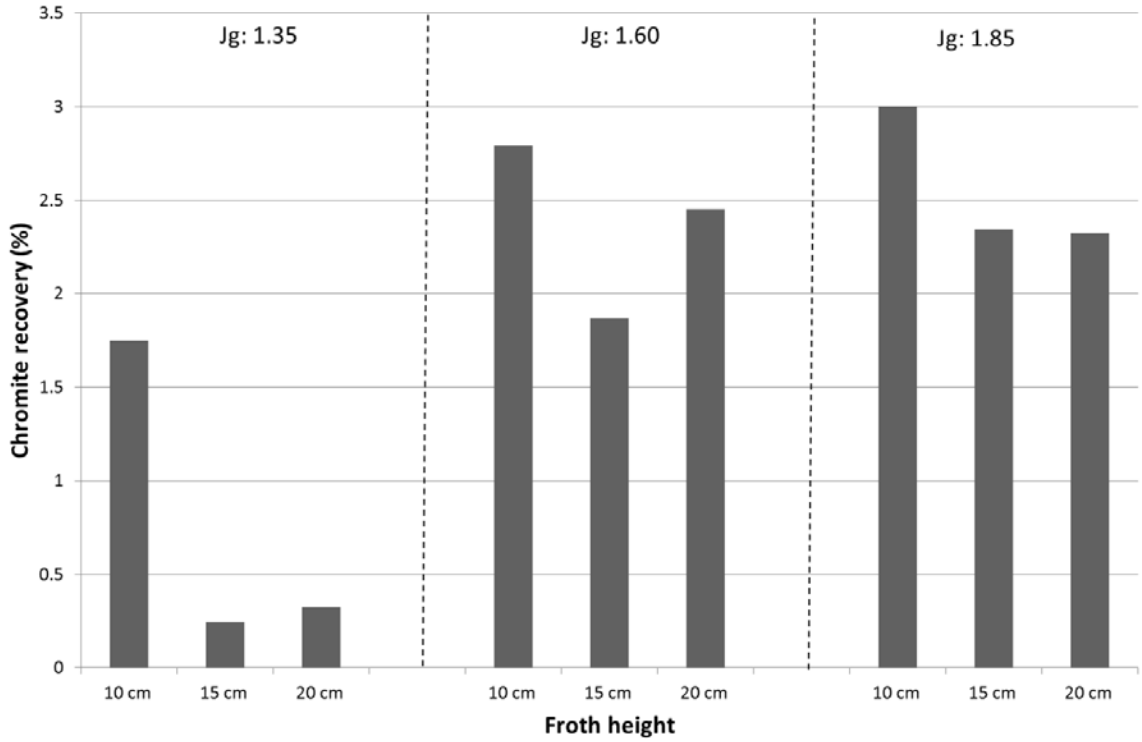

Figure 4. 5: Chromite recoveries for tests conducted at froth heights of 10, 15 and 20 cm and Jg of 1.35, 1.60 and 1.85 in the absence of depressant.

To investigate the effect of increasing superficial air rate on the recovery of chromite, the froth height was kept constant whilst varying the air rate. Figure 4.5 illustrates that there was an increase in chromite recovery as the superficial air rate was increased; a trend which was most obvious for froth heights of 10 and 15 cm. At a froth height of 20 cm, the chromite recovery increased when superficial air rate was increased from 1.35 to 1.60 cm/s, and decreased when superficial air rate was further increased to 1.85 cm/s.

Chromite is a hydrophilic gangue mineral which is mainly recovered through its entrainment in the water collected in the concentrate (Hay & Roy, 2010). It was therefore pertinent to compare the amount of water and chromite recovered, and this is shown in Figure 4.6.

The figure shows that there is a direct relationship between the amount of water recovered and the chromite recovered i.e. increasing the water recovered increased the amount of chromite recovered, which is in agreement with the idea that chromite is largely recovered via the mechanism of entrainment.

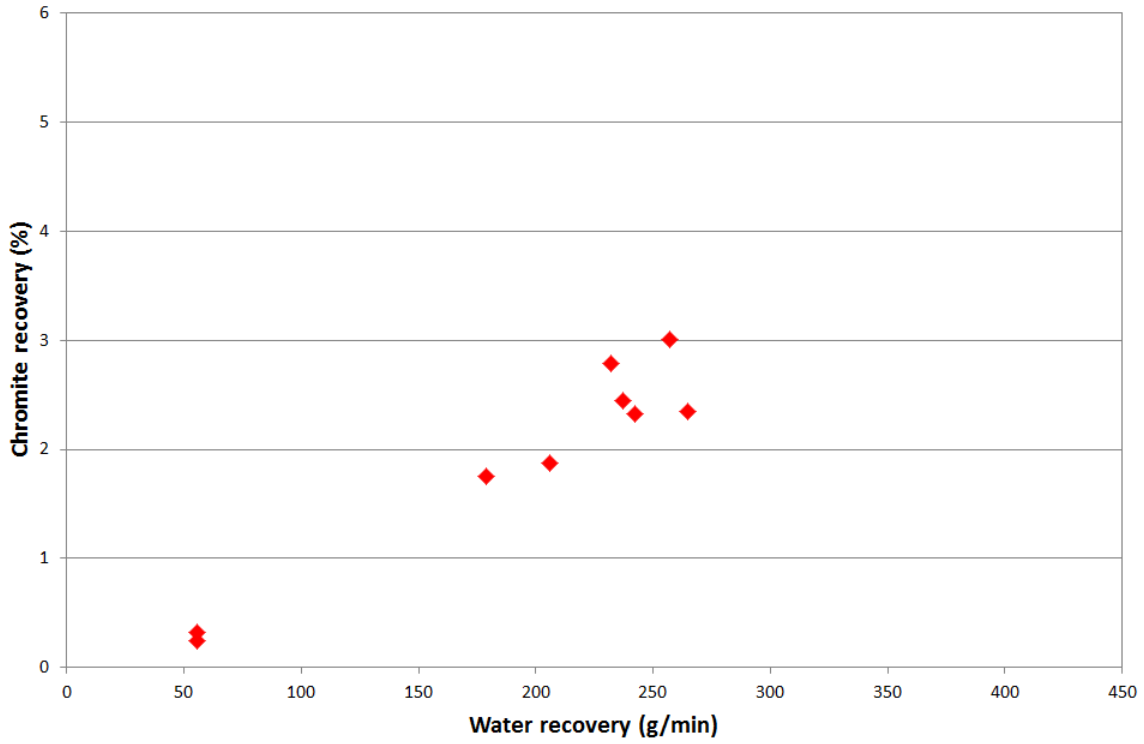

Figure 4. 6: Chromite recovery as a function of water recovery for tests conducted at froth heights of 10, 15 and 20 cm and Jg of 1.35, 1.60 and 1.85 in the absence of depressant.

Particle size analysis was conducted using a Malvern Mastersizer to determine the average size of the particles present in the concentrates; the results obtained are shown in Figure 4.7. The figure shows the d50's of the concentrates collected, which is the particle size that 50 % of the particles in a sample is finer than.

From Figure 4.7 it is apparent that different trends are observed when different superficial air rates were used. At a superficial air rate of 1.35 cm/s larger particles were collected at a 15 cm froth height than at a 10 cm froth height, the average particle size then decreased when froth height was increased from 15 to 20 cm. At a superficial air rate of 1.60 cm/s smaller particles were collected with deeper froths, whilst changing froth height at a superficial air rate of 1.85 cm/s had very little effect on the size of the particles that were collected.

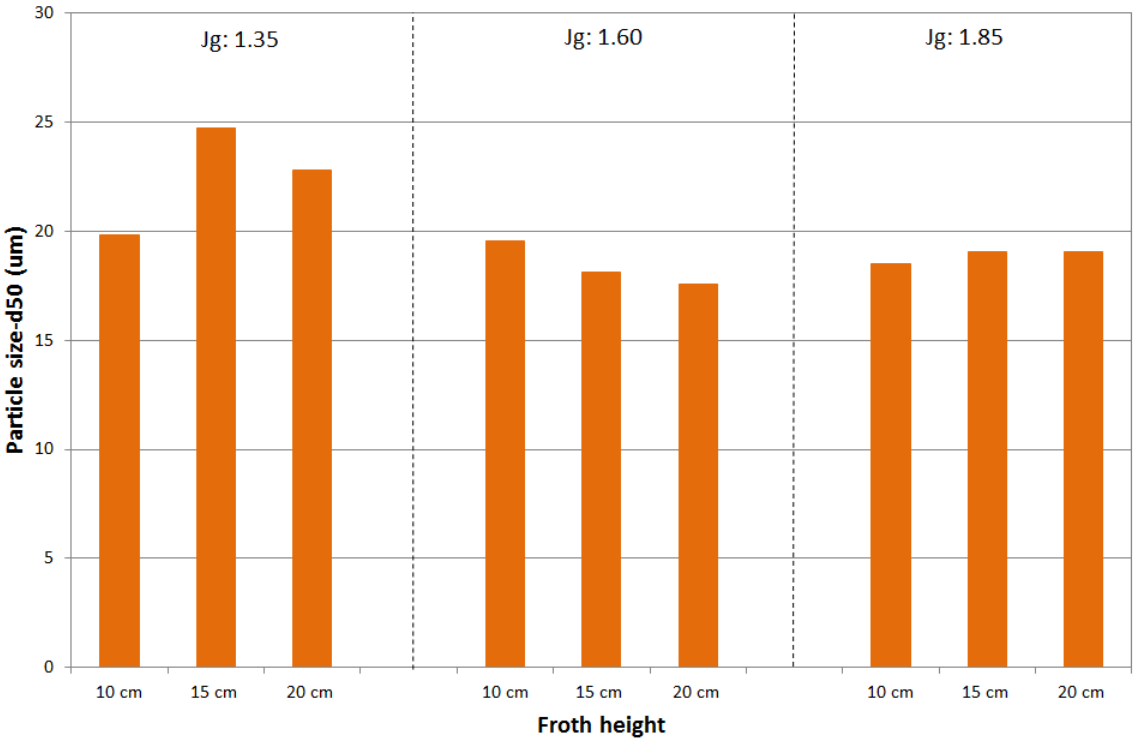

Figure 4. 7: D_{50} for all tests conducted at froth heights of 10, 15 and 20 cm and Jg of 1.35, 1.60 and 1.85 in the absence of depressant.

Whilst keeping the froth height constant at 10 cm, and changing the superficial air rate, the particle size remained constant for all three air rates. At a froth height of 15 cm, the particle size decreased when superficial air rate was increased from 1.35 to 1.60 cm/s but plateaued when superficial air rate was increased from 1.60 to 1.85 cm/s. A similar effect was noted when using a froth height of 20 cm.

4.2.2. Effect of froth height and air rate on froth stability at a depressant dosage of 100 g/t

The study was repeated with some modification to the pulp chemistry through the addition of a depressant along with the frother and collector that were previously added. The depressant that was added was a guar gum, Sendep 348, at a dosage of 100 g/t.

The solids and water recoveries that were obtained at these test conditions are shown in Figure 4.8.

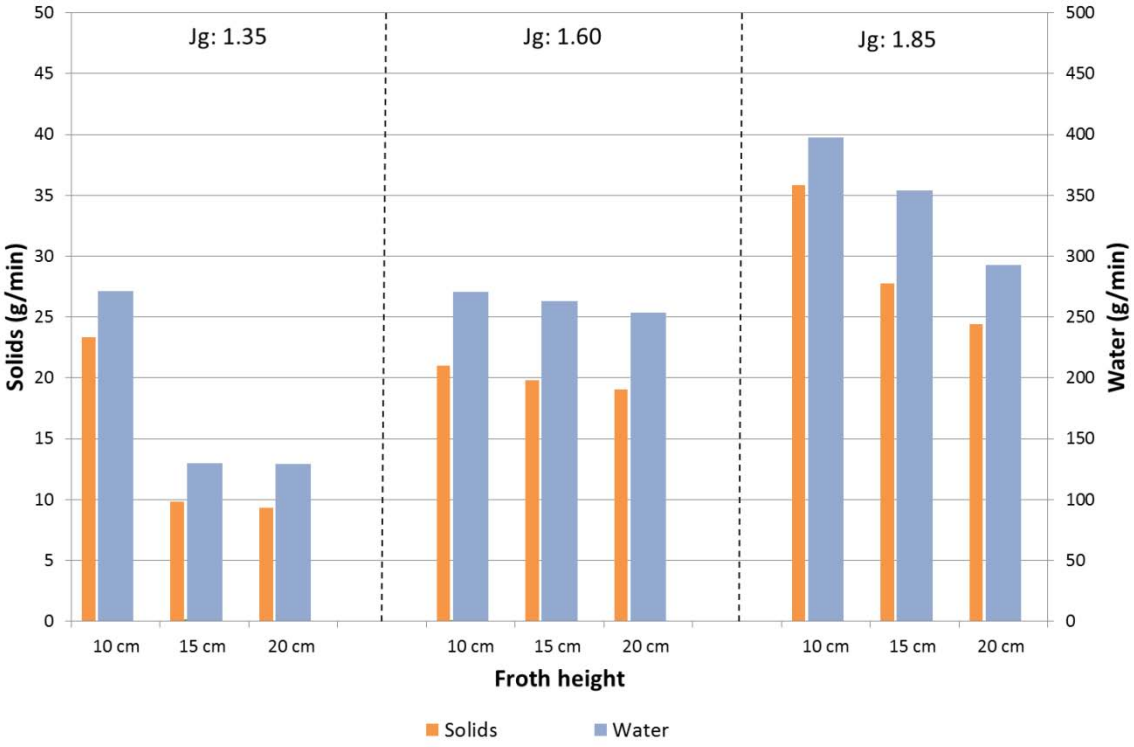

Figure 4. 8: Solids and water recovered from tests conducted at froth heights of 10, 15 and 20 cm and Jg of 1.35, 1.60 and 1.85 at a depressant dosage of 100 g/t.

When the tests were conducted with a superficial air rate of 1.35 cm/s, a decrease in solids and water recoveries was observed when froth height was increased from 10 to 15 cm, followed by no further decrease when froth height was further increased from 15 to 20 cm. This trend is similar to that which was observed when the experiments were conducted without depressant. When the experiments were repeated at the higher superficial air rates, 1.60 and 1.85 cm/s, a decrease in both solids and water recoveries was observed as the froth height was increased. This trend was more evident at an air rate of 1.85 cm/s than at 1.60 cm/s.

To evaluate the effect of changing air rate on froth stability the tests were conducted at a constant froth height whilst the air rate was varied. At a 10 cm froth height, the solids and water recoveries were relatively unchanged when superficial air rate was increased from 1.35 to 1.60 cm/s, which was followed by an increase in solids and water recoveries when superficial air rate was increased from 1.60 to 1.85 cm/s. At froth heights of 15 and 20 cm there was a constant increase in solids and water recoveries as the superficial air rates were increased.

The top of froth bubble burst rate was also evaluated for these test conditions and the results obtained are shown in Figure 4.9.

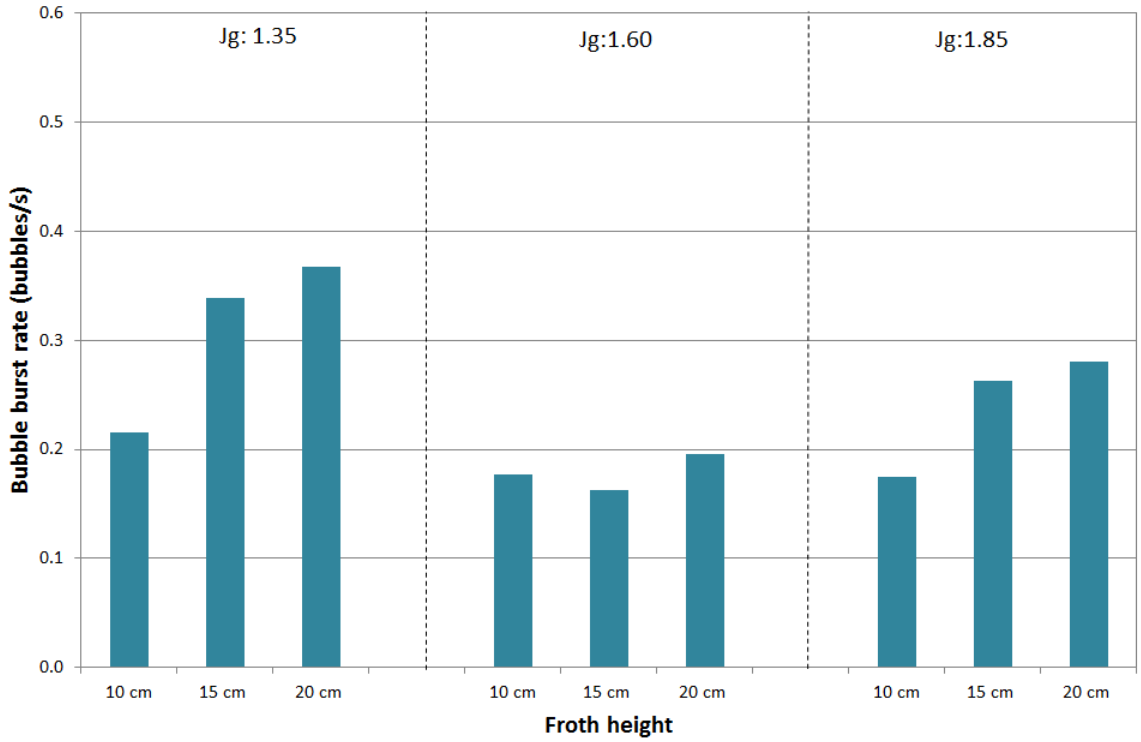

Figure 4. 9: Top-of-froth bubble burst rate for tests conducted at froth heights of 10, 15 and 20 cm and Jg of 1.35, 1.60 and 1.85 at a depressant dosage of 100 g/t.

At superficial air rates of 1.35 cm/s and 1.85 cm/s there was an increase in top of froth bubble burst rate as the froth height increased. At a superficial air rate of 1.60 cm/s the bubble burst rates observed were relatively constant, the difference between the maximum and minimum values were 0.03 bubbles/s, which is very small in comparison to the 0.15 and 0.11 bubbles/s ranges observed at superficial air rates of 1.35 and 1.85 cm/s respectively. The trends observed at all three air rates, are a mirror image of the solids water recovery trends shown in Figure 4.8.

When testing the effect of increasing superficial air rate, a slight decrease in burst rate was observed at a froth height of 10 cm. At froth heights of 15 and 20 cm, there was a decrease in burst rate when the superficial air rate was increased from 1.35 to 1.60 cm/s followed by an increase when air rate was further increased from 1.60 to 1.85 cm/s.

In order to examine the relationship between the top of froth bubble burst rate and the water recovery, the two factors were plotted as a function of each other as shown in Figures 4.10. As in the previous section the figures show that there is an inverse relationship between the amount of water recovered and the top of froth bubble burst rate as the froth height was increased. The figures also show that generally there was an increase in the burst rate as the froth height increased, which suggests that the stability of the froth decreased with increasing froth height. The trends were formulated at the different air rates and the shifts shown in Figure 4.10 show that there was an increase in the stability of the froth between 1.35 and 1.60 cm/s followed by a decrease thereafter.

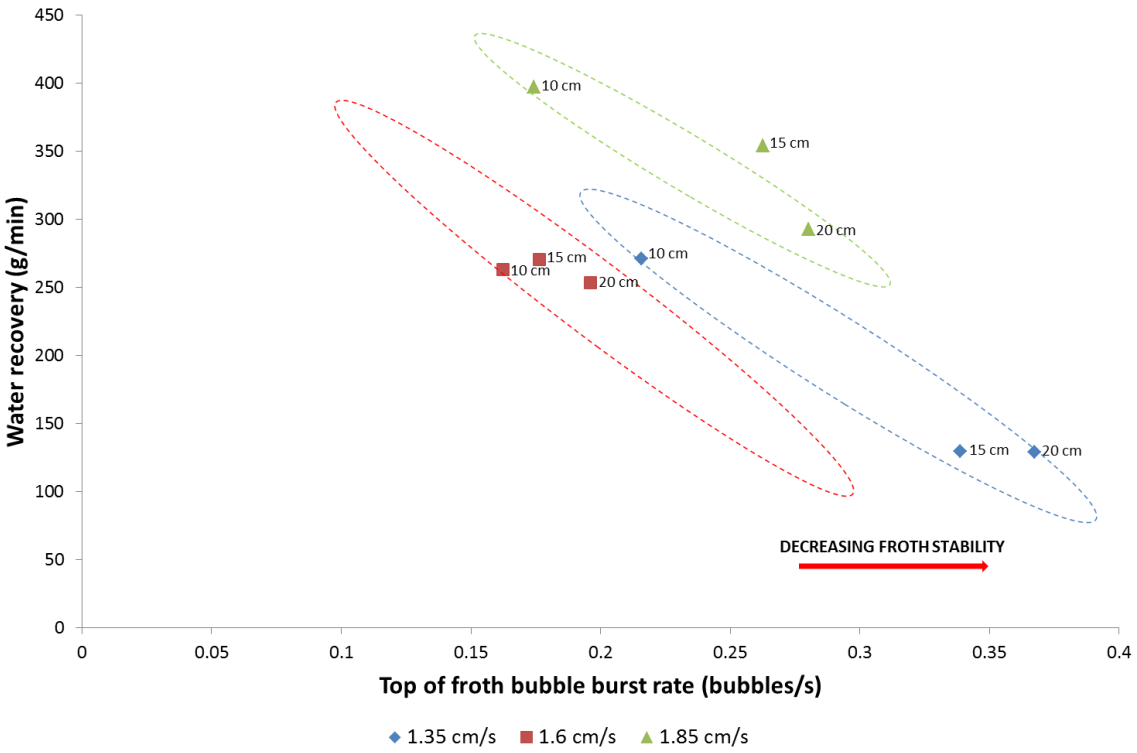

Figure 4. 10: Water recovery as a function of top of froth burst rate for tests investigating effect of changing froth height and air rate on froth stability at 10, 15 and 20 cm froth heights and at Jg of 1.35, 1.60 and 1.85 at 100 g/t depressant dosage.

The PGM recoveries that were obtained from the column flotation experiments conducted under these conditions are shown in Figures 4.11. The increase in froth height from 10 to 15 and then to 20 cm at a superficial air rate of 1.35 cm/s resulted in a decrease in the recovery of platinum and palladium from approximately 70% to 65%. A similar trend was noted at a superficial air rate of 1.85 cm/s. The PGM recoveries obtained when using a superficial air rate of 1.60 cm/s were relatively constant as the froth height was increased with differences in the range of 0.14 and 3.5% for the palladium and platinum respectively.

When testing the effect of increasing superficial air rate at a constant froth height, a continuous increase in PGM recovery was observed for froth heights of 10 and 15 cm. A 20 cm froth height resulted in an increase in PGM recovery between air rates of 1.35 and 1.60 cm/s, followed by a decrease between 1.60 and 1.85 cm/s.

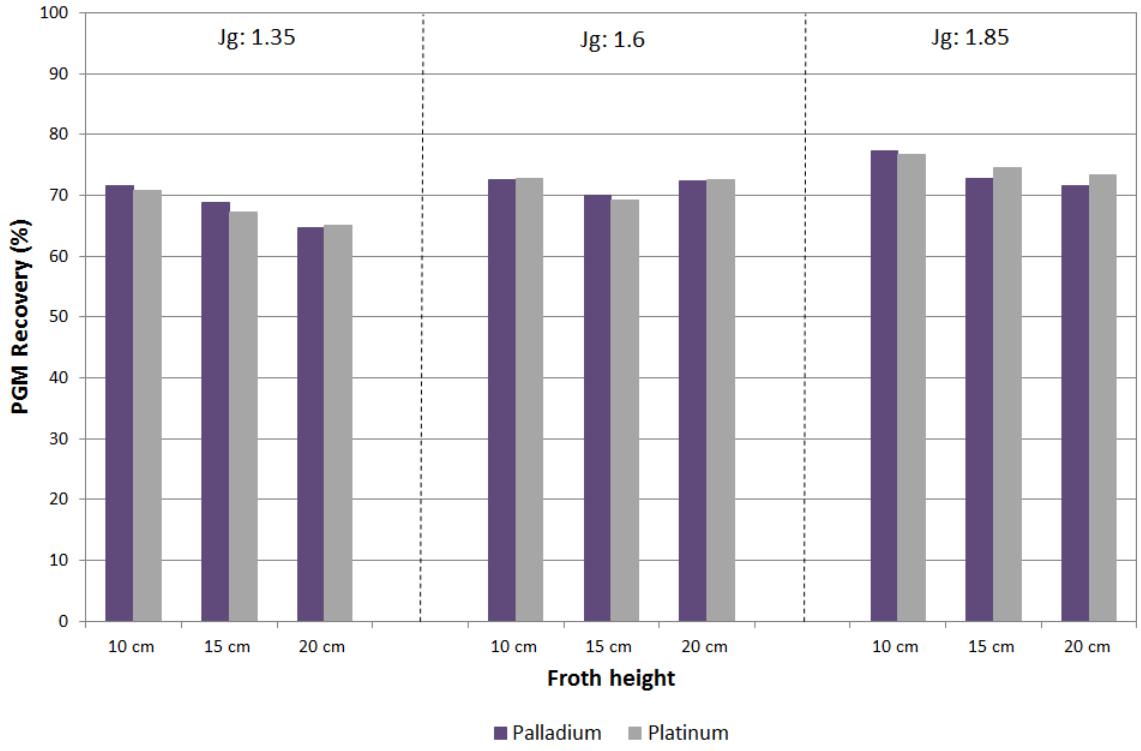

Figure 4. 11: Platinum and palladium recoveries for tests conducted at froth heights of 10, 15 and 20 cm and Jg of 1.35, 1.60 and 1.85 at a depressant dosage of 100 g/t.

The chromite content of the concentrate collected was also determined and the results obtained are shown in Figure 4.12.

At all three superficial air rates investigated there was a decrease in chromite recovery as the froth height was increased. This trend was most pronounced between froth heights of 10 and 15 cm with a further increase in froth height to 20 cm having less of an effect. These trends are similar to those observed for the water recoveries shown in Figure 4.8.

Generally the amount of chromite recovered increased as the superficial air rate was increased, at a constant froth height. This is most evident at the 15 and 20 cm froth heights. At a froth height of 10 cm, the chromite recovery decreased when the superficial gas rate was increased from 1.35 to 1.60 cm/s and increased when superficial gas rate was increased from 1.60 to 1.85 cm/s.

Tests conducted at froth heights of 15 and 20 cm showed an increase in chromite recovery as the superficial air rate was increased. A 10 cm froth height resulted in a decrease in chromite recovery when superficial gas rate was increased from 1.35 to 1.60 cm/s followed by a significant increase when superficial gas rate was increased from 1.60 to 1.85 cm/s.

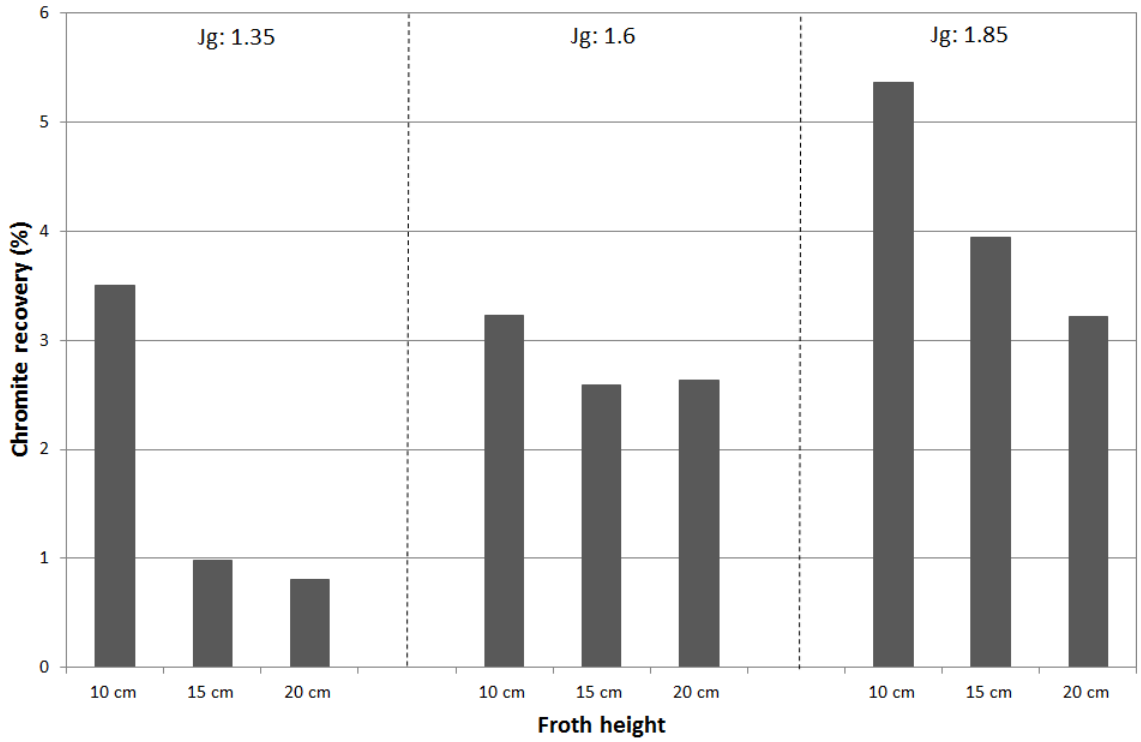

Figure 4. 12: Chromite recoveries for tests conducted at froth heights of 10, 15 and 20 cm and Jg of 1.35, 1.60 and 1.85 at a depressant dosage of 100 g/t.

The similarity between the chromite and water recovery trends was investigated further by plotting chromite recovery as a function of water recovery as shown in Figure 4.13. The trend produced by this data shows that there is a direct relationship between the chromite recovered and the water recovered that is, an increase in the water recovered resulted in an increase in the amount of chromite recovered. This trend suggests that chromite is recovered via the mechanism of entrainment and was also observed when the tests were conducted in the absence of depressant.

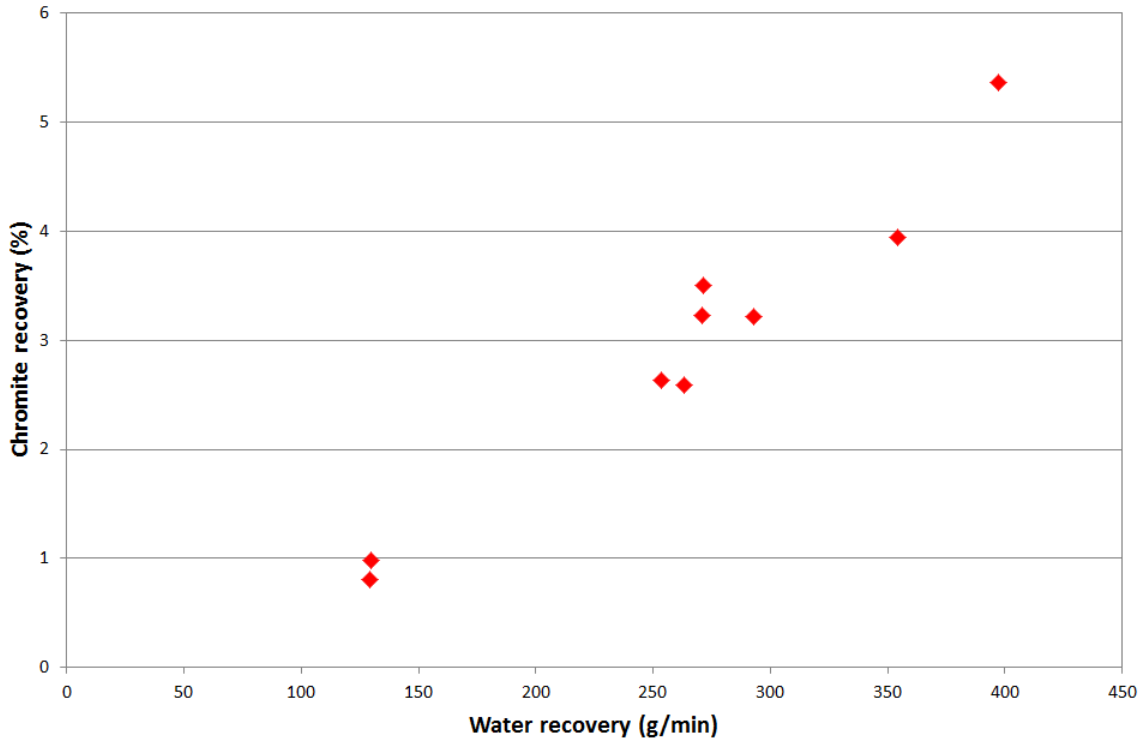

Figure 4. 13: Chromite recovery as a function of water recovery for tests conducted at froth heights of 10, 15 and 20 cm and Jg of 1.35, 1.60 and 1.85 at a depressant dosage of 100 g/t.

Particle size analysis of the concentrates collected was conducted and the average particle sizes obtained are shown in Figure 4.14. Superficial air rates of 1.35 and 1.85 cm/s resulted in a decrease in average particle size as the froth height was increased which implies that deeper froths resulted in the recovery of smaller particles than shallower froths. At a superficial gas rate of 1.60 cm/s the average particle size remained relatively constant as the froth height was increased.

When changing superficial air rate at froth heights of 10 and 15 cm, there was a decrease in the average particle size as the air rate was increased from 1.35 to 1.60 cm/s, this was followed by an increase in particle size when superficial air rate was increased from 1.60 and 1.85 cm/s. At a froth height of 20 cm, the average size of particles recovered remained constant at a d_{50} of approximately 18 µm.

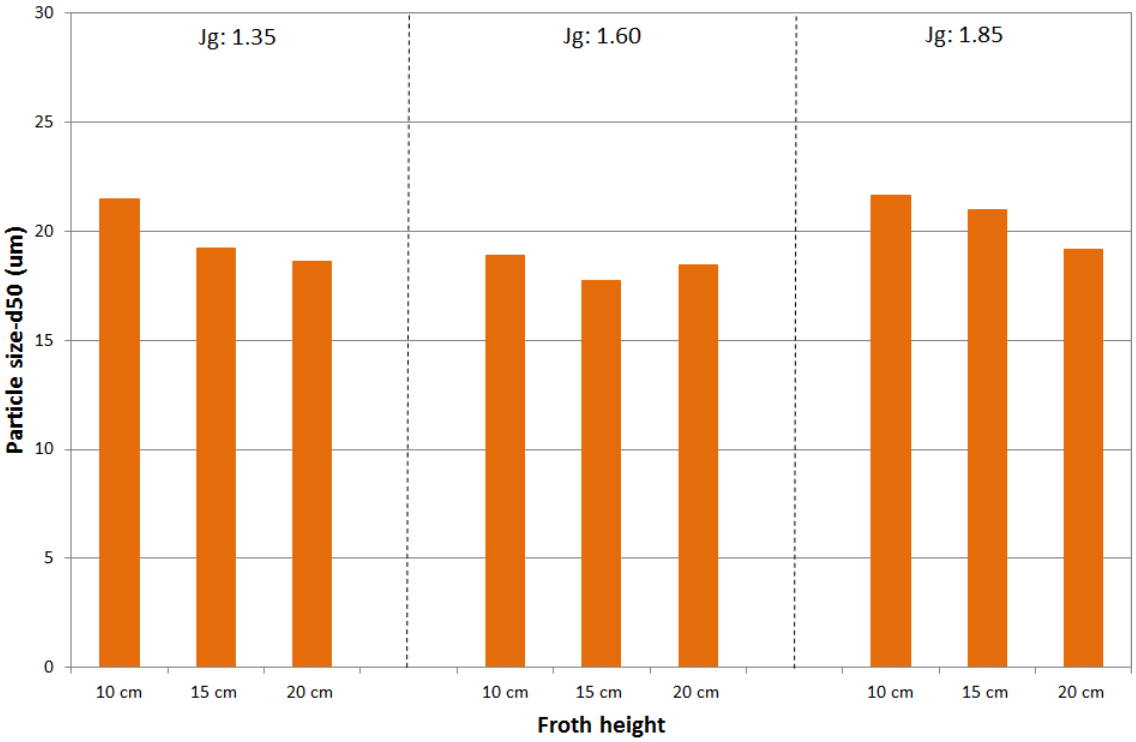

Figure 4. 14: D_{50} for all tests conducted at froth heights of 10, 15 and 20 cm and Jg of 1.35, 1.60 and 1.85 at a depressant dosage of 100 g/t.

4.2.3. Effect of froth height and air rate on froth stability at a depressant dosage of 300 g/t

In the third investigation the depressant dosage was increased to 300 g/t, and the frother and collector dosages were kept constant at 25.2 ppm and 80 g/t respectively.

The solids and water recoveries obtained under these test conditions are shown in Figure 4.15. At a superficial air rate of 1.35 cm/s there was a decrease in both solids and water recoveries when froth height was increased from 10 to 15 cm, with no further reduction in solids and water recoveries when froth height was further increased to 20 cm. This trend is similar to the trends observed in the absence of a depressant and at a depressant dosage of 100 g/t. Tests conducted at a superficial air rate of 1.60 cm/s showed little change in both the solids and water recovered as the froth height was increased, with ranges of 1.7 and 15.3 g/min for the solids and water recoveries respectively. At a superficial air rate of 1.85 cm/s, there was an increase in recoveries when froth height was increased from 10 to 15 cm, followed by a decrease when froth height was increased to 20 cm.

In general, there was an increase in recoveries for froth heights of 10 and 15 cm when superficial gas rate was increased. At a froth height of 20 cm, there was an increase in recoveries when superficial air rate was increased from 1.35 to 1.60 cm/s, followed by a decrease in recoveries when superficial air rate was increased further to 1.85 cm/s.

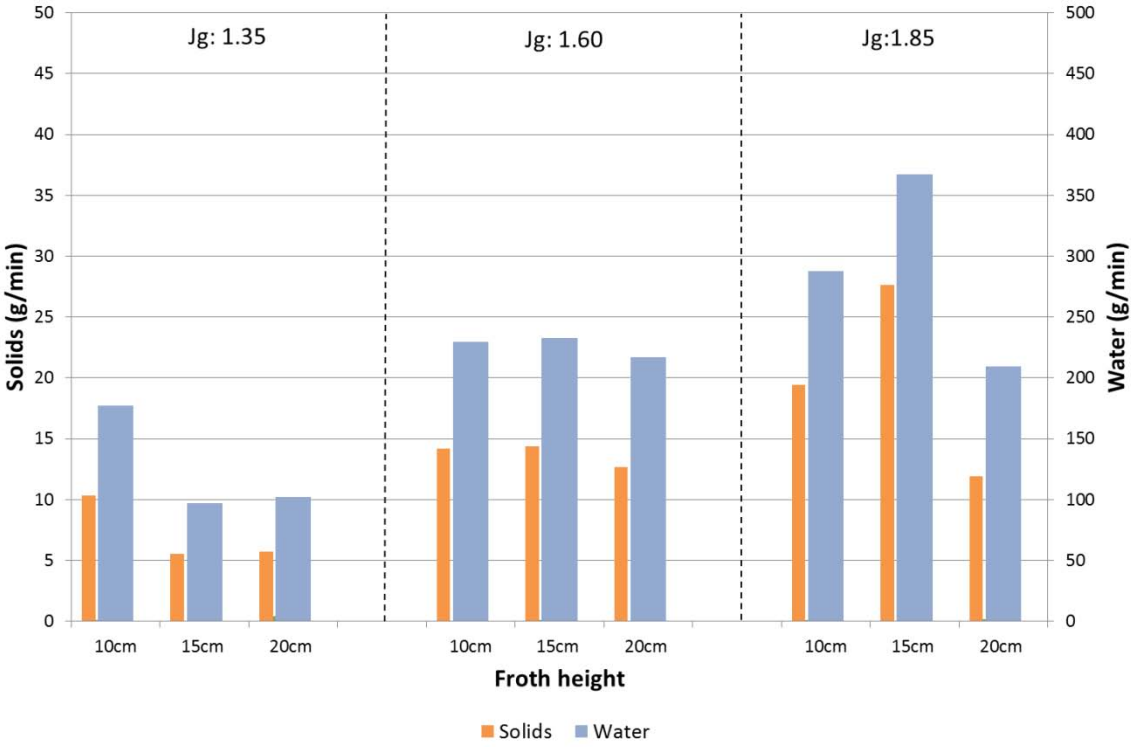

Figure 4.15: Solids and water recovered from tests conducted at froth heights of 10, 15 and 20 cm and Jg of 1.35, 1.60 and 1.85 at a depressant dosage of 300 g/t

The top of froth bubble burst rates for these test conditions are shown in Figure 4.16**.** When the tests were conducted at a superficial air rate of 1.35 cm/s there was an increase in bubble burst rate as the froth height was increased. This is contrary to the trends observed at air rates of 1.60 and 1.85 cm/s which show that there was a decrease in burst rate as the froth height was increased.

Changing superficial air rate at a constant froth height of 10 cm resulted in an increase in burst rate as the air rate was increased. Froth heights of 15 and 20 cm showed a decrease in burst rate when superficial air rate was increased from 1.35 to 1.60 cm/s followed by an increase in burst rate when superficial air rate was further increased to 1.85 cm/s.

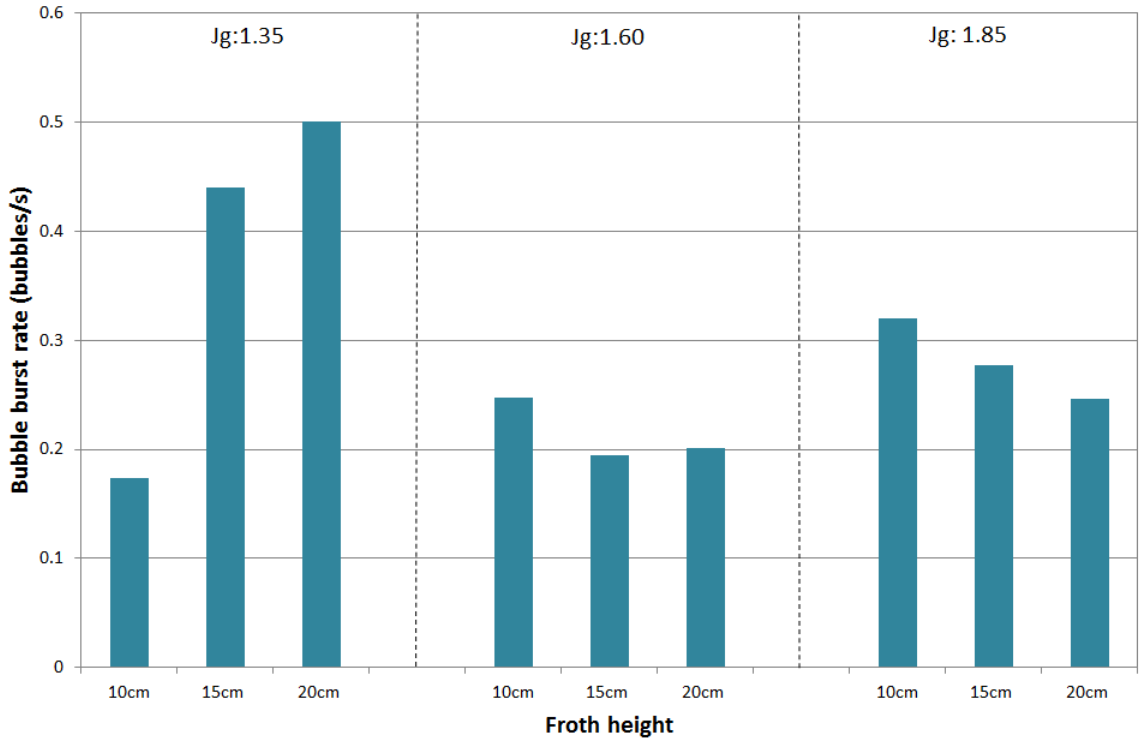

Figure 4. 16: Top-of-froth bubble burst rate for tests conducted at froth heights of 10, 15 and 20 cm and Jg of 1.35, 1.60 and 1.85 at a depressant dosage of 300 g/t.

As in the previous sections the top of froth bubble burst was plotted as a function of water recovery as shown in Figures 4.17. In this case, however, the relationship between the burst rate and the water recovery is not as apparent, as the data are scattered; which could be due to the large amount of depressant present in the pulp. At an air rate of 1.35 cm/s there was an increase in the bubble burst rate with increasing froth height, which suggests that the froth became less stable as the froth height was increased. No other conclusions could be drawn about the structure of the froth and its stability.

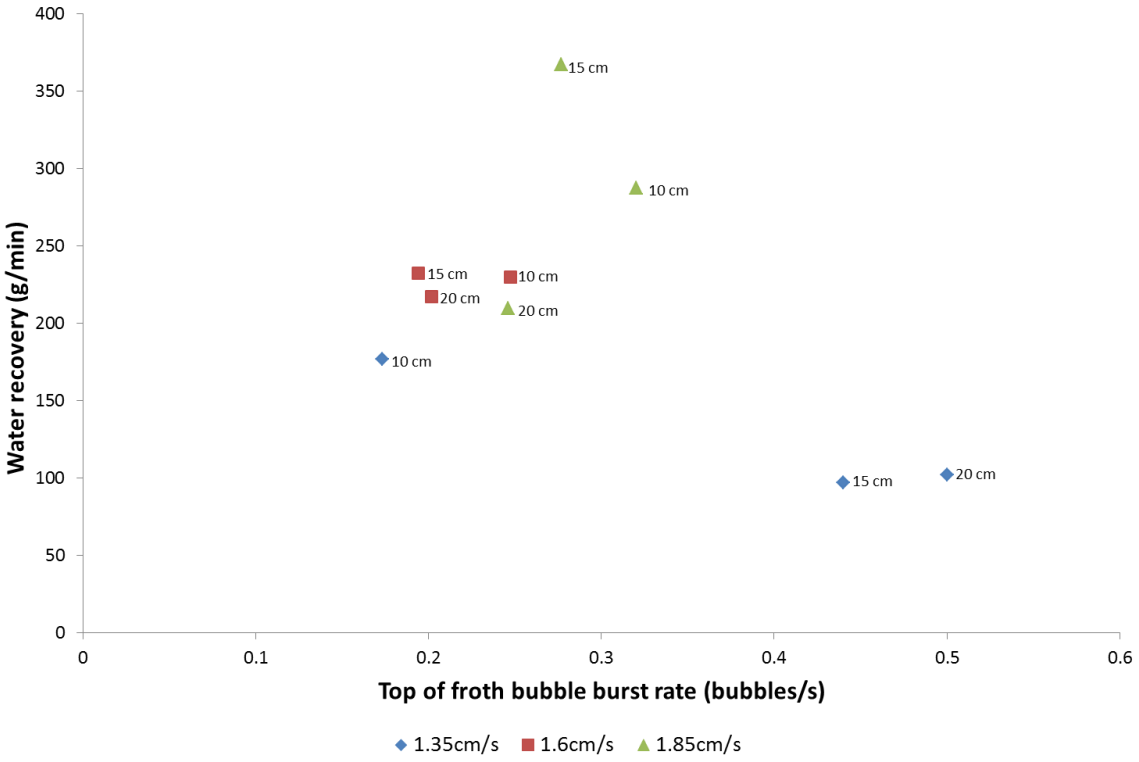

Figure 4. 17: Water recovery as a function of top of froth burst rate for tests investigating effect of changing froth height and air rate on froth stability at 10, 15 and 20 cm at Jg of 1.35, 1.60 and 1.85 at 300 g/t depressant dosage.

Assays of the concentrates were conducted and the PGM content obtained is shown in Figure 4.18. At superficial air rates of 1.35 and 1.60 cm/s there was a decrease in PGM recovery as the froth height was increased from 10 to 15 cm, followed by an increase in recoveries when froth height was further increased to 20 cm. When the tests were conducted at a superficial air rate of 1.85 cm/s, there was a slight increase in PGM recovery when froth height was increased from 10 to 15 cm, followed by a decrease when froth height was further increased to 20 cm.

When the superficial air rate was increased at a froth height of 15 cm a continuous increase in PGM recovery was noted. Tests conducted at froth heights of 10 and 20 cm resulted in an increase in PGM recovery when superficial air rate was increased from 1.35 to1.60 cm/s followed by a decrease in PGM recovery when superficial air rate was further increased to 1.85 cm/s.

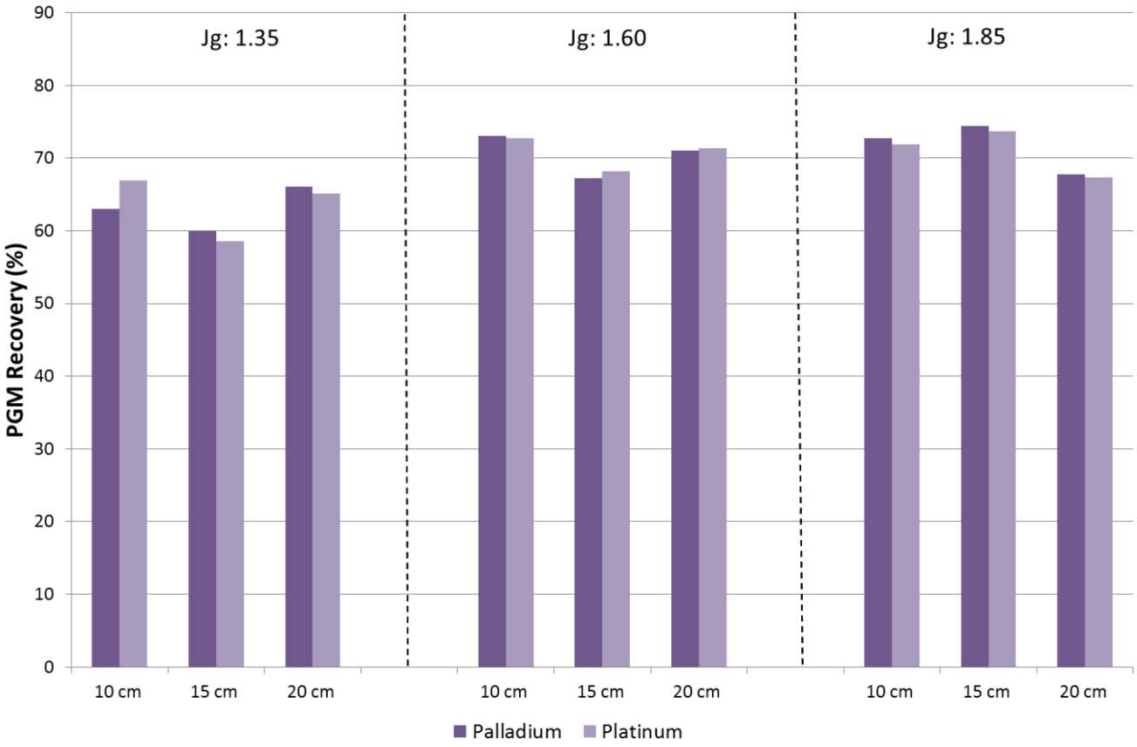

Figure 4. 18: Platinum and palladium recoveries for tests conducted at froth heights of 10, 15 and 20 cm and Jg of 1.35, 1.60 and 1.85 at a depressant dosage of 300 g/t.

The corresponding chromite recoveries for these test conditions are shown in Figure 4.19. When the tests were conducted at a superficial air rate of 1.35 cm/s there was a decrease in chromite recovery when froth height was increased from 10 to 15 cm, followed by a small increase when the froth height was further increased to 20 cm. At a superficial air rate of 1.60 cm/s there was a decrease in chromite recovery as the froth height was increased. The tests conducted at a superficial air rate of 1.85 cm/s showed an increase in chromite recovery when froth height was increased from 10 to 15 cm, followed by a decrease when froth height was further increased to 20 cm.

Tests conducted to investigate the effect of increasing air rate showed that there was an increase in chromite recovery as the superficial air rate was increased for froth heights of 10 and 15 cm. At a froth height of 20 cm there was an increase in chromite recovery when superficial gas rate was increased from 1.35 to 1.60 cm/s followed by a decrease when superficial gas rate was further increased to 1.85 cm/s.

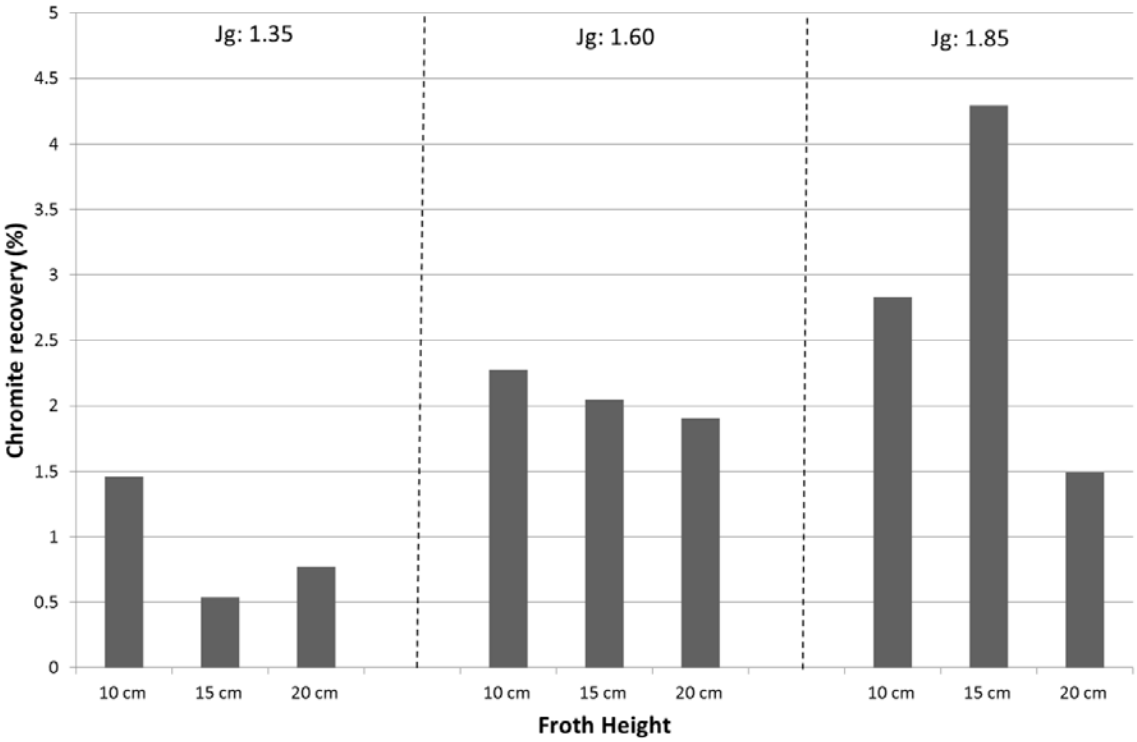

Figure 4. 19: Chromite recoveries for tests conducted at froth heights of 10, 15 and 20 cm and Jg of 1.35, 1.60 and 1.85 at a depressant dosage of 300 g/t.

The chromite recoveries as a function of water recovery are shown in Figure 4.20.
As shown previously the results exhibit the classical entrainment relationship once again emphasizing that chromite is mainly recovered via the mechanism of entrainment.

Figure 4.21 shows the average particle size for the concentrates obtained under these experimental conditions. At superficial air rates of 1.35 and 1.60 cm/s there was an increase in the average particle size as the froth height was increased. At a superficial air rate of 1.85 cm/s the average particle size initially increased slightly when froth height was increased from 10 to 15 cm, but decreased when froth height was further increased to 20 cm.

When evaluating the effect of changing air rate at constant froth heights of 10 and 15 cm, there was an increase in the average particle size as the superficial air rate was increased. At a froth height of 20 cm, there was a decrease in average particle size when superficial air rate was increased from 1.35 to 1.60 cm/s, with particle size not showing any change when froth height was further increased to 20 cm.

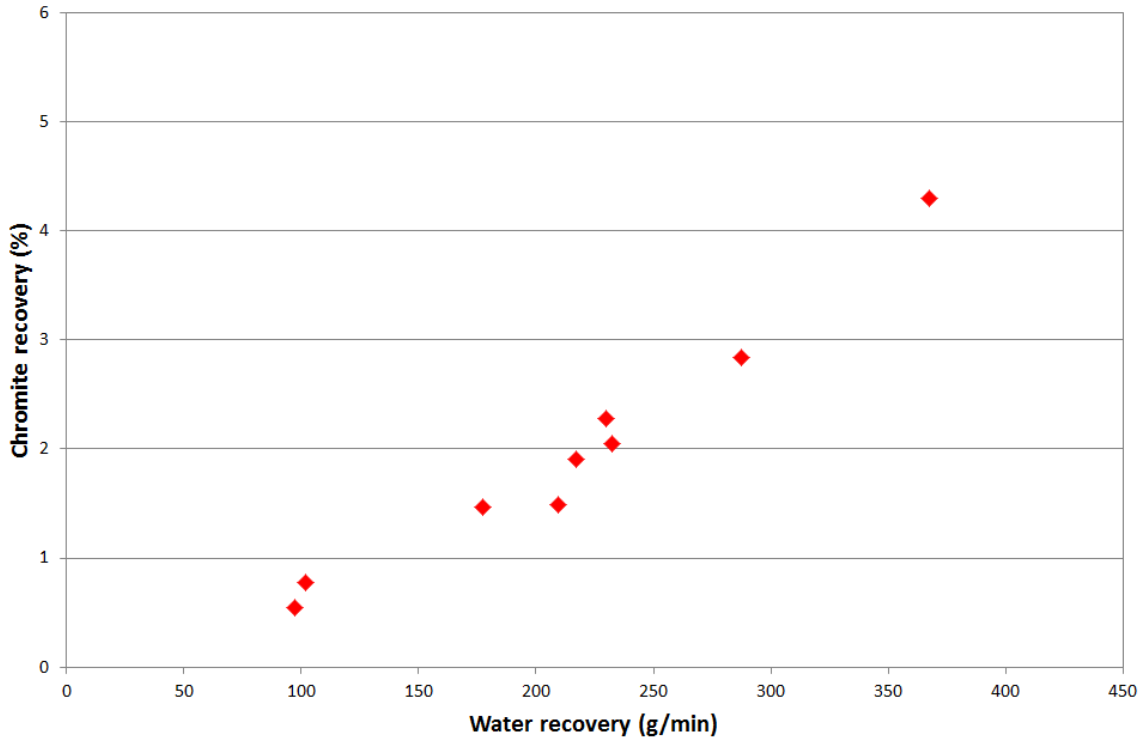

Figure 4. 20: Chromite recovery as a function of water recovery for tests conducted at froth heights of 10, 15 and 20 cm and Jg of 1.35, 1.60 and 1.85 at a depressant dosage of 300 g/t.

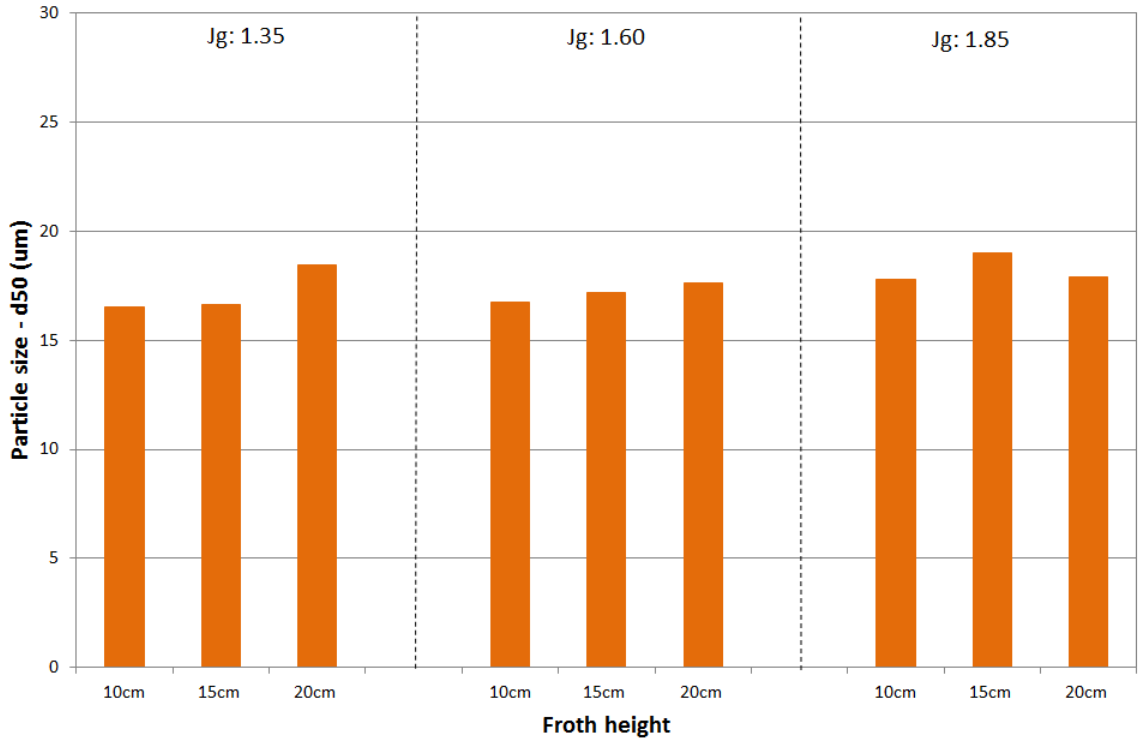

Figure 4. 21: D_{50} for all tests conducted at froth heights of 10, 15 and 20 cm and Jg of 1.35, 1.60 and 1.85 at a depressant dosage of 300 g/t.

4.3. The effect of depressant dosage on froth stability at a constant superficial air rate

This section is divided into three sub-sections each focusing on the effect of changing depressant when operating at froth heights of 10, 15 and 20 cm and superficial air rates of 1.35, 1.60 and 1.85 cm/s.

Test conditions

As in section 4.2, the pulp was conditioned using collector, SIBX, at a dosage of 80 g/t and frother, Dow 200, at a dosage of 25.2 ppm. The depressant dosages used were 0, 100 and 300 g/t depending on the individual experiment. For the first investigation, the air rate was set to 1.35 cm/s and the height of froth in the in column was maintained at 10, 15 or 20 cm.

The tests were then repeated using superficial air rates of 1.60 and 1.85 cm/s. Since the same data set from section 4.2 was used, the effect of changing froth height will not be analysed in this section.

4.3.1. The effect of depressant dosage on froth stability at a superficial air rate of 1.35 cm/s

The solids and water recovered for this set of conditions is shown in Figure 4.22. From this data set it is evident that at the three froth heights investigated, there was an increase in both solids and water recoveries when the depressant dosage was increased from 0 to 100 g/t followed by a decrease when the dosage was further increased to 300 g/t. This increase was most pronounced when the experiments were conducted using a 10 cm froth height.

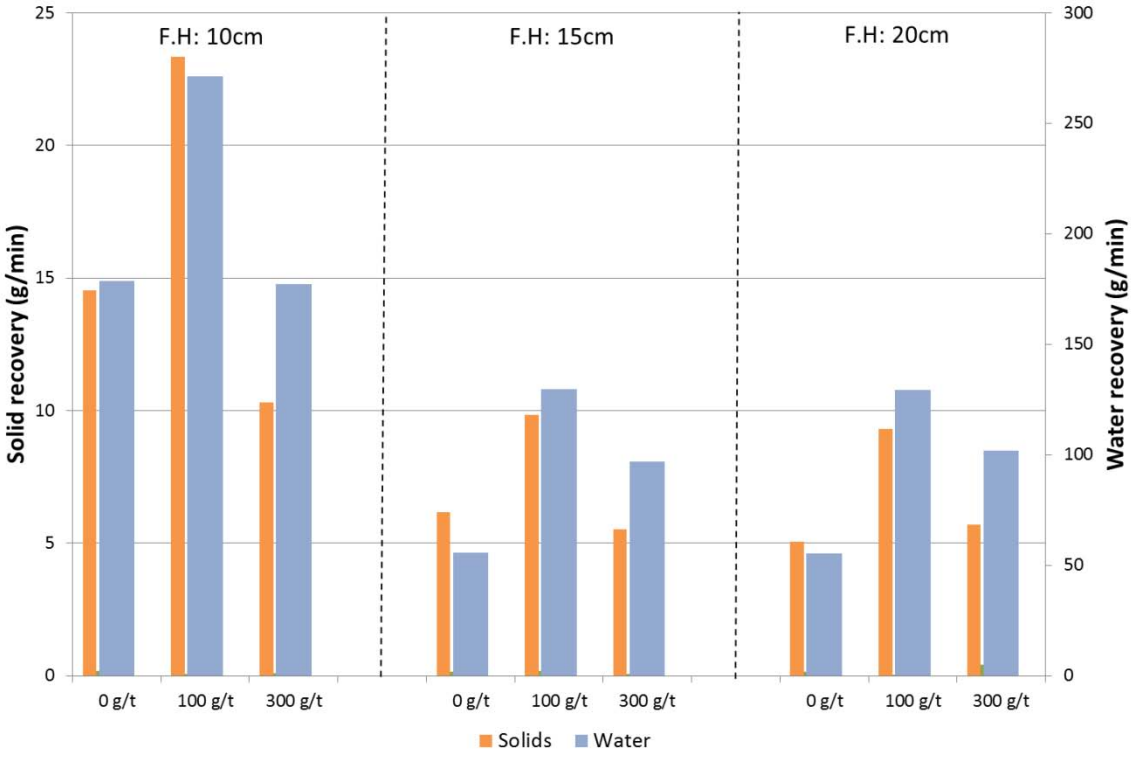

Figure 4. 22: Solids and water recovered from tests conducted at froth heights of 10, 15 and 20 cm and depressant dosages of 0, 100 and 300 g/t at a Jg of 1.35 cm/s.

The corresponding bubble burst rate data are shown in Figure 4.23 where different trends were observed for the three froth heights investigated. At a froth height of 10 cm there was an increase in the bubble burst rate when the depressant dosage was increased from 0 to 100 g/t, which was followed by a decrease when the dosage was further increased to 300 g/t. At a froth height of 15 cm there was a slight decrease in burst rate when the depressant dosage was increased from 0 to 100 g/t followed by an increase thereafter. When the 20 cm froth height was used, the burst rate increased with increasing depressant dosage.

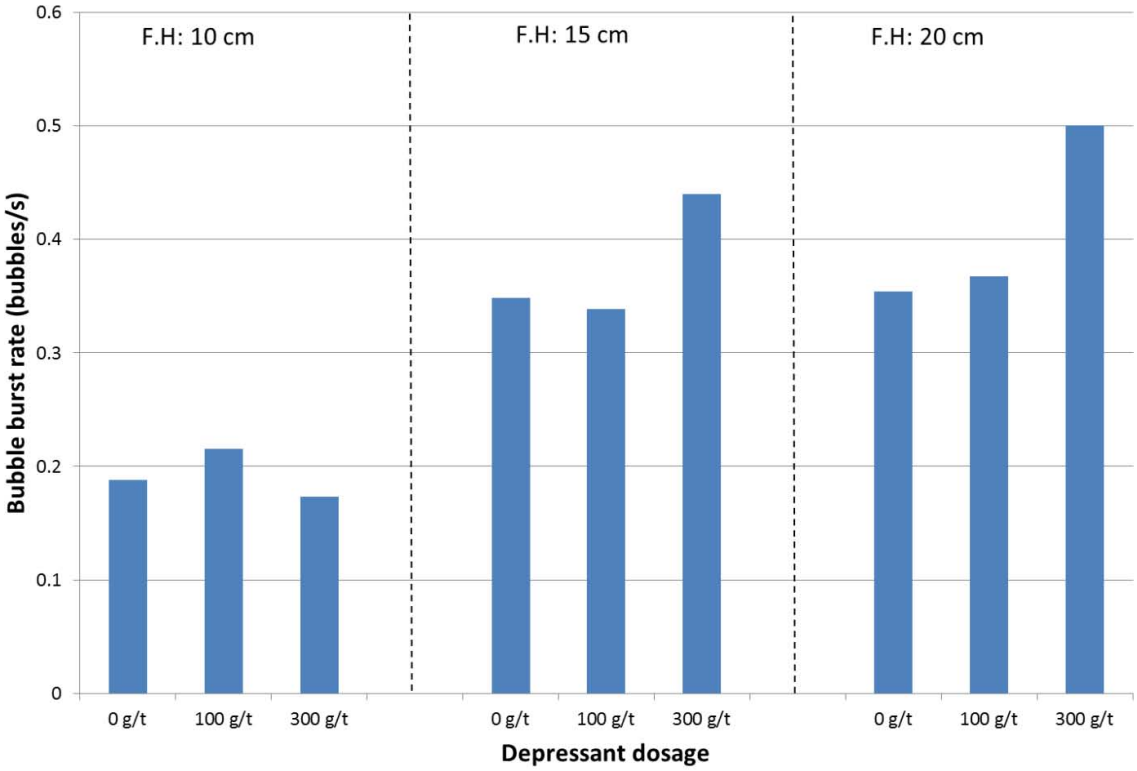

Figure 4. 23: Top-of-froth bubble burst rate for tests conducted at froth heights of 10, 15 and 20 cm and depressant dosages of 0, 100 and 300 g/t at a Jg of 1.35 cm/s.

The relationship between the top of froth bubble burst rate and the water recovery is shown in Figure 4.24. These relationships were drawn with increasing froth height at different depressant dosages. And the figure shows that the trends are shifted to the right as the depressant dosage is increased from 0 to 100 g/t. Which suggests that there was a decrease in the stability of the froth when the depressant dosage was increased from 0 to 100 g/t. The data obtained at 300 g/t was very scattered and could not be used to interpret stability.

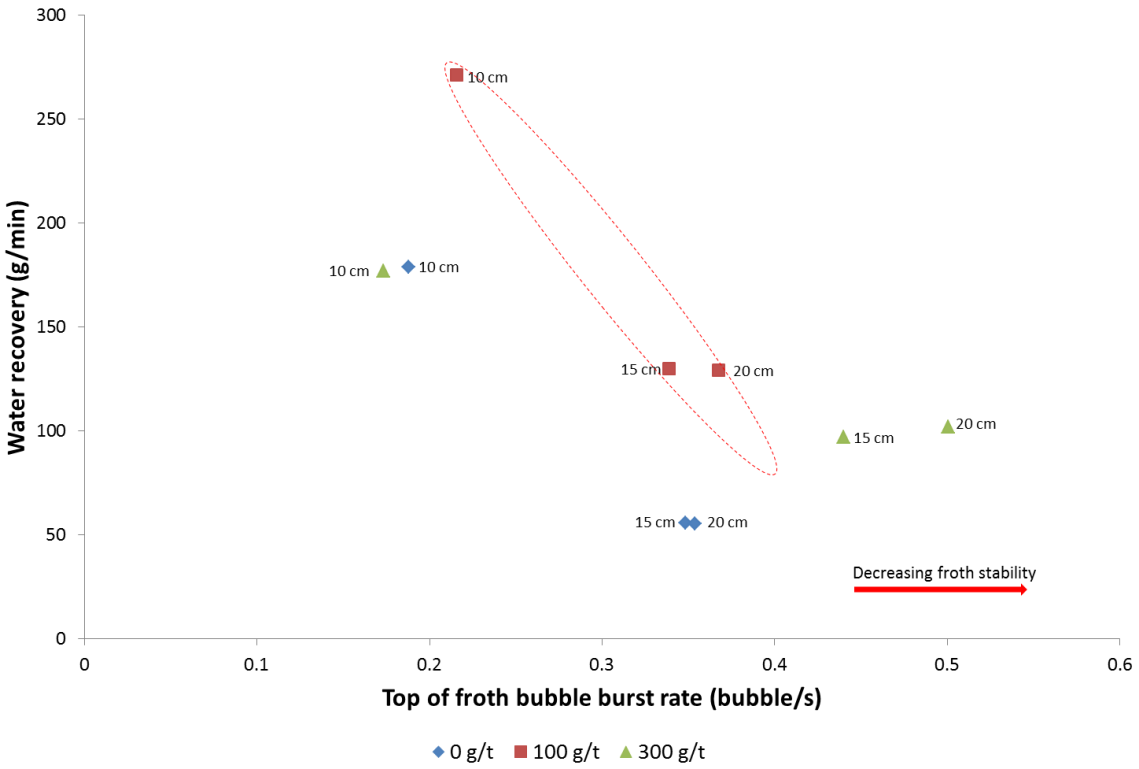

Figure 4. 24: Top-of-froth bubble burst rate as a function of water recovery for tests conducted at froth heights of 10, 15 and 20 cm and depressant dosages of 0, 100 and 300 g/t at a Jg of 1.35 cm/s.

The corresponding PGM recoveries are shown in Figure 4.25.With the exception of the results at a froth height of 20 cm, the PGM recoveries showed similar results to those observed for the solid and water recoveries in Figure 4.22. When 10 and 15 cm froth heights were used in the column a peak in recovery was observed at the 100 g/t depressant dosage. At a froth height of 20 cm the PGM recovery increased as the depressant dosage was increased.

At the three froth heights investigated the chromite recoveries showed peaks in recovery at a depressant dosage of 100 g/t. The peak was more apparent at the froth height of 10 cm and least apparent at the 20 cm froth height as shown in Figure 4.26.

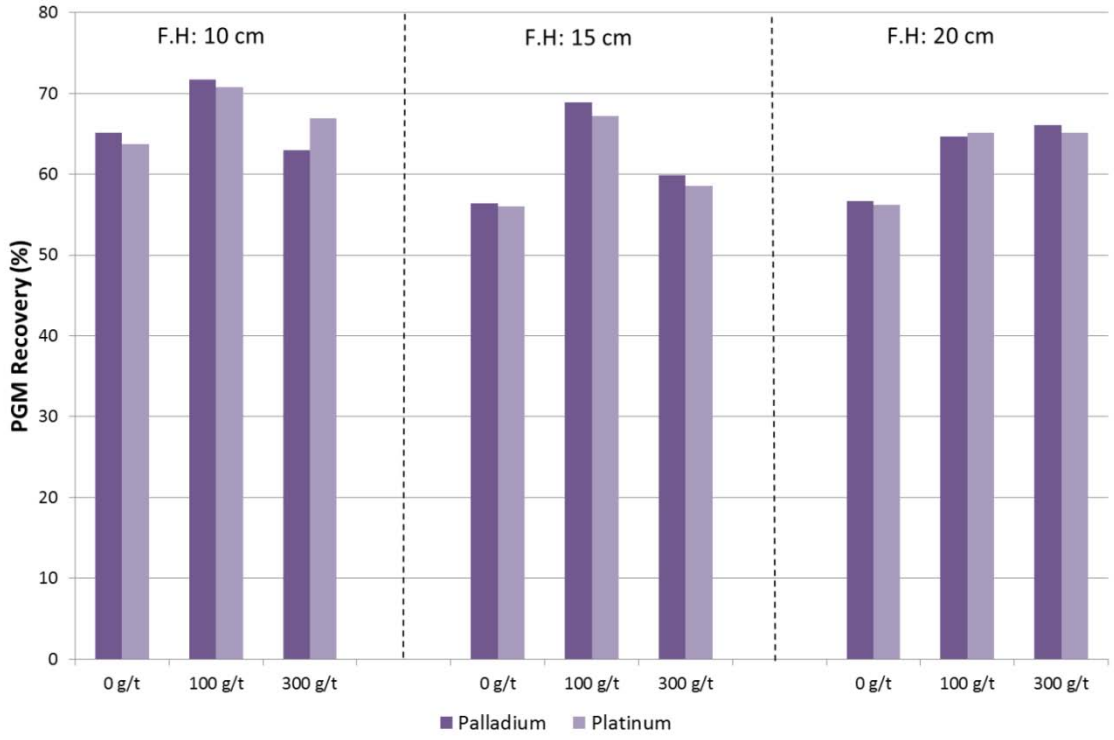

Figure 4. 25: Platinum and palladium recoveries for tests conducted at froth heights of 10, 15 and 20 cm and depressant dosages of 0, 100 and 300 g/t at a Jg of 1.35 cm/s.

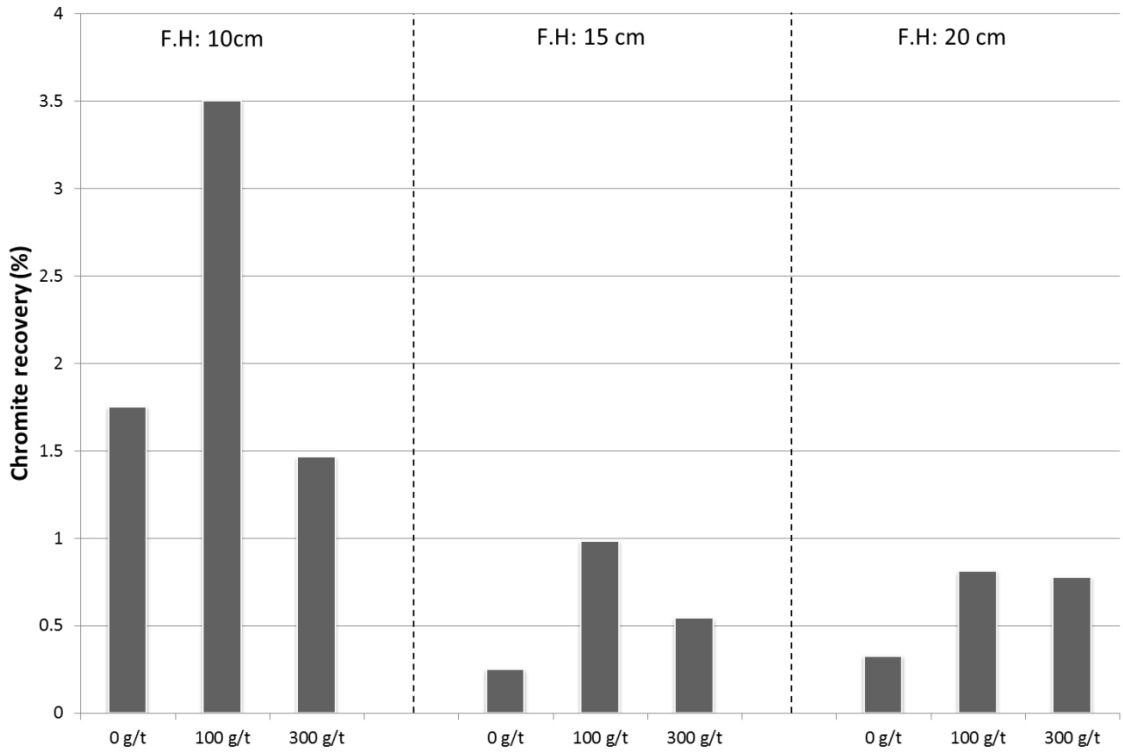

Figure 4. 26: Chromite recoveries for tests conducted at froth heights of 10, 15 and 20 cm and depressant dosages of 0, 100 and 300 g/t at a Jg of 1.35 cm/s.

Figure 4.27 shows the relationship between chromite recovery and water recovery. As in the previous sections, there is a direct relationship between the water and chromite recoveries that is the chromite recovery increases as the water recovery increases.

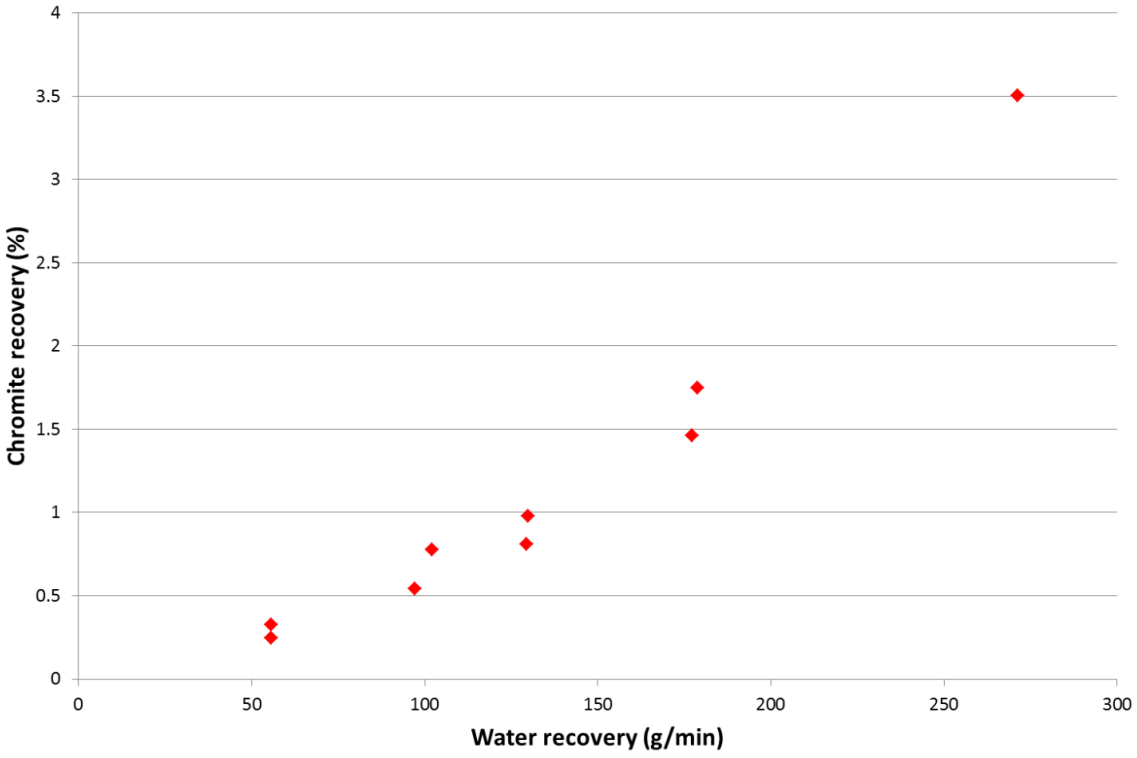

Figure 4. 27: Chromite recovery as a function of water recovery for tests conducted at froth heights of 10, 15 and 20 cm and depressant dosages of 0, 100 and 300 g/t at a Jg of 1.35 cm/s.

The effect of depressant dosage on the particle size distribution was different for the three froth heights that were investigated as shown in Figure 4.28. At a froth height of 10 cm, there was an increase in the particle size between the depressant dosages of 0 and 100 g/t, after which the particle size significantly decreased. At a froth height of 15 cm, there was a continuous decrease in the particle size as the depressant dosage was increased. And at a froth height of 20 cm the particle size decreased between dosages of 0 and 100 g/t after which it plateaued.

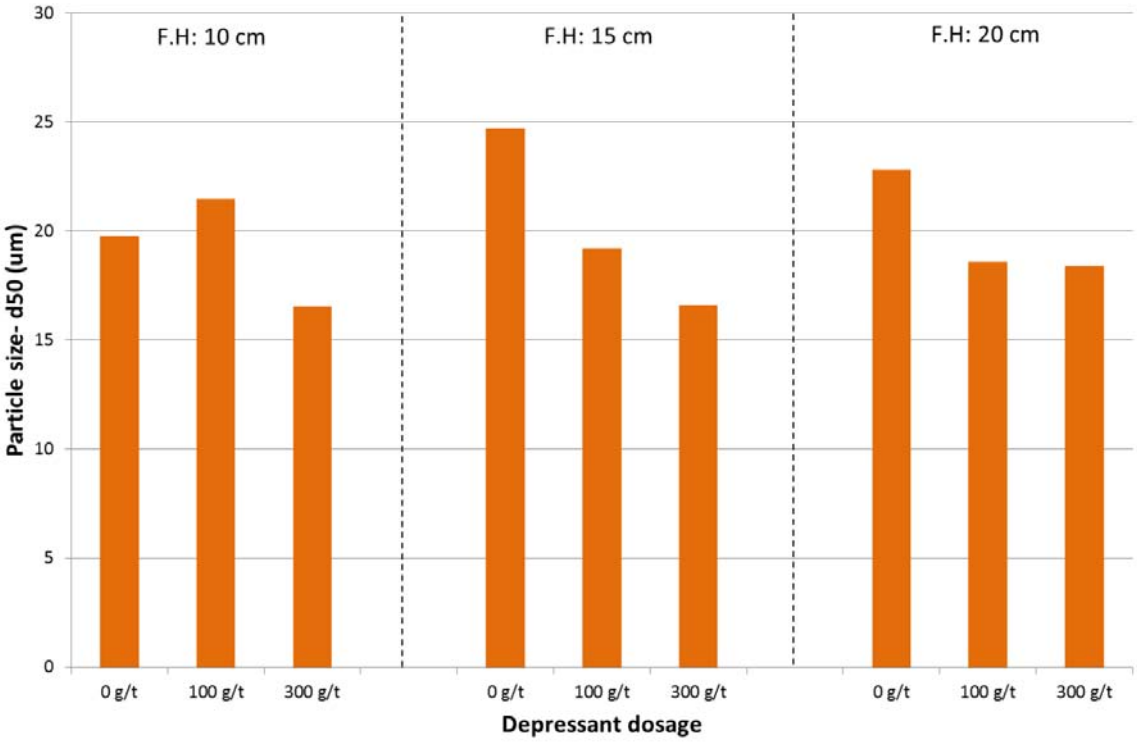

Figure 4. 28: D_{50} for all tests conducted at depressant dosages of 0, 100, and 300 g/t and froth heights of 10, 15 and 20 cm at a Jg of 1.35 cm/s.

4.3.2. The effect of depressant dosage on froth stability at a superficial air rate of 1.60 cm/s

The experiments were repeated using a superficial air rate of 1.60 cm/s and the solids and water recoveries are shown in Figure 4.29. At this air rate the solids and water recovery trends were very similar at the three froth heights investigated. Similar to the tests conducted at 1.35 cm/s, both recoveries increased between the depressant dosages of 0 and 100 g/t and thereafter decreased, resulting in the formation of a peak at 100 g/t.

The corresponding bubble burst rate data are shown in Figure 4.30; as the depressant dosage was increased from 0 to 100 g/t the top of froth bubble burst rate decreased, and when the depressant was further increased to 300 g/t the burst rate also increased. At all three froth heights investigated the burst rate trend formed a mirror image of the water recovery data in Figure 4.29, which shows that under these conditions there was a very good relationship between the two.

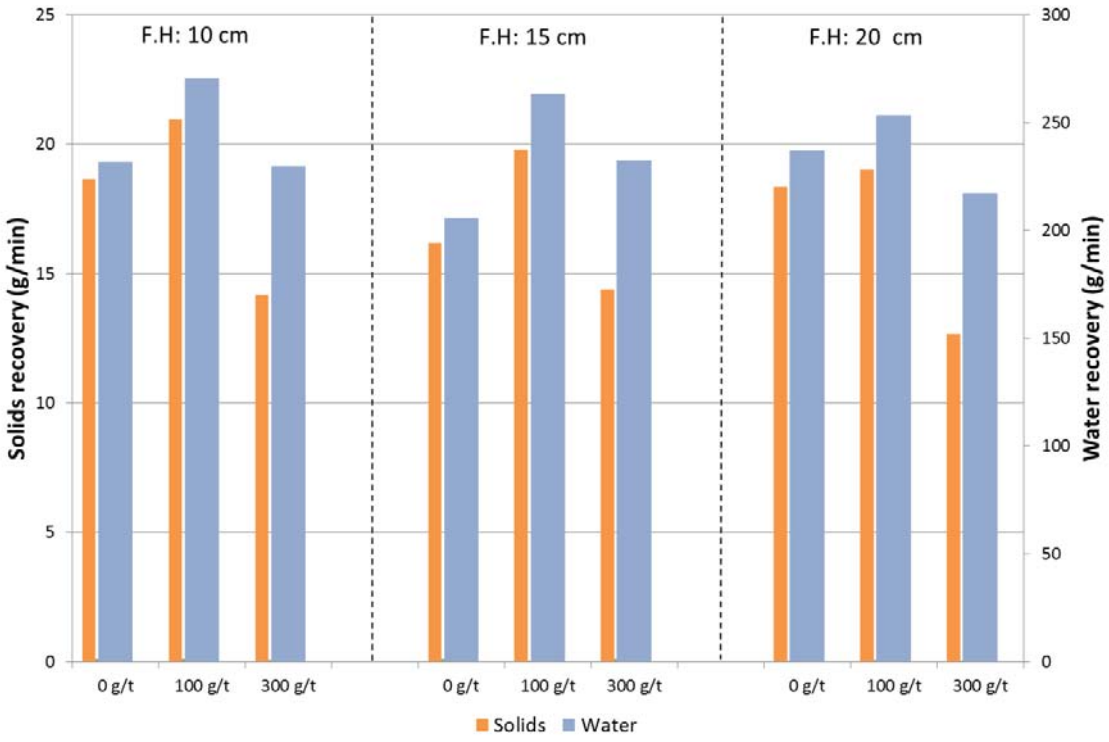

Figure 4. 29: Solids and water recovered from tests conducted at froth heights of 10, 15 and 20 cm and depressant dosages of 0, 100 and 300 g/t at a Jg of 1.60 cm/s.

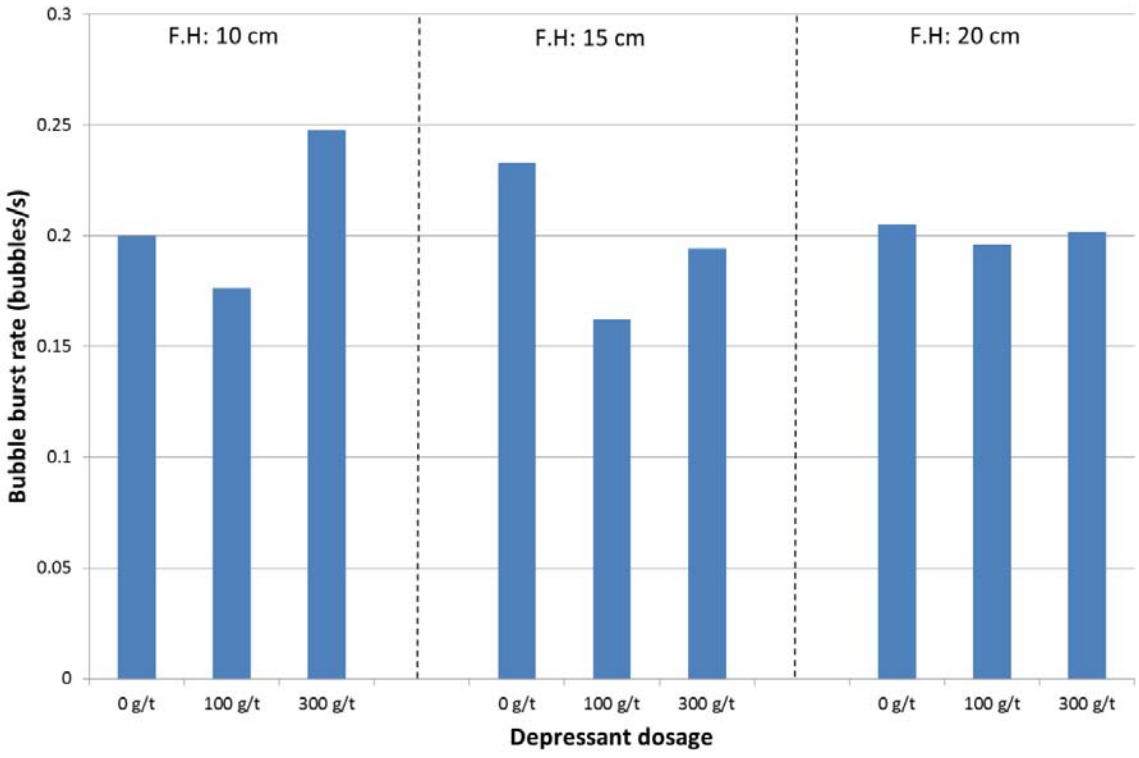

Figure 4. 30: Top-of-froth bubble burst rate for tests conducted at froth heights of 10, 15 and 20 cm and a depressant dosage of 0, 100 and 300 g/t at a Jg of 1.60 cm/s.

The relationship between water recovery and top of froth burst rate was further investigated and the plot obtained is shown in Figure 4.31. Under these conditions, all the data pointsaccumulate along one trend line. Which shows that at a superficial air rate of 1.60 cm/s there were negligible differences in the stability of the froth as the depressant dosage was increased.

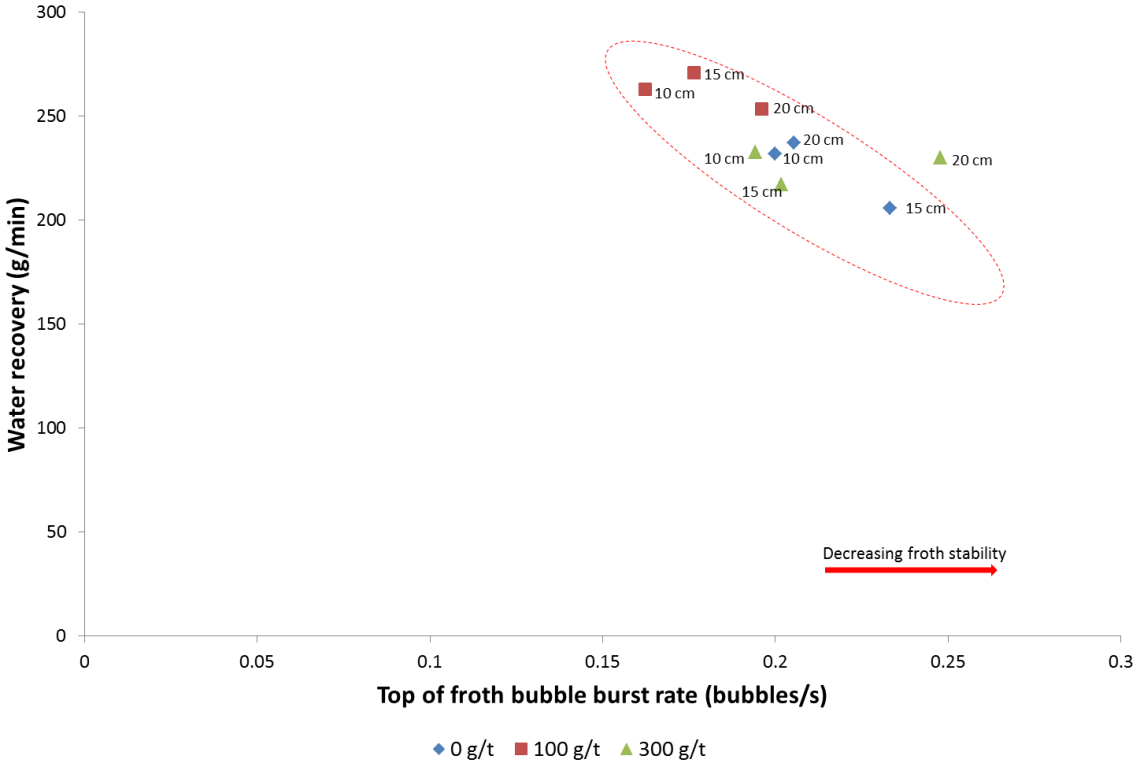

Figure 4. 31: Top-of-froth bubble burst rate as a function of water recovery for tests conducted at froth heights of 10, 15 and 20 cm and depressant dosages of 0, 100 and 300 g/t at a Jg of 1.60 cm/s.

The PGM recoveries showed two distinct trends as the depressant dosage was increased as shown in Figure 4.32. At a froth height of 10 cm, the recoveries increased with increasing depressant dosage; whilst at a froth height of 15 and 20 cm there was a peak in the PGM recoveries at 100 g/t depressant dosage.

The chromite recoveries are shown in Figure 4.33, and these showed that at froth heights of 10 and 15 there was an increase in the chromite recoveries as the depressant dosage was increased. At 20 cm there was a slight peak in the chromite recovery at a depressant dosage of 100 g/t.

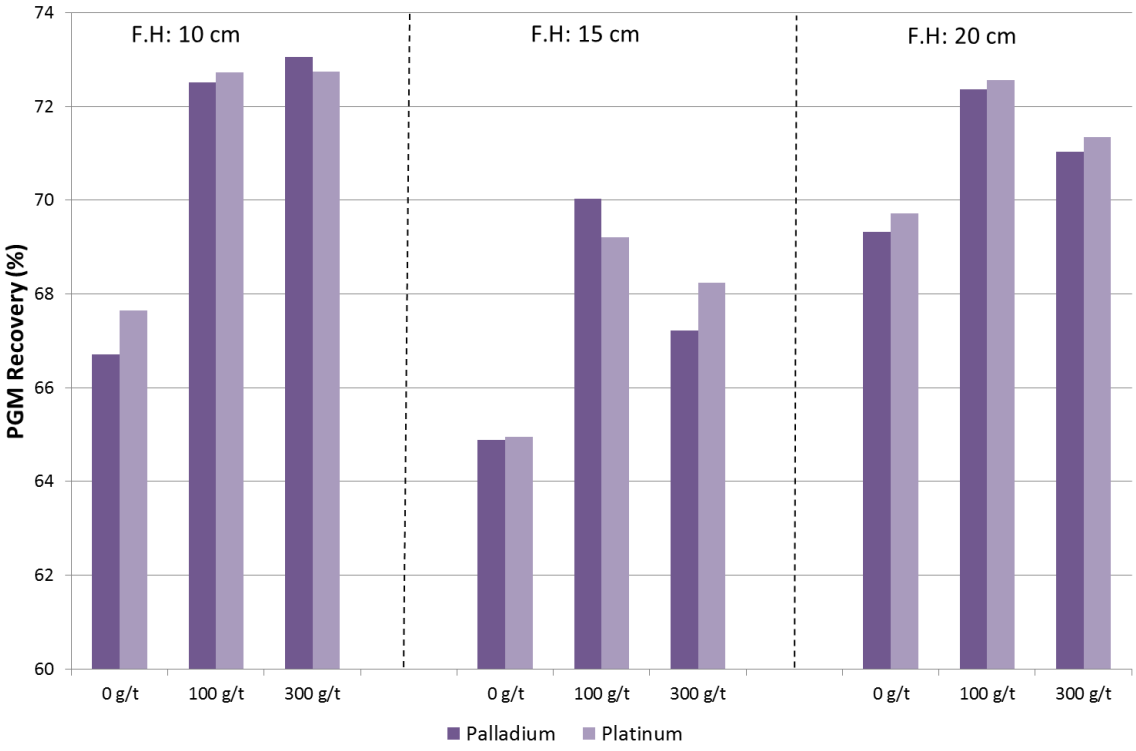

Figure 4. 32: Platinum and palladium recoveries for tests conducted at froth heights of 10, 15 and 20 cm and depressant dosages of 0, 100 and 300 g/t at a Jg of 1.60 cm/s.

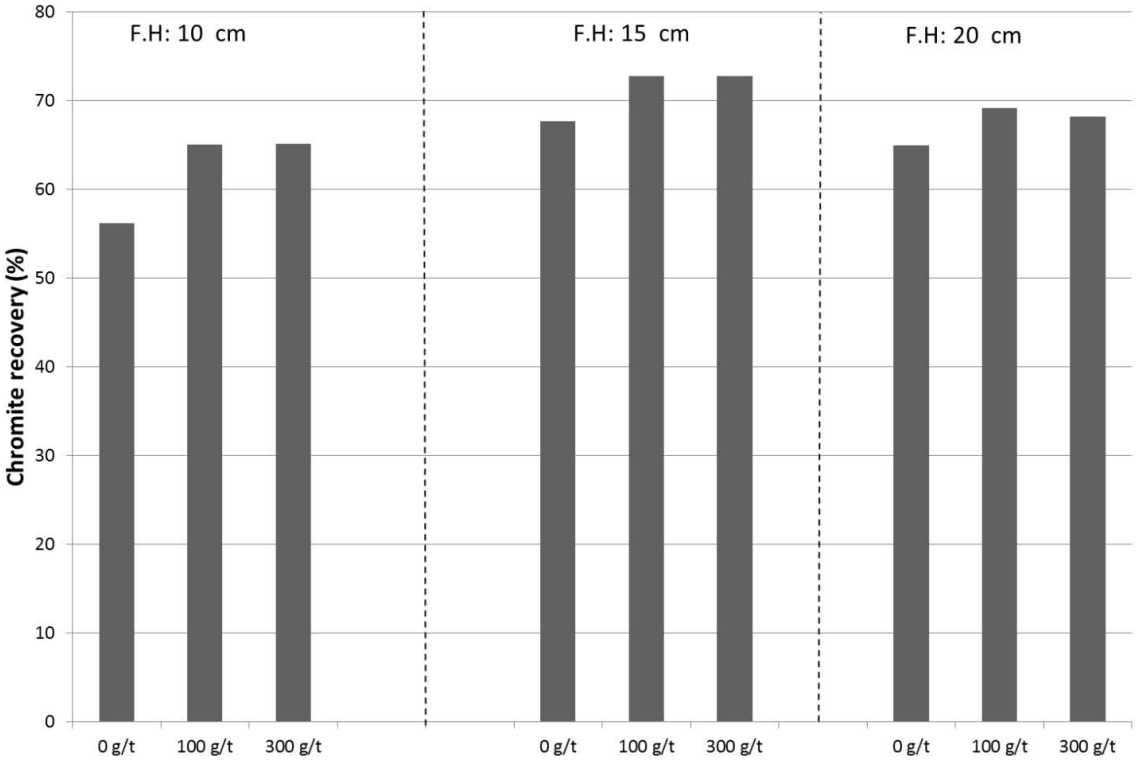

Figure 4. 33: Chromite recoveries for tests conducted at froth heights of 10, 15 and 20 cm and depressant dosages of 0, 100 and 300 g/t at a Jg of 1.60 cm/s.

As seen previously, there was a direct relationship between the chromite recovery and the water recovery as shown in Figure 4.34.

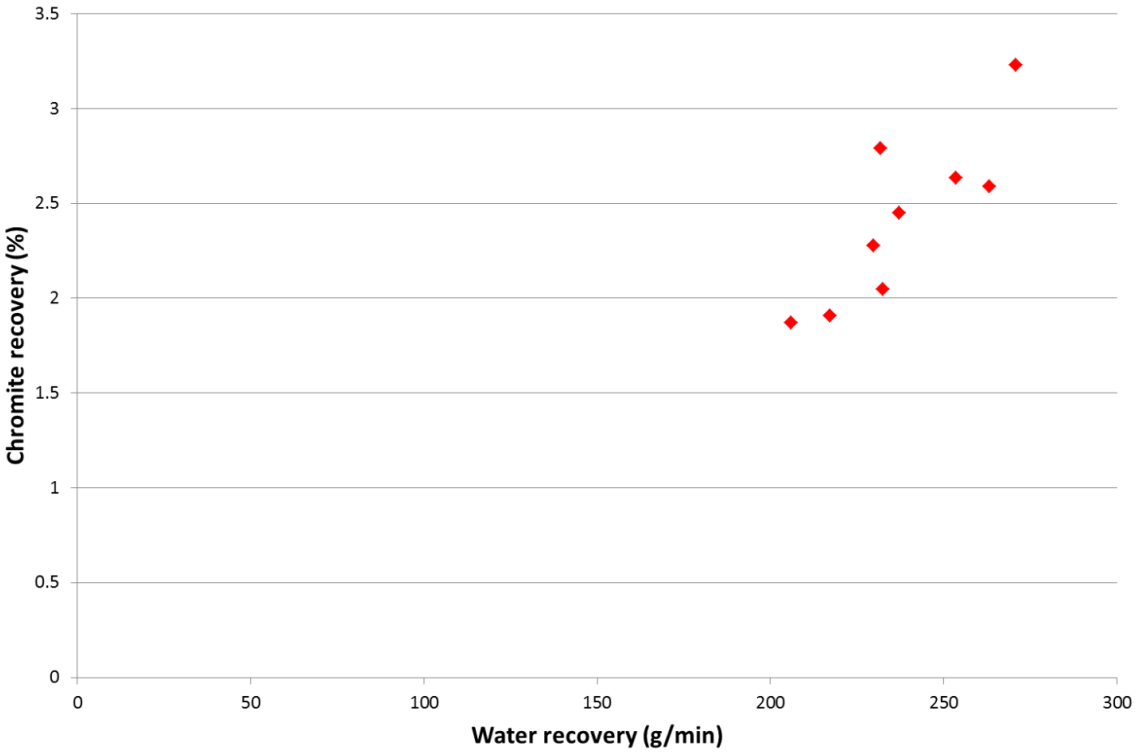

Figure 4. 34: Chromite recovery as a function of water recovery for tests conducted at froth heights of 10, 15 and 20 cm and depressant dosages of 0, 100 and 300 g/t at Jg of 1.60 cm/s.

The particle size distribution under these conditions is shown in Figure 4.35, which shows that for froth heights of 10 and 15 cm there was a decrease in particle size as the depressant dosage was increased. And at 20 cm froth height there was a peak in the particle size at a depressant dosage of 100 g/t as the depressant dosage was increased.

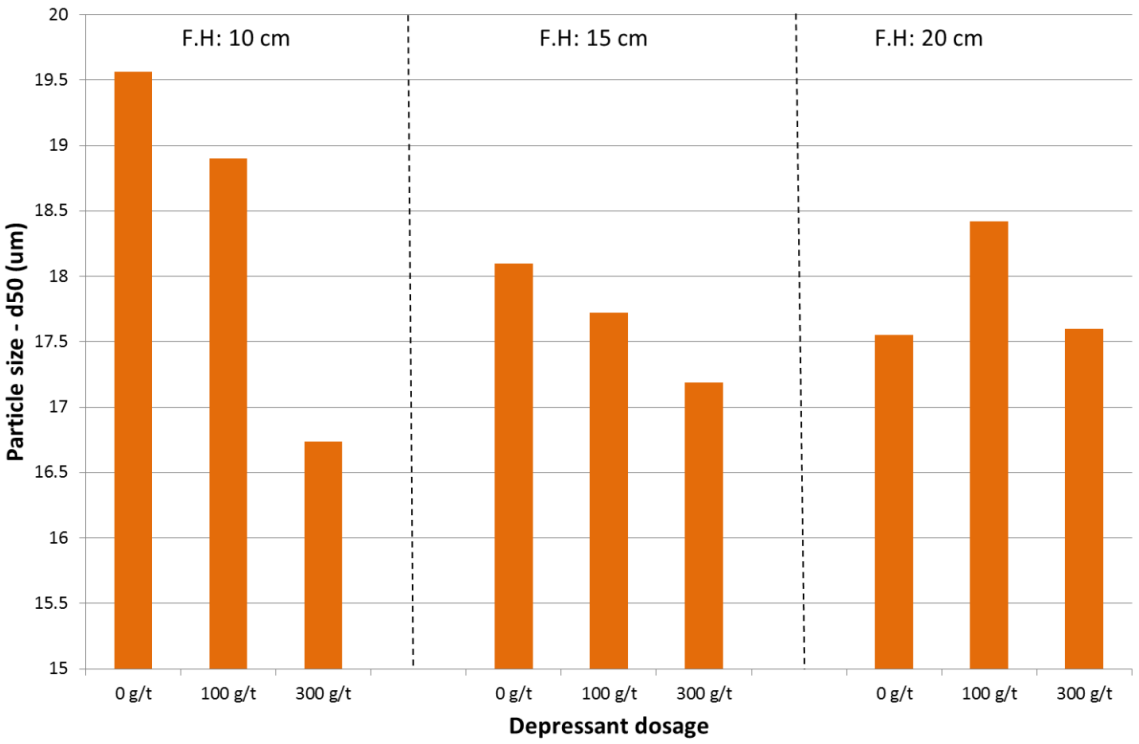

Figure 4. 35: D_{50} for all tests conducted at depressant dosages of 0, 100, and 300 g/t and froth heights of 10, 15 and 20 cm at a Jg of 1.60 cm/s.

4.3.3. The effect of depressant dosage on froth stability at an air rate of 1.85 cm/s

The last investigation was conducted at a constant air rate of 1.85 cm/s while changing the depressant dosage and froth height.

The solids and water recoveries that were obtained at this air rate are shown in Figure 4.36. This shows that at froth heights of 10 and 20 cm there was a peak in both solids and water recoveries at 100 g/t depressant dosage, when the depressant dosage was increased from 0 to 300 g/t. At 15 cm froth height both recoveries increased with increasing depressant dosage.

The corresponding bubble burst rate data are shown in Figure 4.37 which shows that there were three different trends at the different froth heights as the depressant dosage was increased. When a froth height of 10 cm was used, there was a decrease in bubble burst rate when depressant dosage was increased from 0 to 100 g/t, followed by an increase thereafter. At 15 cm froth height the bubble burst rate increased with increasing depressant dosage, and at 20 cm froth height the burst rate increased between depressant dosages of 0 and 100 g/t and decreased between 100 and 300 g/t.

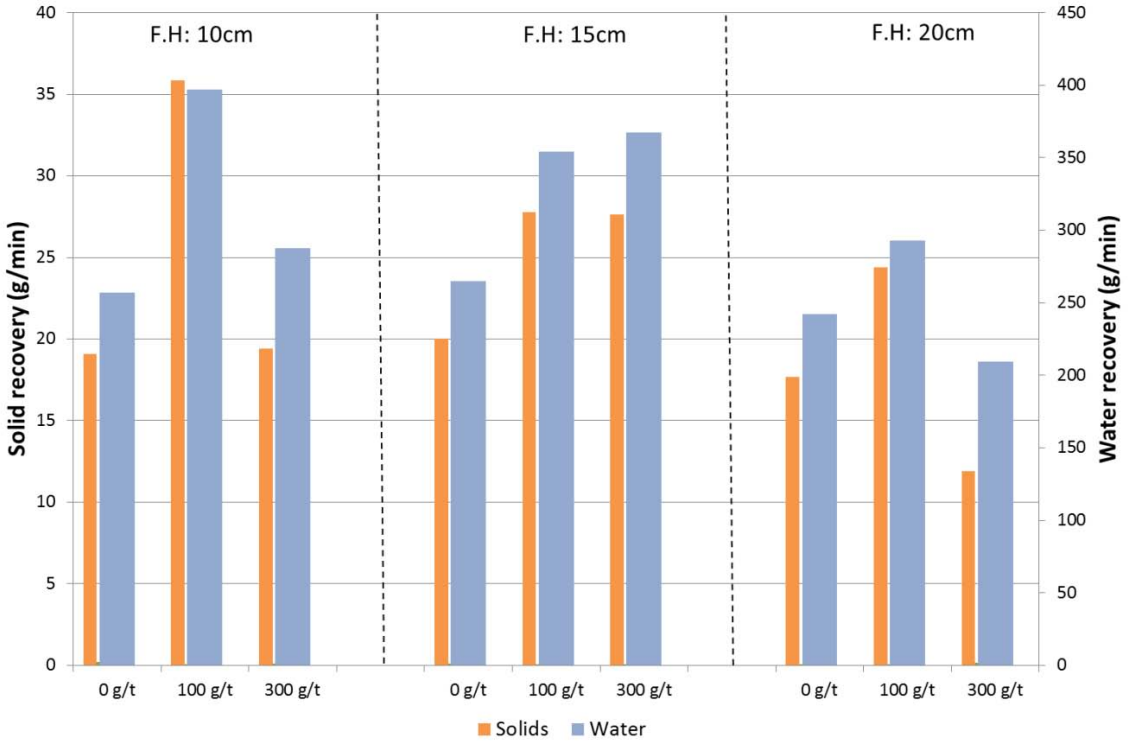

Figure 4. 36: Solids and water recovered from tests conducted at froth heights of 10, 15 and 20 cm and depressant dosages of 0, 100 and 300 g/t at a Jg of 1.85 cm/s.

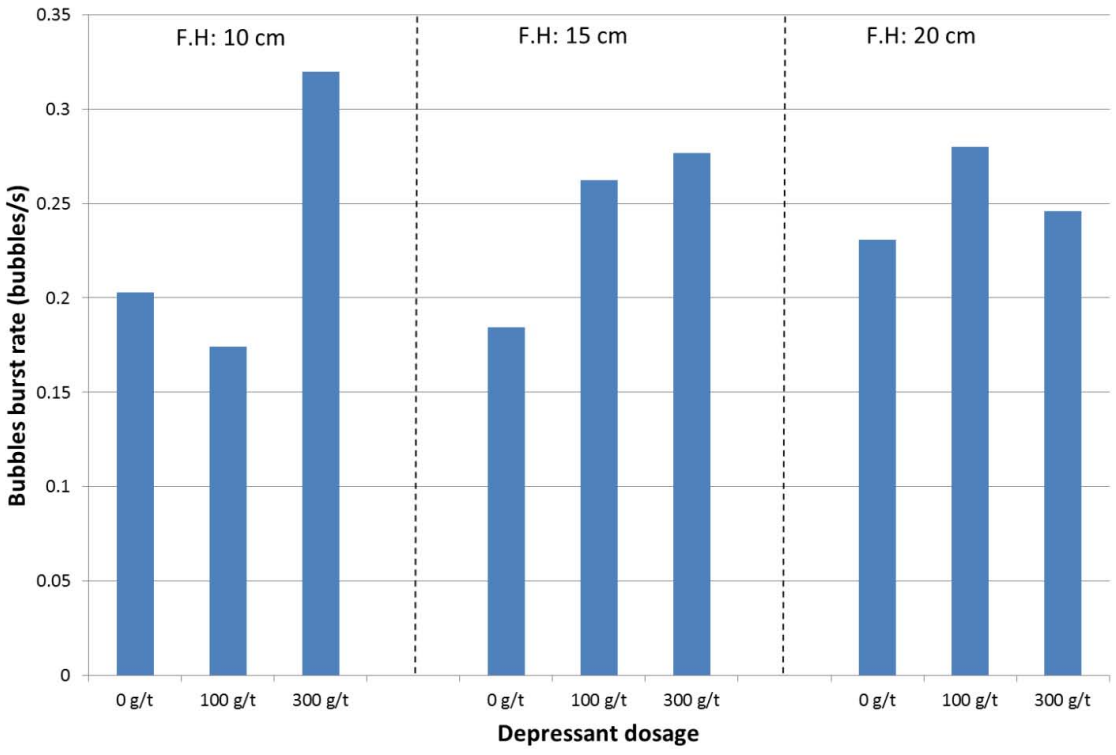

Figure 4. 37: Top-of-froth bubble burst rate for tests conducted at froth heights of 10, 15 and 20 cm and a depressant dosage of 0, 100 and 300 g/t at a Jg of 1.85 cm/s.

The relationship between the bubble burst rate and water recovery is shown in Figure 4.38. As the depressant dosage was increased these trends were shifted to the right due to an increase in the top of froth bubble burst rate, this suggests the froth became less stable with increasing depressant dosage.

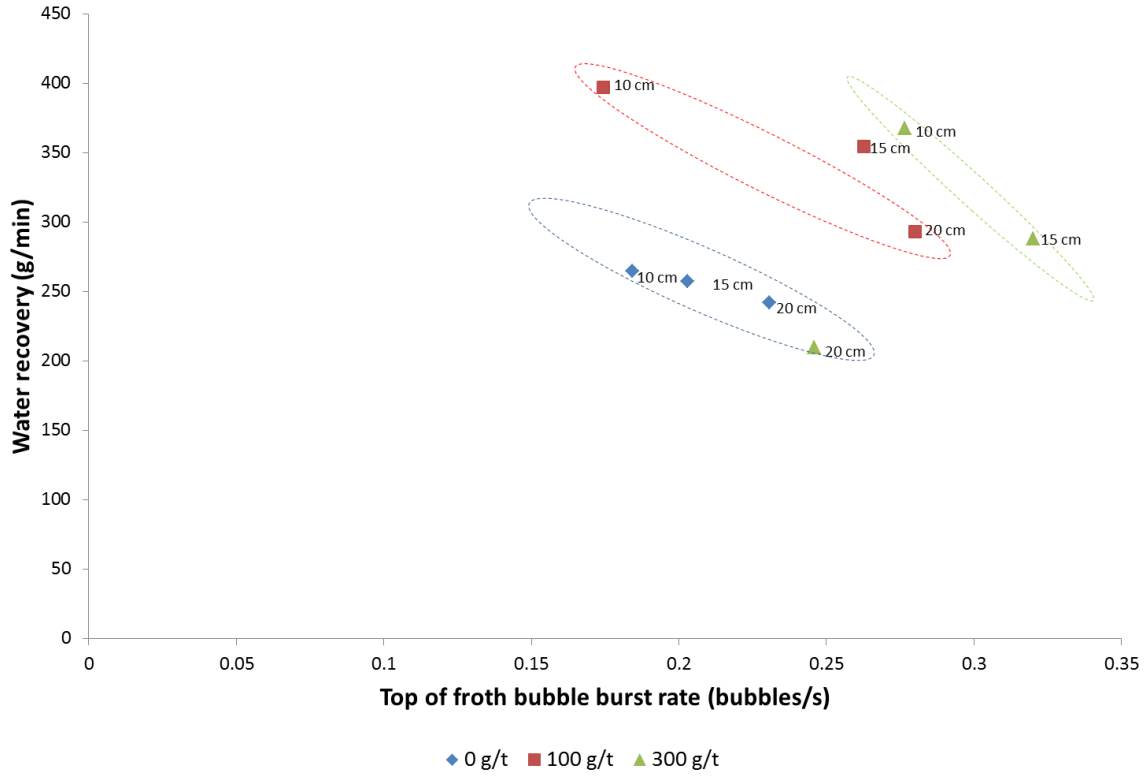

Figure 4. 38: Top-of-froth bubble burst rate as a function of water recovery for tests conducted at froth heights of 10, 15 and 20 cm and depressant dosages of 0, 100 and 300 g/t at a Jg of 1.85 cm/s.

The PGM recoveries for these tests are shown in Figure 4.39. At 10 and 20 cm froth height there was an increase in PGM recovery when depressant dosage was increased from 0 to 100 g/t, further increase in depressant dosage resulted in a decrease in the recoveries. At a froth height of 15 cm the palladium recovery increased with increasing depressant dosage, and the platinum recovery peaked at a depressant dosage of 100 g/t, but was more subtle that those observed at 10 and 20 cm froth heights.

The corresponding chromite recovery data are shown in Figure 4.40. At froth heights of 10 and 20 cm there was an increase in chromite recovery when the depressant dosage was increased from 0 to 100 g/t followed by a decrease thereafter. At a froth height of 15 cm, however, the chromite recovery continued to increase as the depressant dosage was increased. These trends were similar to those obtained for the solids and water recoveries.

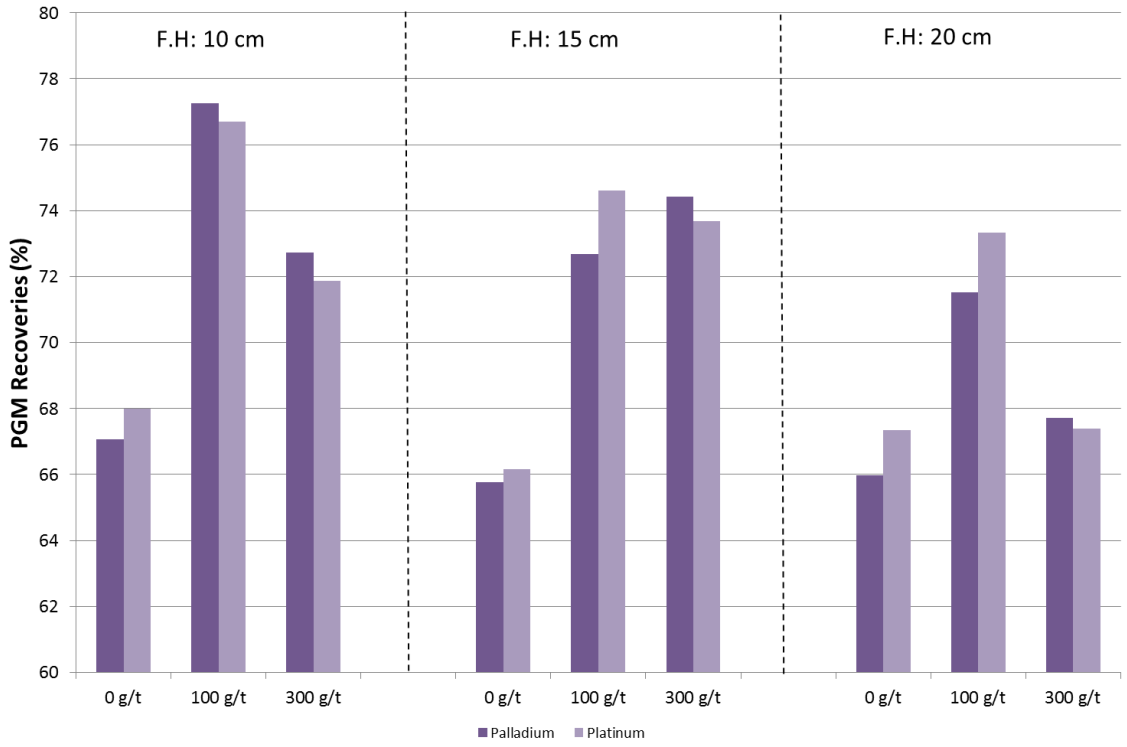

Figure 4. 39: Platinum and palladium recoveries for tests conducted at froth heights of 10, 15 and 20 cm and depressant dosages of 0, 100 and 300 g/t at a Jg of 1.85 cm/s.

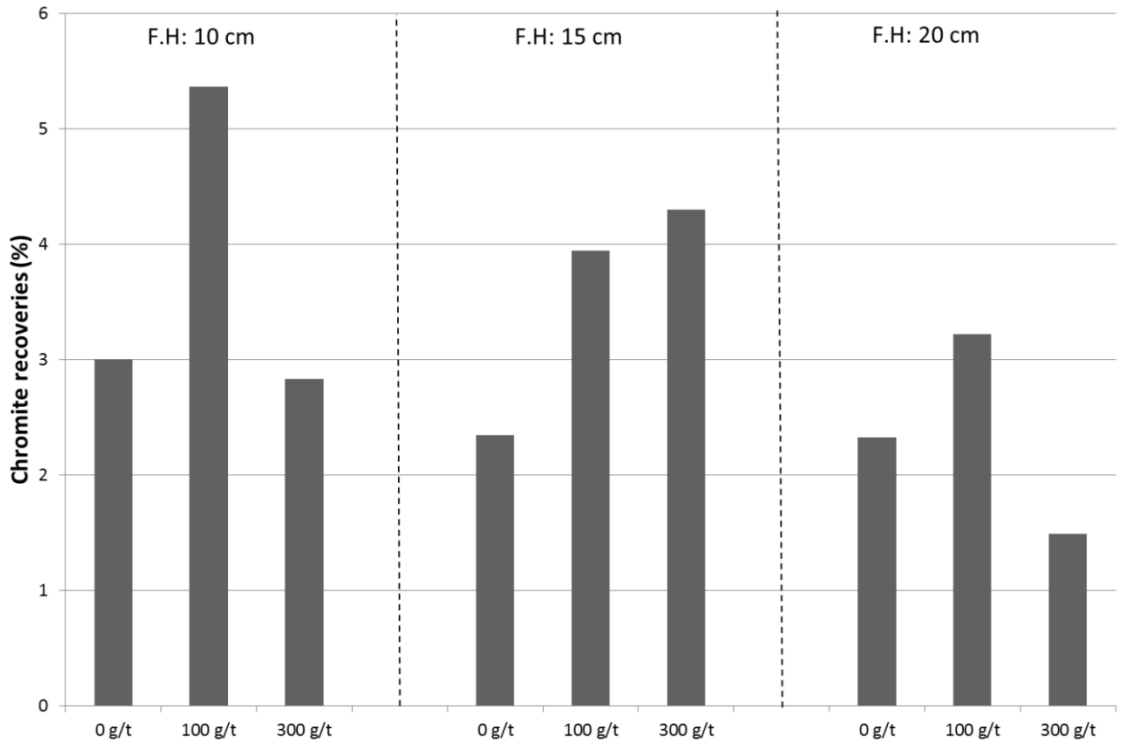

Figure 4. 40: Chromite recoveries for tests conducted at froth heights of 10, 15 and 20 cm and depressant dosages of 0, 100 and 300 g/t at a Jg of 1.85 cm/s.

As in the previous sections there was a direct relationship between the water and chromite recoveries, as shown in Figure 4.41. As the water recovery increased, the chromite recovery also increased.

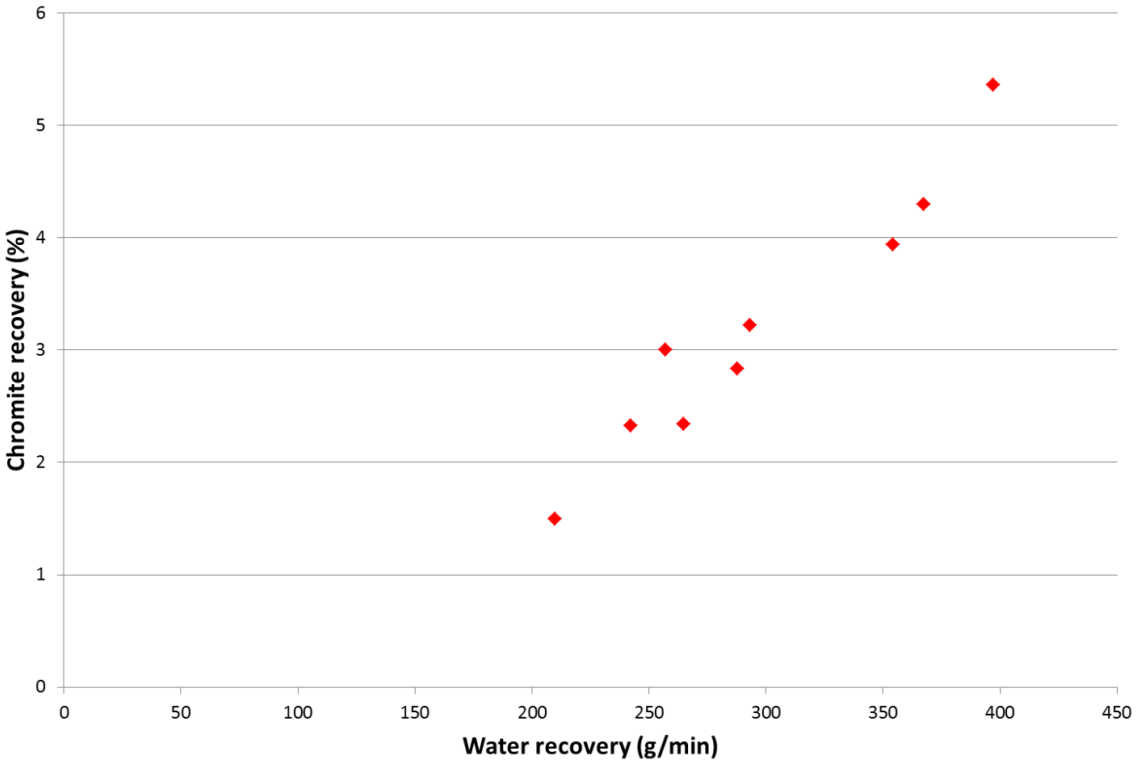

Figure 4. 41: Chromite recovery as a function of water recovery for tests conducted at froth heights of 10, 15 and 20 cm and depressant dosages of 0, 100 and 300 g/t at a Jg of 1.85 cm/s.

Figure 4.42 shows the particle size distribution of the concentrates as the depressant dosage was increased. At froth heights of 10 and 15 cm, the particle size increased when the depressant dosage was increased from 0 to 100 g/t, further increases in dosage resulted in a decrease in particle size. A similar trend was observed at 20 cm froth height, the only difference being that the difference in particle size between 0 and 100 g/t was very slight.

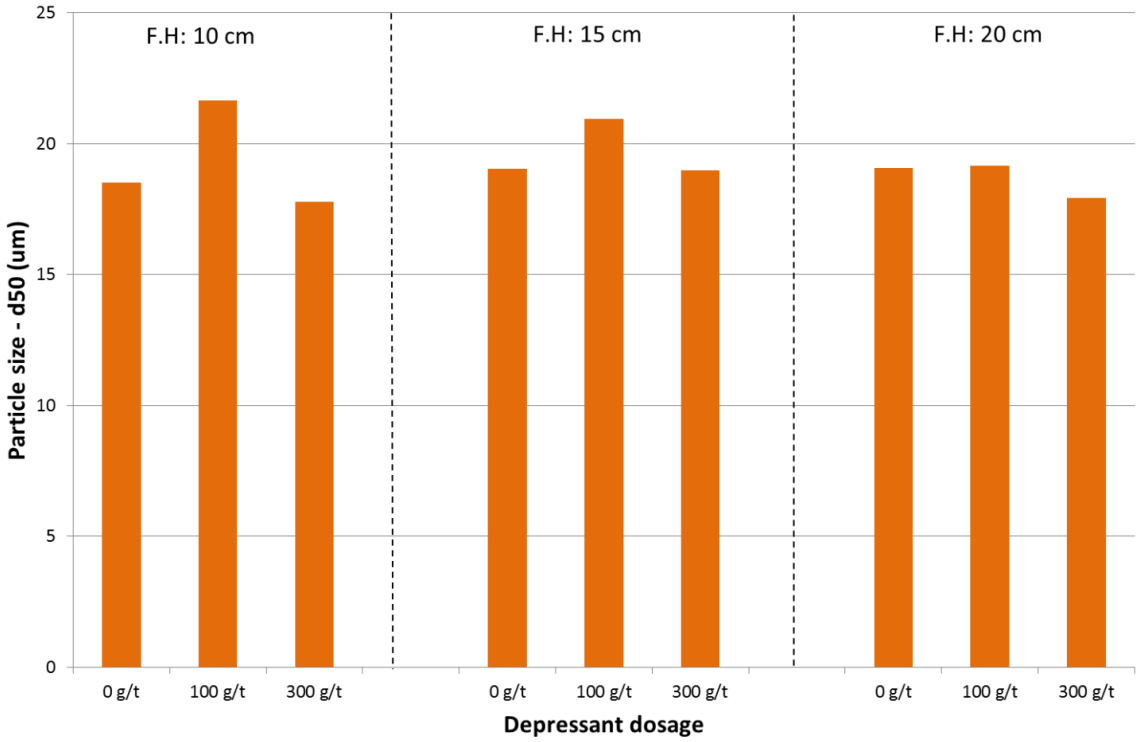

Figure 4. 42: D_{50} for all tests conducted at depressant dosages of 0, 100, and 300 g/t and froth heights of 10, 15 and 20 cm at a Jg of 1.85 cm/s.

CHAPTER FIVE : DISCUSSION

5.1. Introduction

The aim of this study was to investigate the changes in the stability of the froth phase when the froth height, superficial air rate and depressant dosage were varied.

Whilst there are many different methods that have been used to determine froth stability, the method utilised in this study was to compare the relationship between water recovery and the top of froth bubble burst rate. The specific methodology used is described in Chapter Three and the results obtained are shown in Chapter Four. The results from this analysis were then used to account for the changes observed in PGM and chromite recovery, as well as the concentrate particle size distribution.

The chapter is divided into three sections, with each section focusing on the effect of changing one of the aforementioned parameters on the stability of the froth.

5.2. The effect of froth height on froth stability

The first set of experiments was conducted to investigate the effect of changing froth height on the stability of the froth phase. It was expected that increasing the froth height would increase the drainage of water and entrained particles from the froth back into the pulp phase, which would ultimately affect both the recoveries and the grade of the concentrates (Ata et al., 2002, Farrokhpay, 2011).

From this investigation, the solids and water recovery data showed two different trends with increasing froth height. The most dominant trend being the decrease in recoveries as the froth height was increased, this was observed at all air rates when a depressant dosage of 100 g/t was used and also when a superficial air rate of 1.35 cm/s was used with 0 and 300 g/t depressant dosages as shown in Figures 4.1, 4.8 and 4.15. This observation is in agreement with those made by previous researchers (Englebrecht and Woodburn, 1975; Laplante et al., 1983b; Feteris et al., 1987; Tao et al., 2000), where they noted a linear negative relationship between water recovery and froth height. At these conditions there was an increase in bubble burst rate as the froth height was increased as shown in Figures 4.2, 4.9 and 4.16. The increased burst rate was due to the increased drainage of water from the froth which increased the coalescence rate and ultimately the bubble burst rate (Englebrecht and Woodburn, 1975; Feteris et al., 1987; Tao et al., 2000).

The second trend observed is that with increasing froth height there was little change in the water and solids recovered as shown in Figures 4.1, 4.8 and 4.15. This trend was also observed with the bubble burst rate, which showed little change as the froth height was varied. This shows that the burst rate and water recovery are interconnected. At depressant dosages of 0 and 100 g/t the water recovery and burst rate data formed mirror images of each other which showed that there was a strong inverse relationship between the two as shown in Figures 4.3 and 4.10.

An analysis of the relationship between water recovery and bubble burst rate showed that at depressant dosage of 0 and 100 g/t there was a decrease in the stability of the froth as the froth height was increased. This is indicated by the increase in burst rate and decrease in water recovered with increasing froth height as shown in Figures 4.3 and 4.10. Initially there

was a high concentration of naturally floatable gangue that could potentially stabilise the froth; however, with increasing froth height there was increased drainage of these particles and water from the froth back into the pulp phase. This resulted in the formation of dryer froth which resulted in an increase in the coalescence rate. The increased froth height also increased the froth residence time during which these attached particles could detach from the bubbles. This observation was contrary to a study by Hadler et al. (2012) which suggested that when increasing froth height there was a peak where maximum stability was attained.

The recovery of PGMs is also influenced by the stability of the froth phase. Due to their hydrophobic nature, PGMs are recovered in the concentrate through their attachment on the bubble surface. It would thus be expected that as the stability of the froth increases the recovery of PGMs would also increase. This trend is observed in Figure 4.4, at superficial air rate of 1.35 cm/s and Figure 4.11 at air rates of 1.35 and 1.85 cm/s; where there is a decrease in the recovery of PGMs with increasing froth height and decreasing froth stability. However, at a depressant dosage of 0 g/t with superficial air rates of 1.60 and 1.85 cm/s and at a depressant dosage of 100 g/t with a superficial air rate of 1.60 cm/s, the effect of changing froth stability was not as apparent. As the froth height was increased (and froth stability decreased) there were minor deviations in the recovery of PGMs, less than 5 %. These negligible differences could be because the air rates utilised had an overriding effect on the PGM recovery, more so than changes in froth height and froth stability. The increased air rate increased the recovery of particles in the pulp phase which subsequently increased the recovery of PGMs in the froth phase

As a hydrophilic gangue mineral, the recovery of chromite is not influenced by changes in the stability of the froth. However, there was a decrease in the recovery of chromite with increasing froth height. This trend is because chromite is recovered mainly via entrainment as shown by the direct relationship between water and chromite recovery in Figures 4.6 and 4.13. As a result when the froth height was increased, chromite was also drained back into the pulp phase with the water.

The particle size distribution of the concentrate is also potentially controlled by the stability of the froth with more stable froth carrying larger particles. It would thus be expected that since the stability of the froth decreased with increasing froth height the average size of particles recovered would also decrease. This was observed at 0g/t depressant dosage with an air rate of 1.60 cm/s and at 1.35 cm/s between 15 and 20 cm, and 100 g/t depressant dosage with an air rate of 1.35 and 1.85 cm/s. As the froth height was increased there was also a longer residence time during which detachment could occur, as a result the heavier coarser particles were more likely to detach. However, at 0 g/t depressant dosage and an air rate of 1.85 cm/s and at a depressant dosage of 100g/t with an air rate of 1.60 cm/s the d_{50}'s remained relatively constant as the froth height was increased. This is probably because the air rate had an overriding effect on the changes in froth height, so similar sized particles are recovered.

At a depressant dosage of 300 g/t no conclusive deductions could be formulated about the stability of the froth using the bubble burst rate and water recovery data. At this depressant dosage all naturally floatable hydrophobic gangue which could potentially stabilise the froth, was depressed (Wiese, 2009). It can thus be presumed that the under these conditions the froth is highly unstable. In this case the PGM recoveries and particle size could also not be

linked to changing froth height, as they did not decrease with increasing froth height as shown in Figures 4.18 and 4.21.

However, the chromite recovery decreased with increasing froth height as observed at the lower depressant dosages evaluated. This is further indication that chromite is recovered via entrainment and is thus not affected by the stability of the froth.

5.3. The effect of air rate on froth stability

The second set of experiments was conducted to investigate the effect of changes in superficial air rate on the stability of the froth. A decrease in air rate could increase the stability of the froth due to low turbulence in the system which promotes bubble loading and ultimately prevents coalescence. However, a low superficial air rate also increases the froth residence time and subsequently bubble coalescence (Klassen and Mokrousov, 1963; Tao et al., 2000; Engelbrecht and Woodburn, 1975). Whilst increasing superficial air rates reduce the froth residence time, it also lowers bubble loading which increases the rate of bubble coalescence (Barbian et al., 2003; Ventura-Medina et al., 2003). It has been established that when increasing the superficial air rate from a low turbulence region to a high turbulence region, there is an optimum (intermediate) air rate at which maximum stability can be attained (Hadler and Cilliers, 2009).

Generally, at the three depressant dosages investigated there was an increase in water recovery as the superficial air rate was increased as shown in Figures 4.1, 4.8 and 4.15. This result was expected as the increase in superficial air rate would transport more entrained solids from the pulp phase into the froth phase. Increasing air rate would also increase the gas hold up which would result in more water in the lamellae of bubbles and more attached solids reporting to the concentrate.

Unlike the water recovery data, the bubble burst rate data appeared to be more varied with increasing superficial air rate as seen in Figures 4.2, 4.9 and 4.16. This is in contrast to the results observed in section 5.1 where the bubble burst rate data mirrored the water recovery data. The most recurring trend was a decrease in the bubble burst rate when the superficial air rate was increased from 1.35 to 1.60 cm/s followed by an increase when the superficial air rate was further increased from 1.60 to 1.85 cm/s. This was in agreement with the observations made by Hadler and Cilliers (2009) which showed that the stability of the froth went through a peak as the air rate was increased. In this case, this was indicated by the low burst rate at 1.60 cm/s.

The second trend observed was a decrease in the bubble burst rate with increasing superficial air rate; the increased air rate reduced the time available for coalescence which ultimately reduced the bubble burst rate. This trend is in line with observations by Barbian et al. (2003) and Ventura Medina et al. (2003) who found that the froth became more stable with increasing air rate. This trend was only observed at a 15 cm froth height with no depressant in the system and at 10 cm froth height in the presence of 100 g/t depressant.

An analysis of the bubble burst rate and water recovery plots was used to gain more insight on the stability of the froth. This was done by comparing the trends when evaluating the effect of changing froth height at the different air rates. From the interpretation of Figures 4.3, 4.10 and 4.17 it is evident that different depressant dosages affected the interaction between air rate and froth stability differently.

At a depressant dosage of 0 g/t there was a rightward shift in the froth stability trends when the superficial air rate was increased, that is, for the same amount of water recovered the froth produced at 1.85 cm/s would have a higher burst rate than that at 1.35 or 1.60 cm/s. This suggests that as the air rate was increased the froth became less stable as observed by Barbian et al. (2003) and Ventura-Medina et al. (2003). This trend also corresponds with the decreasing limb of the air recovery graph proposed by Hadler and Cilliers (2009); highlighted in Figure 5.1.

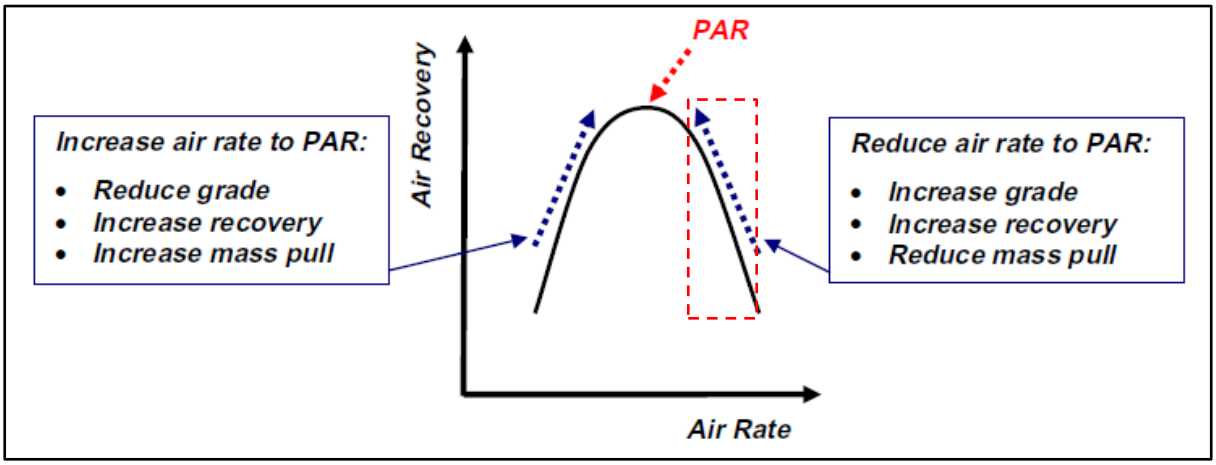

Figure 5. 1: Schematic showing general effect of air recovery optimisation on flotation performance, highlighting the decreasing limb of the air recovery plot with the red box [Adapted from (Hadler and Cilliers, 2010)]

At this depressant dosage the differences in stability are more pronounced between superficial air rates of 1.35 and 1.60 cm/s, than between 1.60 and 1.85 cm/s. This is reflected in the PGM recoveries where the recoveries decreased between superficial air rates of 1.35 and 1.60 cm/s after which they plateaued as shown in Figure 4.4. This shows that the stability of the froth impacted the amount of valuable minerals recovered.

An analysis of the particle size distribution of the concentrates showed two different trends as shown in Figures 4.7. At froth heights of 15 and 20 cm there was a decrease in the size of particles when the superficial air rate was increased from 1.35 to 1.60 cm/s followed by a plateauing off, which corresponded to the froth stability trends. For a 10 cm froth height there was no change in the particle size as the superficial air rate was increased. This could be because the froth produced was so stable that changes in the air rate did not have much of an influence on the particle size.

At a depressant dosage of 100 g/t there appears to be an increase in the stability of the froth when the superficial air rate was increased from 1.35 to 1.60 cm/s followed by a decrease in stability when the superficial air rate was further increased as shown in Figure 4.10. This trend confirms the suppositions drawn from the dominant burst rate data which proposed that the there was a peak in the stability of the froth at 1.60 cm/s.

However, the PGM recoveries appear to be influenced more by the increase in the superficial air rate than by changes in froth stability. Figure 4.11 showed that PGM recoveries generally increased as the air rate is increased. The particle size data shown in

Figure 4.14 showed that the smallest particles were recovered when the froth was most stable.

At the highest depressant dosage of 300 g/t no trends in froth stability could be established as shown in Figure 4.17. As explained in section 5.1, at a depressant dosage of 300 g/t the froth phase is highly unstable due to the absence of naturally hydrophobic froth stabilising gangue (Wiese, 2009). Since no discernable froth stability trends could be established it could not be used to explain the PGM and particle size results. However, at this dosage, both the PGM and particle size increased with increasing superficial air rate. This was more apparent with the PGM recoveries than the particle size as shown in Figures 4.18 and 4.21.

At all three depressant dosages the recovery of chromite was not affected by the stability of the froth as chromite is not recovered by true flotation, but rather by the mechanism of entrainment as evidenced from the direct relationship between water recovery and chromite recovery as shown in Figures 4.6, 4.13 and 4.20 .The air rate had a greater effect on the recovery of chromite and generally there was an increase in chromite recovery as the superficial air rate was increased. This was expected since an increase in air flow rate would result in an increase in water recovered to the concentrate in the lamellae surrounding the bubbles.

5.4. The effect of depressant dosage on froth stability

From section 5.1 and 5.2 it is evident that the amount of depressant present in the system had a large effect on both the stability of the froth and the amount of solids that were recovered. Depressants are added to the system to make naturally hydrophobic gangue more hydrophilic (Wills & Napier-Munn, 2006) which reduces their recovery in the concentrate and in so doing improves the grades of the concentrate of the final product.

Removing the naturally floatable gangue would reduce the amount of hydrophobic particles in the system which could potentially destabilise the froth phase (Bradshaw et al., 2005).Therefore with increasing depressant dosage the stability of the froth and recoveries of water and valuable minerals would be expected to decrease.

The results in section 4.3 showed that, solids and water recoveries increased when the depressant dosage was increased from 0 to 100 g/t after which it decreased when the depressant dosage was further increased. This trend was observed at all three superficial air rates that were investigated as seen in Figures 4.22, 4.29 and 4.36. The trends observed are contrary to expectations; as previously described the amount of solids and water would be expected to decrease as the concentration of depressant increased. The anomaly observed between 0 and 100 g/t can be explained by a study conducted by Perez-Garibay et al. (2002) in which they found that when using a flotation column, increasing the pulp density increased recoveries, however, above a pulp density of 25 % pulp density the recoveries declined as shown in Figure 5.2.

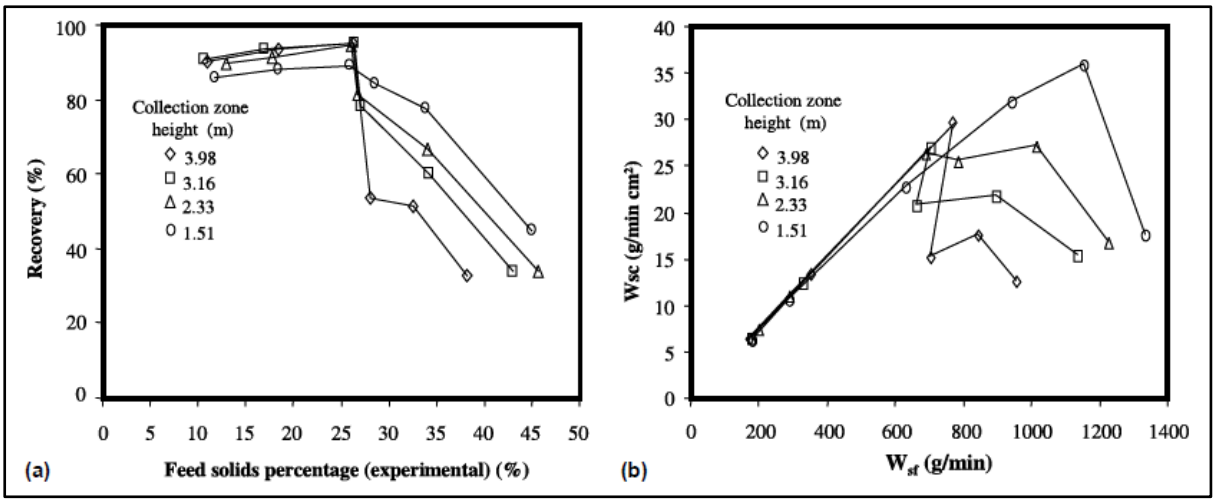

Figure 5. 2: a) Effect of the feed solids content on the solids recovery ; b) effect of the feed solids mass flow on the carrying capacity [Adapted from (Perez Garibay et al., 2002)]

This was attributed to higher pulp densities forming highly loaded bubble particle aggregates with densities close to 1. As a result the bubble-particle aggregates sunk (or did not float as efficiently) and the mineralised bubbles were recovered in the tailings. In this investigation tests were conducted with a 30% solid pulp density so when no depressant was used there was a higher concentration of particles (due to the presence of the naturally floatable gangue). As a result the bubbles were highly loaded which prevented them from floating up to the top of froth as easily. Addition of depressant at a dosage of 100 g/t reduced the bubble loading and allowed efficient transportation of solids to the launder. Further evidence of this effect occurring in this study is the recovery of mineralised bubbles in the tailings which is shown by the reduced PGM recoveries observed at a depressant dosage of 0 g/t. This trend is contrary to the expectation that at a depressant dosage of 0 g/t there would be a more stable froth which would ultimately result in the recovery of more hydrophobic valuable minerals.

The water recovery and bubble burst rate plots analysed at superficial air rates of 1.35 and 1.85 cm/s showed a decrease in the stability of the froth as the depressant dosage was increased as depicted by Figures 4.24 and 4.38. This decrease in stability could be attributed to the reduction in froth stabilising hydrophobic gangue particles due to the addition of depressant.

From Figure 4.31 it is evident that at a superficial air rate of 1.60 cm/s there was no change in froth stability as the depressant dosage was varied. As explained in section 5.2, the froth phase was found to be most stable at a superficial air rate of 1.60 cm/s. It can thus be inferred that if the froth had already reached its maximum stability due to changes in superficial air rate, then changes in depressant dosage would have no further effect on the stability of the froth phase. The effect of superficial air rate on the stability of the froth is thus greater than the effect of depressant dosage.

At all air rates that were tested it is evident that the recovery of solids was more influenced by the transportation of particles from the column to the launder than by the effect of froth stability.

The PGM recoveries were not solely influenced by the stability of the froth but could also be attributed to the effect of bubble loading. As a result the trends observed are very similar to those observed for solids and water recoveries as shown in Figures 4.22, 4.29 and 4.36. For the tests conducted at superficial air rates of 1.35 and 1.85 cm/s, the decrease in PGM recovery when the depressant dosage was increased from 100 to 300 g/t could also be attributed to the formation of less stable froth. At a superficial air rate of 1.60 cm/s the PGM recoveries decreased but this cannot be attributed to changes in froth stability as there were no indications of changes in stability under these conditions.

With the exception of the recoveries measured at a superficial air rate of 1.60 cm/s the chromite recoveries appear to have similar trends to those observed for the water recoveries described above that is there is a peak in chromite recovery at a depressant dosage of 100 g/t. As described previously in sections 5.1 and 5.2 the chromite recovery was found to be directly related to the water as shown in Figures 4.27, 4.34 and 4.41. Chromite is naturally hydrophilic so its recovery would not be expected to be affected by the addition of depressant. In this case the changes in chromite recovery could be attributed to the bubble loading and reduced transportation of bubble particles into the launder. This reduction in transportation would also affect the water surrounding each bubble in which the entrained particles such as chromite are carried. At higher depressant dosages that is between 100 and 300 g/t, the decrease in chromite recovery could also be due to the rimming of chromite by hydrophobic particles such as talc, a phenomenon that was observed by Hay and Roy (2010). As a result the recovery of chromite would decrease as the talc was depressed.

For all the froth heights investigated at a superficial air rate of 1.35 cm/s and at 10 and 15 cm froth heights at a superficial air rate of 1.60 cm/s air rate there was a decrease in particle size as the depressant dosage was increased. As previously stated, at a depressant dosage of 0 g/t the bubbles were highly loaded which reduced their buoyancy. This lower buoyancy in conjunction with the low superficial air rates facilitated the transportation of coarser particles up to the top of the column without interference due to turbulence. At a superficial air rate of 1.35 cm/s the decrease in particle size could also be attributed to the decrease in the stability of the froth when the depressant dosage was increased from 100 to 300 g/t. The highly unstable froth that was formed when 300 g/t depressant was used resulted in the detachment of coarser particles.

At the remaining conditions there was a peak in the particle size as the depressant dosage was increased. The peaks show that at the higher superficial air rates the particle size distribution was also affected by the bubble loading when there was no depressant in the system which reduced the buoyancy of the bubbles. The slow moving bubbles were exposed to the turbulent system produced by the high superficial air rates which increases the detachment of the heavier coarse particles from the bubble surface. A similar trend was not noted when an air rate of 1.35 cm/s was used because the lower air rate produced a more quiescent flow which did not cause excessive detachment. When depressant dosage was increased from 100 to 300 g/t the decrease in particle size was influenced more by the destabilization of the froth and detachment of coarse particles.

5.5. Summary of Discussion

This chapter has highlighted the different froth stability trends observed when the depressant dosage, froth height and superficial air rate are altered. These trends were determined by the concentration of particles in the flotation cell which was altered by the addition of

depressant. In the absence of depressant, the froth formed was highly stable which resulted in slight changes in stability as the air rate was increased. When a depressant dosage of 100 g/t was utilised, there was a decrease in froth stability with increasing froth height, whilst an increase in air rate resulted in a peak forming at the intermediate air rate. The addition of 300 g/t depressant produced highly unstable froth and as a result no froth stability trends could be established.

CHAPTER SIX : CONCLUSIONS AND RECOMMENDATIONS

6.1. Conclusions

This study investigated the effect of changing froth height, superficial air rate and depressant dosage on the stability of the froth phase. The stability of the froth was evaluated at the different conditions by qualitatively comparing the relationship between bubble burst rate and water recovery. This information was then compared to the valuable mineral and gangue recovery data.

The conclusions drawn from this study will be addressed by answering the key questions posed in Chapter One.

1. **What is the effect of changing froth height on the stability of the froth phase?**

The results of this investigation showed that generally when the froth height was increased the stability of the froth decreased. This observation was made when tests were conducted using depressant dosages of 0 and 100 g/t. With increasing froth height there was an increase in the amount of liquid and entrained particles that drained back into the pulp; which resulted in an increase in the bubble coalescence rate and ultimately reduced the stability of the froth.

When a depressant dosage of 300 g/t was used, the froth formed was unstable due to the depression of the majority of the naturally floatable gangue. Since the froth was already unstable, changes in froth height had little effect on the stability of the froth.

2. **What is the effect of changing air rate on the stability of the froth phase?**

In this investigation it was established that the stability of the froth was largely influenced by the concentration of particles within the pulp phase. This was noted from the different froth stability trends that were observed when the depressant dosage was varied.

In the absence of depressant there was a high concentration of particles, mainly naturally floatable gangue, which could potentially stabilise the froth, present in the system. As a result there were minor decreases in the stability of the froth as the superficial air rate was increased. The decrease in stability was due to an increase in turbulence in the system as the air rate was increased.

When a depressant dosage of 100 g/t was used the froth formed was moderately stable which resulted in different froth stability trends from those observed when no depressant was used. Initially, the stability of the froth increased with increasing air rate, this was attributed to a reduction in the froth residence time which reduced the time available for bubble coalescence to occur. The increase in froth stability was also due to an increase in the amount of solids that were present in the froth phase, and could potentially reduce coalescence. Further increases in air rate, however, resulted in the destabilization of the froth phase, and this was due to an increase in the amount of turbulence within the system which resulted in the destruction of the froth.

When a depressant dosage of 300 g/t was used, the froth was highly unstable and as a result no froth stability trends could be established when the superficial air rate was increased.

3. **What is the effect of changing depressant dosage on the stability of the froth phase?**

In this study the concentration of particles was altered by changing the depressant dosage. When the tests were conducted using superficial air rates of 1.35 and 1.85 cm/s there was a continuous decrease in the stability of the froth phase as the depressant dosage was increased. This decrease was due to the reduction in the concentration of froth stabilising gangue with increasing depressant dosage which resulted in the formation of less stable froth.

At a superficial air rate of 1.60 cm/s the stability of the froth remained constant with increasing depressant dosage. An analysis of the results from the tests conducted at increasing superficial air rate established that an air rate of 1.60 cm/s produced stable froth and as a result changing depressant dosage did not have much of an impact on the froth.

4. **How do changes in froth stability affect the recovery of valuable minerals?**

PGMs are recovered in the concentrate through attachment to bubble surfaces, so an unstable froth would be expected to reduce their recoveries. In this study the impact froth stability was only observed when the tests were conducted with increasing froth height, which showed a decrease in mineral recovery.

When the tests were conducted using different superficial air rates, the recovery of PGMs increased with increasing air rate which was contrary to the froth stability trends. Similarly when the depressant dosage was changed the PGM recovery trends did not correspond to the froth stability trends.

6.2. Recommendations

On the basis of the contributions and findings from this study, recommendations for future work in this field are suggested:

1. This study has suggested that bubble coalescence plays a significant role in altering the stability of the froth. Therefore, a robust method should be developed to quantify the bubble coalescence rate. A more powerful camera should be used to measure the froth bubble size and the curvature effects of the column could also be reduced by using a transparent viewing box such as that used by Ata et al. (2003). An attempt should be made to measure the size of bubbles in the pulp phase using the UCT bubble size analyser in an in-line aerated column. The coalescence rate obtained could then be related to the top of froth bubble burst rate as a means of measuring the stability of the froth phase.

2. One of the limitations of this work was the small number of concentrates that were collected during each test. Tests were not conducted in duplicate (due to the large amount of ore required for each test) and thus there was not enough concentrate to conduct an in depth mineralogical analysis. Tests should be conducted at a lower solids concentration to allow for repeat experiments so that more concentrate can be collected for analysis.

3. Generally, while there were some changes in the stability of the froth phase, these changes were not pronounced under the conditions tested in this study. Changes in

frother dosage and particles properties would be expected to show larger changes. From this study it has been established that the concentration of particles plays a large role on the stability of the froth phase. Future work should investigate the effect of changing frother dosage and particle properties such as particle size, hydrophobicity and concentration on the stability of the froth phase.

4. This project forms part of the Amira P9P project and some of the data that has been generated from this study could be used to validate a froth performance model that was proposed in the Amira P9O project.

5. The mobility of the froth appears to have had a large impact on recoveries, particularly when the depressant dosage was altered; further work should be conducted in the same column to investigate this phenomenon.

REFERENCES

Aktas, Z., Cilliers, J. & Banford, A., 2008. Dynamic froth stability : Particle size, airflow rate and conditioning time effects. *International Journal of Mineral Processing ,* Volume 87, pp. 65-71.

Aldo Miners, 2012. *Technology Industry of Gold Mining.* [Online]
Available at: http://miningeducation.blogspot.com/2012/01/flotation-in-mining.html
[Accessed 8 October 2013].

Alvarez-Silva, M., Wiese, J. & O'Connor, C., 2012. *An investigation into the role of the froth phase in the flotation of UG2 ore using a laboratory column flotation cell.* New Delhi, International Mineral Processing Congress .

Ata, S., Ahmed, N. & Jameson, G., 2002. Collection of hydrophobic particles in the froth phase. *International Journal of Mineral Processing,* Volume 64, pp. 101-122.

Ata, S., Ahmed, N. & Jameson, G., 2003. A study of bubble coalescence in flotation froths. *International Journal of Mineral Processing,* Volume 72, pp. 255-266.

Aveyard, R., Binks, B., Fletcher, P. & Peck, T., 1994. Aspects of aqueous foam stability in the presence of hydrocarbon oils and solid particles. *Advanced Colloid Interface Science,* Volume 48, pp. 93-120.

Baete, S., De Deene, Y., Masschaele, B. & De Neve, W., 2008. Microstructural analysis of foam by use of NMR R2 dispersion. *Journal of Magnetic Resonance,* 193(2), pp. 286-296.

Barbian, N., Hadler, K., Ventura-Medina, E. & Cilliers, J., 2005. The froth stability column: linking froth stability and flotation performance. *Minerals Engineering ,* Volume 18, pp. 317-324.

Barbian, N., Ventura-Medina, J. & Cilliers, J., 2003. Dynamic froth stability in froth flotation. *Minerals Engineering ,* Volume 16, pp. 1111-1116.

Bikerman, J., 1973. *Foam. Applied Physics and Engineering.* 10 ed. Berlin: Springer-Verlag.

Bisshop, J. & White, M., 1976. Study of particle entrainment in flotation froths. *Transactions of the instute of mining and metallurgy ,* pp. C191-194.

Bradshaw, D., Harris, P. & O'Connor, C., 1998. Synergistic interactions between reagents in sulphide flotation. *The Journal of The South African Institute of Mining and Metallurgy ,* pp. 189-194.

Bradshaw, D., Harris, P. & O'Connor, C., 2005. *The effect of collectors and their interactions with depressants on the behaviour of the froth phase in flotation.* Brisbane , Centenary of flotation symposium Brisbane 2005.

Cawthorn, R., 1999. The Platinum and Palladium Resources and the Bushveld Complex. *South African Journal of Science,* Volume 95, pp. 481-489.

Cho, Y. & Laskowski, J., 2002. Effect of flotation frothers on bubble size and foam stability. *International Journal of Mineral Processing,* Volume 64, pp. 69-80.

REFERENCES

Cilliers, J., 2007. The froth in column flotation . In: M. Fuerstenau, G. Jameson & R. Yoon, eds. *Froth Flotation : A Century of Innovation .* Colorado : Society for Mining, Metallurgy and Exploration , pp. 708-729.

Ciros Mining Equipment, 2012. *Quartz Flotation Equipment.* [Online]
Available at: http://www.goldorecrusher.com/beneficiation-plant/quartz-flotation-equipment
[Accessed 8 October 2013].

Corin, K. & Harris, P., 2010. Investigation into the flotation response of a sulphide ore to depressant mixtures. *Minerals Engineering ,* Volume 23, pp. 915-920.

Dippenaar, A., 1982. The destabilization of froth by solids.I. The mechanism of film rupture. *International Journal of Mineral Processing,* Volume 9, pp. 1-14.

Ekmekci, Z., Bradshaw, D., Allison, S. & Harris, P., 2001. *Investigation into the flotation of chromite at the Crocodile River UG2 Plant.* Cape Town : Unpublished Research Report,Mineral Processing Research Unit, Department of Chemical Engineering, University of Cape Town .

Ekmekci, Z., Bradshaw, D., Allison, S. & Harris, P., 2003. Effects of frother type and froth height on the flotation behaviour of chromite in UG2. *Minerals Engineering ,* Volume 16, pp. 941-949.

Engelbrecht, J. & Woodburn, E., 1975. The effect of froth height, aeration rate and gas precipitation on flotation. *Journal of the South African Institute of Mining and Metallurgy ,* Volume 76, pp. 125-132.

Farrokhpay, S., 2011. The significance of froth stability in mineral flotation- A review. *Advances in Colloid and Interface Science ,* Volume 166, pp. 1-7.

Farrokhpay, S., 2012. The importance of rheology in mineral flotation: A review. *Minerals Engineering ,* Volume 36-38, pp. 272-278.

Farrokhpay, S. & Zanin, M., 2011. *Effect of water quality on froth stability in flotation.* Sydney, Chemeca 2011: Engineering A Better World .

Feteris, S., Frew, J. & Jowett, A., 1987. Modelling the effect of froth depth in flotation. *International Journal of Mineral Processing ,* Volume 20, pp. 121-135.

Finch, J. & .Dobby, G., 1990. *Column Flotation.* Oxford: Pergamon.

Finch, J., Cilliers, J. & Yianatos, J., 2007. Column Flotation. In: M. Fuerstenau, G. Jameson & R. Yoon, eds. *Froth flotation : A century of innovation .* Colorado : Society for Mining,Metallurgy and Exploration , pp. 681-708.

Fuerstenau, M. & Han, K., 2003. *Principles of Mineral Processing.* Colorado : Society for Mining,Metallurgy and Exploration,Inc.

Grau, R., Laskowski, J. & Heiskanen, K., 2005. Effect of frothers on bubble size. *International Journal of Mineral Processing ,* Volume 76, pp. 225-233.

Hadler, K. & Cilliers, J., 2009. The relationship between the peak in air recovery and flotation bank performance. *Minerals Engineering,* 22(5), pp. 451-455.

Hadler, K., Greyling, M., Plint, N. & Cilliers, J., 2012. The effect of froth depth on air recovery and flotation performance. *Minerals Engineering ,* 36(38), pp. 248-253.

Hadler, K., Smith, C. & Cilliers, J., 2010. Recovery vs.mass pull: The link to air recovery. *Minerals Engineering ,* Volume 23, pp. 994-1002.

Harris, P., 1982. Frothing Phenomena and frothers. In: R. King, ed. *Principles of flotation .* Johannesburg: South African Institute of Mining and Metallury , pp. 237-250.

Harvey, P., Nguyen, A., Jameson, G. & Evans, G., 2005. Influence of sodium dodecyl sulphate and Dowfroth frothers on froth stability. *Minerals Engineering ,* Volume 18, pp. 311-315.

Hay, M. & Roy, R., 2010. A case study of optimising UG2 flotation performance. Part 1: Bench,pilot and plant scale factors which influence chromite entrainment in UG2 flotation. *Minerals Engineering ,* Volume 23, pp. 855-867.

Hunter, T., Pugh, R., Franks, G. & Jameson, G., 2008. The Role of Particles in Stabilising Foams and Emulsions. *Advances in Colloid and Interface Sciences ,* Volume 137, pp. 57-81.

Johansson, G. & Pugh, R., 1992. The Influence of Particles Size and Hydrophobicity on the Stability of Mineralized Froths. *International Journal of Mineral Processing ,* Volume 34, pp. 1-21.

Kakovsky, I., Grebnev, A. & Silina, E., 1961. The relationship between the flotability of mineral particles of various sizes ,their structures and the consumption of collectors. *Tsvetnye Metal ,* 2(8), pp. 7-16.

Kawatra, S. & Eisele, T., 2001. *Coal Desulfurization : High-Efficiency Preparation Methods.* New York : Taylor and Francis .

Klassen, V. & Mokrousov, V., 1963. *An Introduction to the Theory of Flotation.* London : Butterworth .

Klimpel, R. R., 1995. The influence of frother structure on industrial coal flotation. In: Kawatra, ed. *High Efficiency Coal Preparation .* Littleton : Society for Mining, Metallurgy and Exploration , pp. 141-151.

Lange, A., Skinner, W. & Smart, R., 1997. Fine coarse particle interaction and aggregation in sphalerite flotation. *Minerals Engineering ,* Volume 10, pp. 681-693.

Laplante, A., Toguri, J. & Smith, H., 1983b. The effect of air flow rate on the kinetics of flotation: Part 2. The transfer of material from the froth over the cell lip. *International journal of mineral processing,* Volume 11, pp. 221-234.

Laskowski, J., 2004. Testing flotation frothers. *Physicochemical problems of Mineral Processing,* Volume 38, pp. 13-22.

Livshits, A. & Dudenkov, S., 1965. Some factors in flotation froth stability. *International Mineral Processing ,* Volume 1, pp. 367-371.

Moolman, D., Aldrich, C., van Deventer, J. & Bradshaw, D., 1995. The interpretation of flotation froth surfaces by using digital image analysis and neural networks. *Chemical Engineering Science,* 50(22), pp. 3501-3513.

Morar, H., Hatfield, D., Barbian, N. & Bradshaw, D., 2006. *A comparison of flotation froth stability measurements and their use in the prediction of concentrate grade.* Istanbul, International Mineral Processing Congress.

Morar, S., Bradshaw, D. & Harris, M., 2012. The use of the froth surface lamellae burst rate as a flotation froth stability measurement. *Minerals Engineering,* 36(38), pp. 152-159.

Moudgil, B., 1992. *Enhanced recovery of coarse particles during phosphate flotation,* Florida : Florida Institute of Phosphate Research .

Moys, M., 1978. A study of a plug flow model for flotation froth behaviour. *International Journal of Mineral Processing,* Volume 5, pp. 21-28.

Moys, M., 1984. Residence time distribution and mass transport in the froth phase of the flotation process. *International journal of mineral processing,* Volume 13, pp. 117-142.

Nashwa, V., 2007. *The flotation of high talc-containing ore from the Great Dyke of Zimbabwe,* Pretoria : University of Pretoria .

Penberthy, C., Oosthuyzen, E. & Merkle, R., 2000. The Recovery of Platinum-Group Elements from the UG2 Chromitite Bushveld Complex-A Mineralogical Perspective. *Mineralogy and Petrology,* Volume 68, pp. 213-222.

Perez Garibay, R., Gallegos A, P., Uribe S, A. & Nava A, F., 2002. Effect of collection zone height and operating variables on recovery of overload flotation columns. *Minerals Engineering ,* Volume 15, pp. 325-331.

Pugh, P., 1988a. Macromolecular organic depressants in sulphide flotation - a review 1: principles, types and applications. *International Journal of Mineral Processing ,* Volume 25, pp. 101- 130.

Rahman, R., Ata, S. & Jameson, G., 2012. The effect of flotation variables on the recovery of different particle size in the froth and the pulp. *International Journal of Mineral Processing ,* Volume 106-109, pp. 70-77.

Robinson, A., 1960. Relationship between particle size and collector concentration. *Transactions of the institute of mining and metallurgy,* Volume 69, pp. 45-62.

Schouwstra, R. & Kinloch, E., 2000. A Short Geological Review of the Bushveld Complex. *Platinum Metals Review ,* 44(1), pp. 33-39.

Schulze, H., 1984. *Phsyico-Chemical Elementary Processes in Flotation.* Amsterdam: Elsevier.

Subrahmanyam, T. & Forssberg, E., 1988. Froth stability,particle entrainment and drainage in flotation. *International Journal of Minerals Processing,* Volume 23, pp. 33-53.

Szatkowski, M. & Freyburger, W., 1985. Kinetics of flotation with fine bubbles. *Transactions of the Institute of Mining and Metallurgy,* Volume 94, pp. C61-C70.

Tang, D., Wightman, E., Franzidis, J. & Montes-Atenas, G., 2010. *Assessment of the consistency between different laboratory froth stability measurements.* Brisbane , International Mineral Processing Conference .

Tang, F., Xiao, Z., J, T. & Jiang, L., 1989. The effect of silica dioxide particles upon stabilization of foam. *Journal of colloid and interface science,* 131(2), pp. 498-502.

Tao, D., Luttrell, G. & Yoon, R., 2000. A parametric study of froth stability and its effect on column flotation of fine particles. *International Journal of Mineral Processing ,* Volume 59, pp. 25-43.

Trahar, W., 1980. A rational interpretation of the role of particle size in flotation. *International Journal of Mineral Processing ,* Volume 8, pp. 289-327.

Trahar, W. & Warren, L., 1976. The flotation of very fine particles-a review. *International Journal of Mineral Processing,* Volume 3, pp. 103-131.

Valenta, M., 2007. Balancing the reagent suite to optimise grade and recovery. *Minerals Engineering ,* Volume 20, pp. 979-985.

Ventura-Medina, E., Barbian, N. & Cilliers, J., 2003. *Froth stability and flotation performance.* s.l., XXII International Mineral Processing Congress.

Ventura-Medina, E. & Cilliers, J., 2002. A model to describe flotation performance based on physics of foams and froth images analysis. *International Journal of Mineral Processing ,* 67(1-4), pp. 79-99.

Viera, A. & Peres, A., 2007. The effect of amine type,pH and size range in the flotation of quartz. *Minerals Engineering,* 20(10), pp. 1008-1013.

Whelan, P. F. & Brown, D., 1956. Particle-bubble attachment in froth flotation. *Bulletin of the Institute of Mining and Metallurgy ,* Volume 591, pp. 181-192.

Wiese, J., 2009. *Investigating depresssant behaviour in the flotation of Merensky ore (Masters Thesis),* Cape Town : Department of Chemical Engineering ,University of Cape Town.

Wiese, J., Harris, P. & Bradshaw, D., 2005. The influence of the reagent suite on the flotation of ores from the Merensky Reef. *Minerals Engineering,* Volume 18, pp. 189-198.

Wiese, J., Harris, P. & Bradshaw, D., 2011. The effect of the reagent suite on froth stability in laboratory scale batch flotation tests. *Minerals Engineering ,* Volume 24, pp. 995-1003.

Wills, B. & Napier-Munn, T., 2006. *Will's Mineral Processing Technology: An Introduction to the Practical Aspects of Ore Treatment and Mineral Recovery.* Seventh ed. Queensland: Elsevier Science and Technology Books.

Woodburn, E., Ausint, L. & Stockton, J., 1994. A froth based flotation model. *Chemical Engineering Research and Design,* 72(A2), pp. 211-226.

Xu, D. & Ametov, I. G., 2011. Detachment of coarse particles from oscillating bubbles- the effect of particle contact angle, shape and medium viscosity. *International Journal of Mineral Processing ,* 101(1-4), pp. 50-57.

Xu, M., Quinn, P. & Stratton-Crawley, R., 1996. A feed-line aerated flotation column.Part 1: Batch and continuous testwork. *Minerals Engineering ,* 9(5), pp. 499-507.

Yianatos, J., 1989. *Column flotation modelling and technology.* Cape Town , The Southern African Institution of Mining and Metallurgy .

Zheng, X., Johnson, N. & Franzidis, J., 2006. Modelling of entrainment in industrial flotation cells: Water recovery and degree of entrainment. *Minerals Engineering ,* Volume 19, pp. 1191-1203.

Zhou, Z., Egiebor, N. & Plitt, L., 1993. Frother effects on bubble size estimation in a flotation column. *Minerals Engineering ,* Volume 6, pp. 55-67.

APPENDICES

APPENDIX A: Effect of increasing air rate and froth height in the absence of depressant

RUN 1: 10 CM FROTH HEIGHT AND 1.35 CM/S AIR RATE

	Solids (g/min)	Solids (%)	Water (g/min)
C1	14.9	3.86	182
C2	13.1	3.39	159
C3	14.6	3.80	180
C4	15.6	4.07	194
T1	449	-	641
T2	388	-	646
T3	380	-	645
T4	376	-	620

	Burst rate (bubbles/s)
Beginning	0.20
Middle	0.18
End	0.18
Average	0.19
Standard deviation	0.01

Height from bottom of column (cm)	Bubble size (mm)
191	1.27
190	0.700
189	0.616
188	0.600
187	0.415
Gradient	0.180

Froth height (cm)	10.0
Volume of bubble	0.11
Burst rate (bubbles/sec)	0.19
Air rate through top of column (cm/s)	0.001
Stability factor	7940

	Mass flow (g/min)	Recovery (%)
Palladium	0.0003	65.1
Platinum	0.001	63.7
Chromite	1.05	1.75

Particle size –d50 (μm)	19.8

RUN 2: 15 CM FROTH HEIGHT AND 1.35 CM/S AIR RATE

	Solids (g/min)	Solids (%)	Water (g/min)
C1	5.27	1.37	40.1
C2	6.10	1.59	50.9
C3	6.96	1.81	67.2
C4	6.41	1.67	64.7
T1	470	-	769
T2	421	-	730
T3	404	-	699
T4	414	-	738

	Burst rate (bubbles/s)
Beginning	0.35
Middle	0.28
End	0.41
Average	0.35
Standard deviation	0.07

Height from bottom of column (cm)	Bubble size (mm)
191	1.40
190	1.19
188	1.24
186	0.498
Gradient	0.158

Froth height (cm)	15
Volume of bubble	0.19
Burst rate (bubbles/sec)	0.35
Air rate through top of column (cm/s)	0.004
Stability factor	3760

	Mass flow (g/min)	Recovery (%)
Palladium	0.0003	56.4
Platinum	0.001	56.0
Chromite	0.214	0.247

Particle size –d50 (μm)	24.7

RUN 3: 20 CM FROTH HEIGHT AND 1.35 CM/S AIR RATE

	Solids (g/min)	Solids (%)	Water (g/min)
C1	4.83	1.26	49.4
C2	5.38	1.40	57.4
C3	6.17	1.60	70.4
C4	3.83	0.99	45.0
T1	343	-	667
T2	321	-	663
T3	328	-	634
T4	320	-	656

	Burst rate (bubbles/s)
Beginning	0.38
Middle	0.33
End	0.35
Average	0.35
Standard deviation	0.03
Height from bottom of column (cm)	Bubble size (mm)
191	1.45
189	0.603
187	1.20
Gradient	0.062

Froth height (cm)	20.
Volume of bubble	0.20
Burst rate (bubbles/sec)	0.35
Air rate through top of column (cm/s)	0.004
Stability factor	4813

	Mass flow (g/min)	Recovery (%)
Palladium	0.0002	56.7
Platinum	0.0004	56.2
Chromite	0.196	0.326

Particle size –d50 (μm)	22.7

RUN 4: 10 CM FROTH HEIGHT AND 1.60 CM/S AIR RATE

	Solids (g/min)	Solids (%)	Water (g/min)
C1	18.9	4.91	238
C2	19.2	4.99	240
C3	19.0	4.93	235
C4	17.6	4.57	215
T1	312	-	474
T2	318	-	475
T3	299	-	442
T4	300	-	456

	Burst rate (bubbles/s)
Beginning	0.09
Middle	0.21
End	0.30
Average	0.20
Standard deviation	0.10

Height from bottom of column (cm)	Bubble size (mm)
191	0.972
190	0.868
189	0.659
188	0.740
187	0.559
Gradient	0.096

Froth height (cm)	10
Volume of bubble	0.15
Burst rate (bubbles/sec)	0.20
Air rate through top of column (cm/s)	0.002
Stability factor	5700

	Mass flow (g/min)	Recovery (%)
Palladium	0.0003	66.7
Platinum	0.001	67.6
Chromite	1.61	2.79

Particle size –d50 (μm)	19.6

RUN 5: 15 CM FROTH HEIGHT AND 1.60 CM/S AIR RATE

	Solids (g/min)	Solids (%)	Water (g/min)
C1	14.5	3.78	183
C2	16.5	4.30	211
C3	17.3	4.50	221
C4	16.4	4.25	208
T1	369	-	525
T2	338	-	495
T3	336	-	485
T4	334	-	486

	Burst rate (bubbles/s)
Beginning	0.27
Middle	0.22
End	0.20
Average	0.23
Standard deviation	0.04

Height from bottom of column (cm)	Bubble size (mm)
191	1.57
190	1.52
189	1.24
188	1.30
187	1.20
Gradient	0.092

Froth height (cm)	15
Volume of bubble	0.25
Burst rate (bubbles/sec)	0.23
Air rate through top of column (cm/s)	0.003
Stability factor	4370

	Mass flow (g/min)	Recovery (%)
Palladium	0.0003	64.9
Platinum	0.0004	65.0
Chromite	1.30	1.87

Particle size –d50 (μm)	18.1

RUN 6: 20 CM FROTH HEIGHT AND 1.60 CM/S AIR RATE

	Solids (g/min)	Solids (%)	Water (g/min)
C1	17.2	4.47	221
C2	17.8	4.61	229
C3	17.8	4.64	230
C4	20.7	5.37	269
T1	300	-	464
T2	307	-	436
T3	307	-	436
T4	270	-	406

	Burst rate (bubbles/s)
Beginning	0.21
Middle	0.22
End	0.19
Average	0.21
Standard deviation	0.02

Height from bottom of column (cm)	Bubble size (mm)
191	1.18
190	0.958
189	1.10
188	0.984
Gradient	0.045

Froth height (cm)	20
Volume of bubble	0.07
Burst rate (bubbles/sec)	0.21
Air rate through top of column (cm/s)	0.0008
Stability factor	24900

	Mass flow (g/min)	Recovery (%)
Palladium	0.0003	69.3
Platinum	0.0005	69.7
Chromite	1.56	2.45

Particle size –d50 (μm)	17.6

RUN 7: 10 CM FROTH HEIGHT AND 1.85 CM/S AIR RATE

	Solids (g/min)	Solids (%)	Water (g/min)
C1	17.6	4.57	238
C2	18.8	4.89	255
C3	18.6	4.82	249
C4	21.4	5.55	287
T1	304	-	497
T2	311	-	486
T3	317	-	476
T4	287	-	451

	Burst rate (bubbles/s)
Beginning	0.22
Middle	0.20
End	0.19
Average	0.20
Standard deviation	0.02

Height from bottom of column (cm)	Bubble size (mm)
191	2.26
190	1.50
189	1.53
188	1.21
187	1.30
Gradient	0.222

Froth height (cm)	10
Volume of bubble	0.46
Burst rate (bubbles/sec)	0.20
Air rate through top of column (cm/s)	0.006
Stability factor	1780

	Mass flow (g/min)	Recovery (%)
Palladium	0.0003	67.1
Platinum	0.0005	68.0
Chromite	1.77	3.00

Particle size –d50 (μm)	18.5

RUN 8: 15 CM FROTH HEIGHT AND 1.85 CM/S AIR RATE

	Solids (g/min)	Solids (%)	Water (g/min)
C1	17.7	4.60	240
C2	20.6	5.36	275
C3	22.0	5.71	290
C4	19.7	5.13	255
T1	371	-	555
T2	389	-	513
T3	372	-	471
T4	390	-	501

	Burst rate (bubbles/s)
Beginning	0.19
Middle	0.20
End	0.17
Average	0.18
Standard deviation	0.02

Height from bottom of column (cm)	Bubble size (mm)
190	0.975
188	0.877
186	0.632
Gradient	0.086

Froth height (cm)	15
Volume of bubble	0.09
Burst rate (bubbles/sec)	0.18
Air rate through top of column (cm/s)	0.001
Stability factor	15000

	Mass flow (g/min)	Recovery (%)
Palladium	0.0003	65.8
Platinum	0.0005	66.2
Chromite	1.84	2.34

Particle size –d50 (μm)	19.0

RUN 9: 20 CM FROTH HEIGHT AND 1.85 CM/S AIR RATE

	Solids (g/min)	Solids (%)	Water (g/min)
C1	16.5	4.29	231
C2	18.1	4.71	249
C3	17.3	4.50	233
C4	18.8	4.88	255
T1	319	-	488
T2	311	-	460
T3	322	-	474
T4	327	-	449

	Burst rate (bubbles/s)
Beginning	0.27
Middle	0.24
End	0.19
Average	0.23
Standard deviation	0.04

Height from bottom of column (cm)	Bubble size (mm)
191	1.15
189	1.03
187	0.987
Gradient	0.041

Froth height (cm)	20
Volume of bubble	0.32
Burst rate (bubbles/sec)	0.23
Air rate through top of column (cm/s)	0.004
Stability factor	4500

	Mass flow (g/min)	Recovery (%)
Palladium	0.0003	66.0
Platinum	0.0005	67.3
Chromite	1.61	2.32

Particle size –d50 (μm)	19.1

APPENDIX B: Effect of increasing air rate and froth height with 100 g/t depressant

RUN 10: 10 CM FROTH HEIGHT AND 1.35 CM/S AIR RATE

	Solids (g/min)	Solids (%)	Water (g/min)
C1	24.1	6.27	276
C2	23.6	6.14	272
C3	22.3	5.80	263
C4	23.3	6.06	274
T1	324	-	474
T2	447	-	564
T3	293	-	464
T4	310	-	465

	Burst rate (bubbles/s)
Beginning	0.19
Middle	0.22
End	0.23
Average	0.22
Standard deviation	0.02

Height from bottom of column (cm)	Bubble size (mm)
191	0.699
189	0.664
188	0.508
Gradient	0.064

Froth height (cm)	10
Volume of bubble	0.06
Burst rate (bubbles/sec)	0.22
Air rate through top of column (cm/s)	0.0008
Stability factor	13000

	Mass flow (g/min)	Recovery (%)
Palladium	0.0004	71.7
Platinum	0.0006	70.7
Chromite	2.41	3.50

Particle size –d50 (μm)	21.5

RUN 11: 15 CM FROTH HEIGHT AND 1.35 CM/S AIR RATE

	Solids (g/min)	Solids (%)	Water (g/min)
C1	8.84	2.30	113
C2	10.4	2.71	136
C3	11.2	2.92	151
C4	8.89	2.31	119
T1	374	-	660
T2	368	-	645
T3	347	-	598
T4	344	-	624

	Burst rate (bubbles/s)
Beginning	0.34
Middle	0.34
End	0.34
Average	0.34
Standard deviation	0.002

Height from bottom of column (cm)	Bubble size (mm)
188	0.990
187	0.823
186	0.621
Gradient	0.185

Froth height (cm)	15
Volume of bubble	0.05
Burst rate (bubbles/sec)	0.34
Air rate through top of column (cm/s)	0.0009
Stability factor	16000

	Mass flow (g/min)	Recovery (%)
Palladium	0.0004	67.2
Platinum	0.0006	68.9
Chromite	0.717	0.981

Particle size –d50 (μm)	19.2

RUN 12: 20 CM FROTH HEIGHT AND 1.35 CM/S AIR RATE

	Solids (g/min)	Solids (%)	Water (g/min)
C1	8.14	2.12	104
C2	9.87	2.57	137
C3	10.2	2.66	146
C4	9.06	2.35	130
T1	383	-	635
T2	450	-	722
T3	378	-	609
T4	354	-	602

	Burst rate (bubbles/s)
Beginning	0.40
Middle	0.31
End	0.39
Average	0.37
Standard deviation	0.05
Froth height (cm)	20
Volume of bubble	0.13
Burst rate (bubbles/sec)	0.37
Air rate through top of column (cm/s)	0.003
Stability factor	7090

Height from bottom of column (cm)	Bubble size (mm)
190	0.912
188	0.854
186	0.886
184	0.602
Gradient	0.045

	Mass flow (g/min)	Recovery (%)
Palladium	0.0003	64.6
Platinum	0.001	65.1
Chromite	0.65	0.811

Particle size –d50 (μm)	18.6

RUN 13: 10 CM FROTH HEIGHT AND 1.60 CM/S AIR RATE

	Solids (g/min)	Solids (%)	Water (g/min)
C1	19.4	5.05	254
C2	21.4	5.56	277
C3	20.4	5.31	262
C4	22.6	5.88	290
T1	340	-	484
T2	344	-	475
T3	343	-	442
T4	286	-	390

	Burst rate (bubbles/s)
Beginning	0.15
Middle	0.24
End	0.13
Average	0.18
Standard deviation	0.06

Height from bottom of column (cm)	Bubble size (mm)
191	0.946
190	0.751
189	0.794
188	0.631
187	0.572
Gradient	0.087

Froth height (cm)	10
Volume of bubble	0.15
Burst rate (bubbles/sec)	0.18
Air rate through top of column (cm/s)	0.002
Stability factor	6420

	Mass flow (g/min)	Recovery (%)
Palladium	0.0003	72.51
Platinum	0.001	72.7
Chromite	2.15	3.23

Particle size –d50 (μm)	18.9

RUN 14: 15 CM FROTH HEIGHT AND 1.60 CM/S AIR RATE

	Solids (g/min)	Solids (%)	Water (g/min)
C1	19.7	5.12	265
C2	20.0	5.19	266
C3	18.5	4.81	244
C4	21.0	5.46	278
T1	335	-	492
T2	362	-	479
T3	364	-	486
T4	317	-	446

	Burst rate (bubbles/s)
Beginning	0.17
Middle	0.12
End	0.19
Average	0.16
Standard deviation	0.04

Height from bottom of column (cm)	Bubble size (mm)
191	0.985
190	0.831
189	0.770
188	0.823
187	0.782
Gradient	0.037

Froth height (cm)	15
Volume of bubble	0.12
Burst rate (bubbles/sec)	0.16
Air rate through top of column (cm/s)	0.001
Stability factor	13300

	Mass flow (g/min)	Recovery (%)
Palladium	0.0003	70.0
Platinum	0.001	69.2
Chromite	1.86	2.59

Particle size –d50 (μm)	17.7

RUN 15: 20 CM FROTH HEIGHT AND 1.60 CM/S AIR RATE

	Solids (g/min)	Solids (%)	Water (g/min)
C1	20.8	5.40	275
C2	16.4	4.25	217
C3	17.9	4.66	240
C4	21.0	5.46	282
T1	347	-	447
T2	380	-	500
T3	342	-	479
T4	296	-	419

	Burst rate (bubbles/s)
Beginning	0.22
Middle	0.20
End	0.17
Average	0.20
Standard deviation	0.02

Height from bottom of column (cm)	Bubble size (mm)
191	1.07
190	1.25
189	1.26
188	1.23
187	1.04
Gradient	0.010

Froth height (cm)	20
Volume of bubble	0.22
Burst rate (bubbles/sec)	0.20
Air rate through top of column (cm/s)	0.003
Stability factor	7700

	Mass flow (g/min)	Recovery (%)
Palladium	0.0003	72.4
Platinum	0.001	72.6
Chromite	1.84	2.63

Particle size –d50 (μm)	18.4

RUN 16: 10 CM FROTH HEIGHT AND 1.85 CM/S AIR RATE

	Solids (g/min)	Solids (%)	Water (g/min)
C1	36.6	9.50	409
C2	37.0	9.62	405
C3	32.8	8.54	365
C4	37.0	9.61	409
T1	351	-	431
T2	354	-	408
T3	355	-	427
T4	302	-	351

	Burst rate (bubbles/s)
Beginning	0.15
Middle	0.19
End	0.18
Average	0.17
Standard deviation	0.02

Height from bottom of column (cm)	Bubble size (mm)
191	0.668
190	0.645
189	0.602
Gradient	0.066

Froth height (cm)	10
Volume of bubble	0.23
Burst rate (bubbles/sec)	0.17
Air rate through top of column (cm/s)	0.002
Stability factor	4060

	Mass flow (g/min)	Recovery (%)
Palladium	0.0004	77.2
Platinum	0.001	76.7
Chromite	4.03	5.36

Particle size –d50 (μm)	21.6

RUN 17: 15 CM FROTH HEIGHT AND 1.85 CM/S AIR RATE

	Solids (g/min)	Solids (%)	Water (g/min)
C1	25.8	6.69	332
C2	27.8	7.22	35
C3	26.6	6.92	342
C4	30.9	8.03	387
T1	368	-	488
T2	369	-	468
T3	356	-	466
T4	319	-	408

	Burst rate (bubbles/s)
Beginning	0.24
Middle	0.30
End	0.24
Average	0.26
Standard deviation	0.03

Height from bottom of column (cm)	Bubble size (mm)
190	0.928
188	0.766
186	0.749
Gradient	0.045

Froth height (cm)	15
Volume of bubble	0.10
Burst rate (bubbles/sec)	0.26
Air rate through top of column (cm/s)	0.001
Stability factor	10300

	Mass flow (g/min)	Recovery (%)
Palladium	0.0003	72.7
Platinum	0.001	74.6
Chromite	3.05	3.94

Particle size –d50 (μm)	21.0

RUN 18: 20 CM FROTH HEIGHT AND 1.85 CM/S AIR RATE

	Solids (g/min)	Solids (%)	Water (g/min)
C1	23.8	6.19	291
C2	26.2	6.82	313
C3	24.3	6.33	289
C4	23.1	6.01	279
T1	414	-	502
T2	392	-	476
T3	401	-	474
T4	366	-	505

	Burst rate (bubbles/s)
Beginning	0.28
Middle	0.29
End	0.27
Average	0.28
Standard deviation	0.01

Height from bottom of column (cm)	Bubble size (mm)
191	1.03
190	0.795
188	0.838
186	0.707
Gradient	0.050

Froth height (cm)	20
Volume of bubble	0.36
Burst rate (bubbles/sec)	0.28
Air rate through top of column (cm/s)	0.006
Stability factor	3300

	Mass flow (g/min)	Recovery (%)
Palladium	0.0004	71.5
Platinum	0.001	73.3
Chromite	2.55	3.21

Particle size –d50 (μm)	19.2

APPENDIX C: Effect of increasing air rate and froth height with 300 g/t depressant

RUN 19: 10 CM FROTH HEIGHT AND 1.35 CM/S AIR RATE

	Solids (g/min)	Solids (%)	Water (g/min)
C1	9.72	2.53	170
C2	9.32	2.42	163
C3	10.9	2.83	185
C4	11.4	2.95	190
T1	372	-	586
T2	365	-	632
T3	345	-	551
T4	319	-	513

	Burst rate (bubbles/s)
Beginning	0.20
Middle	0.20
End	0.12
Average	0.17
Standard deviation	0.05

Height from bottom of column (cm)	Bubble size (mm)
191	1.18
190	0.966
189	0.871
188	0.974
187	0.746
Gradient	0.087

Froth height (cm)	10
Volume of bubble	0.16
Burst rate (bubbles/sec)	0.17
Air rate through top of column (cm/s)	0.002
Stability factor	6100

	Mass flow (g/min)	Recovery (%)
Palladium	0.0003	63.0
Platinum	0.001	66.9
Chromite	1.03	1.46

Particle size –d50 (μm)	16.5

RUN 20: 15 CM FROTH HEIGHT AND 1.35 CM/S AIR RATE

	Solids (g/min)	Solids (%)	Water (g/min)
C1	5.14	1.34	82.8
C2	5.78	1.50	100
C3	5.59	1.45	104
C4	5.63	1.46	101
T1	490	-	773
T2	416	-	692
T3	420	-	695
T4	412	-	654

	Burst rate (bubbles/s)
Beginning	0.47
Middle	0.39
End	0.46
Average	0.44
Standard deviation	0.04

Height from bottom of column (cm)	Bubble size (mm)
191	1.06
190	0.917
188	0.952
186	0.636
Gradient	0.073

Froth height (cm)	15
Volume of bubble	0.16
Burst rate (bubbles/sec)	0.44
Air rate through top of column (cm/s)	0.004
Stability factor	3500

	Mass flow (g/min)	Recovery (%)
Palladium	0.0003	59.9
Platinum	0.001	58.6
Chromite	0.482	0.541

Particle size –d50 (μm)	16.6

RUN 21: 20 CM FROTH HEIGHT AND 1.35 CM/S AIR RATE

	Solids (g/min)	Solids (%)	Water (g/min)
C1	5.24	1.36	88.0
C2	6.05	1.57	104
C3	7.82	2.03	144
C4	3.74	0.97	71.6
T1	354	-	676
T2	346	-	654
T3	290	-	624
T4	284	-	643

	Burst rate (bubbles/s)
Beginning	0.50
Middle	0.63
End	0.37
Average	0.50
Standard deviation	0.13

Height from bottom of column (cm)	Bubble size (mm)
191	3.11
190	3.01
189	1.99
188	2.07
187	1.33
186	1.08
Gradient	0.432

Froth height (cm)	20
Volume of bubble	0.06
Burst rate (bubbles/sec)	0.50
Air rate through top of column (cm/s)	0.002
Stability factor	10600

	Mass flow (g/min)	Recovery (%)
Palladium	0.0003	66.1
Platinum	0.001	65.1
Chromite	0.436	0.77

Particle size –d50 (μm)	18.4

RUN 22: 10 CM FROTH HEIGHT AND 1.6 CM/S AIR RATE

	Solids (g/min)	Solids (%)	Water (g/min)
C1	14.3	3.71	237
C2	15.0	3.89	242
C3	13.3	3.46	213
C4	14.2	3.68	227
T1	310	-	468
T2	312	-	457
T3	325	-	463
T4	303	-	457

	Burst rate (bubbles/s)
Beginning	0.21
Middle	0.26
End	0.27
Average	0.25
Standard deviation	0.03

Height from bottom of column (cm)	Bubble size (mm)
191	0.956
190	0.900
189	0.868
188	0.742
187	0.687
Gradient	0.070

Froth height (cm)	10
Volume of bubble	0.14
Burst rate (bubbles/sec)	0.25
Air rate through top of column (cm/s)	0.002
Stability factor	4960

	Mass flow (g/min)	Recovery (%)
Palladium	0.0003	73.1
Platinum	0.001	72.7
Chromite	1.41	2.28

Particle size –d50 (μm)	16.7

RUN 23: 15 CM FROTH HEIGHT AND 1.6 CM/S AIR RATE

	Solids (g/min)	Solids (%)	Water (g/min)
C1	12.7	3.29	209
C2	15.0	3.90	244
C3	13.5	3.51	218
C4	16.4	4.25	259
T1	361	-	532
T2	343	-	506
T3	365	-	525
T4	336	-	481

	Burst rate (bubbles/s)
Beginning	0.17
Middle	0.15
End	0.26
Average	0.19
Standard deviation	0.05

Height from bottom of column (cm)	Bubble size (mm)
191	1.74
190	1.91
189	1.70
188	1.39
187	1.45
Gradient	0.109

Froth height (cm)	15
Volume of bubble	0.06
Burst rate (bubbles/sec)	0.19
Air rate through top of column (cm/s)	0.0007
Stability factor	20400

	Mass flow (g/min)	Recovery (%)
Palladium	0.0003	67.2
Platinum	0.001	68.2
Chromite	1.48	2.05

Particle size –d50 (μm)	17.2

RUN 24: 20 CM FROTH HEIGHT AND 1.6 CM/S AIR RATE

	Solids (g/min)	Solids (%)	Water (g/min)
C1	11.3	2.94	201
C2	12.4	3.22	215
C3	12.2	3.16	206
C4	14.8	3.86	248
T1	356	-	541
T2	346	-	515
T3	323	-	489
T4	278	-	432

	Burst rate (bubbles/s)
Beginning	0.20
Middle	0.18
End	0.22
Average	0.20
Standard deviation	0.02

Height from bottom of column (cm)	Bubble size (mm)
191	1.15
190	1.83
189	1.38
188	1.05
Gradient	0.075

Froth height (cm)	20
Volume of bubble	0.16
Burst rate (bubbles/sec)	0.20
Air rate through top of column (cm/s)	0.002
Stability factor	10400

	Mass flow (g/min)	Recovery (%)
Palladium	0.0003	71.0
Platinum	0.001	71.3
Chromite	1.24	1.91

Particle size –d50 (μm)	17.6

RUN 25: 10 CM FROTH HEIGHT AND 1.85 CM/S AIR RATE

	Solids (g/min)	Solids (%)	Water (g/min)
C1	17.2	4.47	265
C2	19.3	5.01	289
C3	20.3	5.27	298
C4	20.9	5.42	299
T1	366	-	559
T2	393	-	504
T3	384	-	507
T4	365	-	459

	Burst rate (bubbles/s)
Beginning	0.29
Middle	0.36
End	0.30
Average	0.32
Standard deviation	0.04

Height from bottom of column (cm)	Bubble size (mm)
191	0.877
189	0.673
187	0.458
Gradient	0.105

Froth height (cm)	10.0
Volume of bubble	0.240
Burst rate (bubbles/sec)	0.320
Air rate through top of column (cm/s)	0.005
Stability factor	2200

	Mass flow (g/min)	Recovery (%)
Palladium	0.0004	72.7
Platinum	0.001	71.9
Chromite	2.21	2.83

Particle size –d50 (μm)	17.8

RUN 26: 15 CM FROTH HEIGHT AND 1.85 CM/S AIR RATE

	Solids (g/min)	Solids (%)	Water (g/min)
C1	25.0	6.50	339
C2	26.0	6.77	354
C3	29.6	7.70	389
C4	29.9	7.77	388
T1	372	-	437
T2	365	-	444
T3	340	-	381
T4	339	-	397

	Burst rate (bubbles/s)
Beginning	0.30
Middle	0.21
End	0.32
Average	0.28
Standard deviation	0.06

Height from bottom of column (cm)	Bubble size (mm)
191	0.999
189	0.804
187	0.711
Gradient	0.070

Froth height (cm)	15.0
Volume of bubble	0.21
Burst rate (bubbles/sec)	0.28
Air rate through top of column (cm/s)	0.004
Stability factor	4200

	Mass flow (g/min)	Recovery (%)
Palladium	0.0004	74.4
Platinum	0.0007	73.7
Chromite	3.37	4.30

Particle size –d50 (μm)	19.0

RUN 27: 20 CM FROTH HEIGHT AND 1.85 CM/S AIR RATE

	Solids (g/min)	Solids (%)	Water (g/min)
C1	11.6	3.02	208
C2	12.4	3.23	219
C3	10.3	2.68	183
C4	13.3	3.45	229
T1	413	-	593
T2	378	-	581
T3	390	-	595
T4	374	-	547

	Burst rate (bubbles/s)
Beginning	0.19
Middle	0.27
End	0.29
Average	0.25
Standard deviation	0.05

Height from bottom of column (cm)	Bubble size (mm)
191	2.79
189	2.56
187	2.13
Gradient	0.166

Froth height (cm)	20.0
Volume of bubble	0.16

Burst rate (bubbles/sec)	0.25
Air rate through top of column (cm/s)	0.002
Stability factor	8300

	Mass flow (g/min)	Recovery (%)
Palladium	0.0004	67.7
Platinum	0.001	67.4
Chromite	1.23	1.49

Particle size –d50 (µm)	17.9

APPENDIX D: Sample calculations

PULP BUBBLE SIZE

The methodology that was used in calculating the pulp bubble size was described in section 3.3.4 and was adapted from a study by Zhou et al (1993). The following values were constant in each calculation.

Column area (m^2)	0.002
Liquid flowrate (m^3/s)	$1.70x10^{-5}$
Jl (m/s)	0.010
g(m/s2	9.81
Density of liquid (kg/m3)	1000
Density of air (kg/m3)	1.29
C	1.50
Cc	247
Bulk viscosity (Pa.s)	0.001
A	$1\ 09x10^{4}$

The pulp bubble size was dependent on the gas hold up, which varied with changing superficial air rate.

Tests conducted at Jg of 1.35 cm/s

Air flow rate (m^3/s)	$2.00x10^{-5}$
Jg	0.014
ε_g	0.133
Bc	$1.05x10^{-7}$
Bubble radius -Rv (m)	$4.00x10^{-4}$
Bubble diameter (mm)	0.771

Tests conducted at Jg of 1.60 cm/s

Air flow rate (m^3/s)	$2.67x10^{-5}$
Jg	0.016
ε_g	0.160
Bc	$1.04x10^{-7}$
Bubble radius -Rv (m)	$4.00x10^{-4}$
Bubble diameter (mm)	0.769

Tests conducted at Jg of 1.85 cm/s

Air flow rate (m^3/s)	$3.08x10^{-5}$
Jg	0.019
ε_g	0.173
Bc	$1.11x10^{-7}$
Bubble radius -Rv (m)	$4.00x10^{-4}$
Bubble diameter (mm)	0.793